UNIVERSITE D'ABOMEY - CALAVI (UAC)

INSTITUT NATIONAL DE L'EAU

Registered under N°: ……/UAC/VR-AA/SA

A DISSERTATION

Submitted

In partial fulfillment of the requirements for the degree of

DOCTOR of Philosophy (PhD) of the University of Abomey-Calavi (Benin Republic)

In the framework of the

Graduate Research Program on Climate Change and Water Resources (GRP-CCWR)

By

KOUAKOU Koffi Abdelaziz

Public defense on: mm/dd/yyyy

======

IMPACT OF CLIMATE CHANGE AND URBANIZATION ON THE CONTINENTAL TERMINAL AQUIFER RECHARGE IN AGHIEN LAGOON AREA (ABIDJAN, CÔTE D'IVOIRE)

======

Supervisors:

Yalo Nicaise, Full Professor, Université d'Abomey-Calavi, Benin.

Bamory Kamagaté, Full Professor, Université Nangui Abrogoua, Côte d'Ivoire.

======

Reviewers:

Name, highest title (Associate or Full Prof), institution or University, Country

======

JURY

Members of the Jury's names	highest title (Associate or Full Prof, University, country)	position in the Jury

Dedication

I dedicate this work to The Almighty, the self-sufficient, the most honorable, and to my late father and my mother.

Everything should be made as simple as possible, but not simpler.

Albert Einstein

Acknowledgment

This PhD work is realized in the framework of the West African Science Service Center on Climate Change and Adapted Land use (WASCAL) and funded by the German Ministry of Education and Research (BMBF) in collaboration with the Benin Ministry of Higher Education and Scientific Research (MESRS).

At the end of this PhD Thesis, I would like to express my gratitude to many people who have contributed to its development in a direct or indirect way. I am delighted to express my profound gratitude to my supervisors: Prof. Yalo Nicaise (Universite d'Abomey Calavi, Benin), Prof. Bamory Kamagaté (Université Nangui Abrogoua, Côte d'Ivoire), and my Advisors: M. Luc Seguis (IRD, UMR Hydrosciences), Prof. SAVANE Issiaka (Université Nangui Abrogoua, Côte d'Ivoire), Dr. Ismaïla Ouattara (Université de Man, Côte d'Ivoire), Dr. Kouassi Kouamé Auguste (Université Nangui Abrogoua, Côte d'Ivoire), Dr. Ouedraogo Moussa (Université de Man, Côte d'Ivoire). I cannot express only with words about all that you did for me to achieve this study.

I want also to thank Mme Saramatou Bahire, M. Diakaria Koné, and all the Members from water resources direction of ONEP (Office National de l'Eau Potable) institution where I did my internship in order to collect piezometric data.

I also appreciate the management of the WASCAL Doctoral Graduate study of Université d'Abomey Calavi and all my colleagues of WASCAL Graduate School for their support in diverse ways, especially my Akan brother from Ghana, Dr. Isaac Larbi and Adama Gassama Jallow.

I would like to thank Dr. Kouakou Koffi Amoulaye, Dr. Danuma, Dr. Soro Dimitri, Dr. Alima Dajuma, Dr. Lereyaha Coulibaly, Diallo Seydou, Didi Sacre Regis, Salomon, Odou Thiery, Ibrahim Sanogo and Djim Mouhamadou Lamine.

Finally, gratitude goes to my family and friends, especially to my late father who passed away during the accomplishment of this work and my dear mother for her Douas all the time, my siblings and Tenindja Soro, for their support, prayers and encouragement when away from home, and throughout the study.

Abstract

This study focuses on the influence of climate and land use/land cover (LULC) change on groundwater recharge over the Continental Terminal catchment (Abidjan aquifer) in the context of urbanization and population growth. The specific objectives of the study were to, (i) assess groundwater recharge regarding the changes in LULC of the Continental Terminal catchment using water balance method, (ii) assess the impact of the Representative Concentration Pathways (RCP4.5) climate change scenario on rainfall, temperature, and groundwater recharge in the near future 2020-2049, and (iii) model and analyze locally impact of climate and LULC change on groundwater balance using MODFLOW model by assessing the interaction between groundwater and surface water. Many data have been used for the study such as, piezometric level data, observations (stations and CHIRPS) climate data, Landsat images (1990, 2000 and 2016) for LULC mapping, Regional Climate Models (RCMs) under RCP4.5 scenario for historical (1982-2011) and near future (2020-2049) period for climate change impact assessment. The results show an increased in built-up and agricultural land, while the forest and shrub areas declined, with water body remaining unchanged over the period 1990-2016. The decline in forest could be imputed to the demographic and socio-economic growth as expressed by the expansion in agriculture and urbanization. Groundwater recharge represents 34%, 21% and 26% of rainfall respectively in 1990, 2000, and 2016. While the runoff during these same years is respectively 20%, 46% and 14% of rainfall total. The ensemble mean projected a warmer climate in the near future (2020-2049) with a 1.73^{o}C increase in mean annual temperature and a 37.32% increase in mean annual rainfall relative to the baseline (1982-2011) period. Groundwater recharge projection was found more depending on climate change parameter, especially changes in rainfall and temperature. Groundwater and lagoon Aghien intaraction show that Aghien lagoon drains the aquifer to 1.10^4 m^3 /day in certain areas where the aquifer is deeper, the lagoon supplies the groundwater by drainage up to $41.10^3 m^3$/day and all the scenarios made to assess future groundwater water level (2060) reveal a drop of hydraulic head and this could impact surface water reserve.

Key words: Land use and land cover change, climate change, MODFLOW, recharge, Ground Water-Surface Water interaction, Continental Terminal, Côte d'Ivoire

Synthèse de la Thèse

Résumé

Cette étude a mis en relief l'influence du changement climatique et de la variation de l'occupation du sol sur la recharge en eau souterraine de la nappe du Continental Terminal (Côte d'Ivoire) dans un contexte d'urbanisation et d'accroissement rapide de la population. Les objectifs assignés à cette étude sont au nombre de trois (3). D'abord, il s'est agi d'estimer la recharge en eau souterraine tout en considérant la variation de l'occupation et de l'utilisation du sol sur la zone d'étude par la méthode couplée du bilan hydrologique et du SCS runoff Curve Number (SCS-CN). Ensuite, l'impact du scénario Representative Concentration Pathways 4.5 (RCP 4.5) sur les précipitations, les températures et la recharge à l'horizon 2022-2049 a été estimé. Pour terminer, nous avons modélisé, de façon locale, l'impact du changement climatique sur l'interaction entre eaux souterraines et le plan d'eau lagunaire d'Aghien à l'aide du logiciel MODFLOW. Les résultats montrent une augmentation des zones habitables et des terres cultivées au détriment des zones forestières et des zones déboisées. Par ailleurs, la superficie des plans d'eau reste inchangée entre 1990 et 2016. La régression progressive de la forêt s'expliquerait par l'accroissement de la démographie et des activités socio-économiques. La recharge en eau souterraine représente 34 %, 21 % et 26 % de la pluviométrie respectivement en 1990, 2000, et 2016. Alors que la part du ruissèlement pendant ces mêmes années est respectivement de 20 %, 46 % et 14 % de la pluviométrie totale. Dans l'ensemble, les modèles climatiques utilisés prévoiraient un climat plus chaud à l'avenir (2020-2049) avec une augmentation de 1,73 °C de la température moyenne annuelle et une augmentation des précipitations moyennes annuelles de 37,32 % par rapport à la période de référence (1982-2011). Il ressort également de cette étude que la recharge prévue dans le futur serait influencée par le changement des paramètres climatiques tels que la température et la précipitation. L'interaction entre l'eau souterraine et la lagune Aghien révèle à partir du bilan global que la lagune Aghien draine la nappe à hauteur de 1.10^4 m^3/j. Dans certaines zones ou la nappe est plus profonde, la lagune alimente la nappe par drainance à hauteur de 41.10^3 m^3/j. Tous les scenarios mis en place pour comprendre la dynamique de la nappe d'eau souterraine dans le future (2060) prédisent une baisse du niveau piézométrique ce qui pourrait impacter quantitativement la réserve en eau de surface de la lagune Aghien.

Mots-clés: Occupation du sol, changement climatique, MODFLOW, recharge, interaction lagune-aquifère, Continental Terminal, Côte d'Ivoire

Introduction

Partout dans le monde, les eaux souterraines jouent un rôle très important dans le processus d'approvisionnement en eau potable des populations, les usages domestiques, l'agriculture, le fonctionnement des industries et autres. Cela les met à rude épreuve et favorise la surexploitation et d'autres formes de pratiques qui ont un impact sur cette ressource. Cette pression est mieux aperçue dans les grandes agglomérations avec le développement de l'agriculture urbaine et des activités industrielles (FAO, 2011)

Ainsi, en Côte d'Ivoire précisément dans le district d'Abidjan, la nappe du Continental Terminal reste la seule source d'approvisionnement en eau potable de la population depuis l'indépendance. Depuis lors, le taux de croissance de la population s'est considérablement accru atteignant 2,6 % (INS, 2014). Cela implique une surexploitation de la ressource due à une forte demande en eau. Ajouté à cela la diminution des précipitations dues aux effets perceptibles de la variabilité climatique émanant du phénomène de changement climatique (Mahé *et al*, 2001; Bigot *et al.*, 2005; Goula *et al.*, 2006; Kouassi *et al.*, 2007; Kouakou *et al.*, 2007; Kanohin *et al.*, 2009; Kouakou, 2011; Tanina *et al.*, 2011). En effet, selon les projections sur la population de la grande métropole d'Abidjan, le taux de croissance devrait atteindre les 13,06 % à l'horizon 2025 (WPP, 2017). Le problème de la satisfaction des besoins en eau de cette métropole dans le futur pourrait se poser avec acuité. Dans un souci d'anticipation, le regard est tourné vers les eaux de surface d'où celle de la lagune Aghien. C'est dans ce cadre qu'un vaste projet a été entrepris depuis 2014, entre les laboratoires GéoSciences et Environnement de l'Université Nangui Abrogoua, HydroSciences Montpellier et le LMI Picass'Eau, dans l'objectif d'étudier la probable utilisation de l'eau de cette lagune pour l'alimentation en eau de la ville d'Abidjan. Plusieurs axes sont à l'étude faisant l'objet de 3 thèses, ils concernent :

- l'estimation des apports liquides et solides des tributaires vers la lagune,
- l'impact de l'urbanisation sur la quantité de l'eau sur les bassins versants des tributaires de la lagune,
- la qualité des eaux des tributaires et des eaux de la lagune Aghien.

Notre travail, quant à lui s'est intéressé aux relations nappe-rivière à travers la modélisation des écoulements des nappes souterraines vers la lagune. Le but est d'estimer la masse d'eau souterraine qui alimente la lagune Aghien. Cette part du souterrain ajoutée à celle des rivières permettra de faire un état des lieux plus ou moins exhaustif quant à l'alimentation de la population urbaine à travers les eaux de ce réservoir naturel qu'est la lagune Aghien.

A ce sujet, la connaissance de la composante quantité des apports de l'eau souterraine à l'eau de surface pourrait-elle contribuer à une maitrise de la gestion future de l'eau destinée à la population d'Abidjan ?

L'effet néfaste du changement climatiques et l'urbanisation galopante pourrait-elle nuire à la recharge de la nappe du Continental Terminal ?

Autant de questions que nous essayerons de répondre dans le cadre ce travail de thèse.

L'objectif assigné à cette étude est d'étudier la dynamique de l'eau souterraine et d'évaluer l'impact du changement climatique et de l'urbanisation sur la recharge afin de satisfaire la demande en eau potable de la population. De façon spécifique, il s'est agi pour nous de :

- estimer la recharge en eau souterraine tout en considérant la variation de l'occupation du sol sur la zone d'étude,
- examiner l'impact du scénario *Representative Concentration Pathways* (RCP4.5) sur les précipitations, les températures à l'horizon 2020-2049
- modéliser et analyser de façon locale l'impact du changement climatique et de l'urbanisation sur le flux hydrique des eaux souterraines (interaction eau souterraine et eau de surface).

Zone d'étude

La zone d'étude est le bassin sédimentaire du Continental Terminal en Côte d'Ivoire. Elle est située dans le Sud-e de la Côte d'Ivoire, entre les latitudes 5°10 et 5°38 Nord et les longitudes 3°45 et 4°21 Ouest (Fig.1). C'est une zone couvrant une superficie d'environ 1160 km² située dans le district d'Abidjan, avec une population estimée à 4 707 404 habitants, soit environ 38,5 % de la population de la Côte d'Ivoire (INS, 2014).

La région est influencée par un climat équatorial de transition et par quatre saisons (Tapsoba, 1995; Tastet, 1979): une longue saison des pluies de mars à juin suivie d'une courte saison sèche de juillet à août; une petite saison des pluies de septembre à fin novembre et une longue saison sèche de novembre à février. La température moyenne mensuelle est de 27 ° C. On observe une précipitation moyenne annuelle enregistrée à la station pluviométrique d'Abidjan allant de 1822 mm à 1611mm entre de 1960 à 2016. La zone d'étude est caractérisée par un relief moyennement assez faible, avec une altitude comprise entre -16 m et 146 m et il est principalement dominé par des terres cultivées, et des forêts.

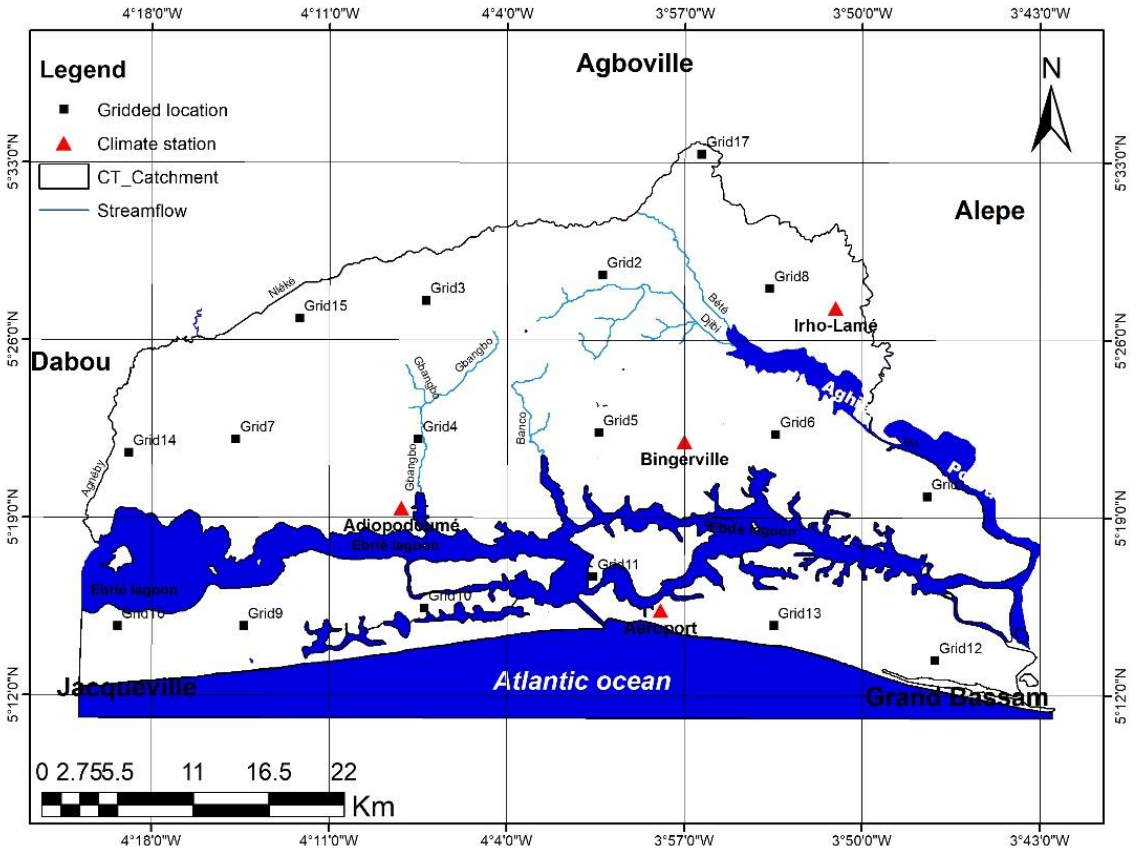

Fig. 1: Bassin sédimentaire du continental terminal subdivisée en grille

Matériel et méthodes

La présente étude a, dans un premier temps, porté sur la mise envidence de l'influence de la variabilité du climat et du changement de l'occupation du sol sur la recharge d'eau souterraine au niveau du Continental Terminal a partie de la méthode du bilan hydrologique. Cela a nécissité l'aquisition d'image landsat des années 1990, 2000 et 2016 afin d'avoir une idée reelle de la dynamique de l'occupation du sol qui pourrait impacter la rechage. Pour ce faire, ces images ont été classifiées utilisant l'algorithme du maximum de vraisemblance. La précision de la classification globale est de 98,29 %, 99,90 % et 93,80 % respectivement pour les images des années 1990, 2000, et 2016 sur la base de la matrice d'erreur. Le ruissellement quant à lui a été déterminé par la méthode *Soil Conservation Service Curve Number* (SCS-CN)qui nécessite la carte d'occupation des sols et la carte du type de sol converti en groupe de sol hydrologique déterminé a parti de la capacité d'infiltration du sol. Ceux-ci seront superposés dans le modèle afin de déterminer une valeur unique de curve number pour chaque polygone. Le modèle SCN-CN utilise une méthode empirique basée sur le bilan hydrologique. La recharge, en définitive, a été déterminée en se basant sur l'équation du bilan hydrologique. Ensuite, l'impact du changement climatique sur la température moyenne annuelle, la pluviométrie annuelle sur la zone d'étude sur la période 2022-2049 a été évalué afin

d'appréhender l'évolution future du climat sur la zone d'etude et d'estimer les recharges futures en eau souterraine. A cet effet, des modeles climatiques ont eté appliqués sur la base de données climatiques observées (station et satellitaire). Les stations au sol concernent celles de Bingerville, de l'aéroport d'Abidjan, de la Mé et d'Adiopodoumé. Les données satellitaires proviennent du modèle climatique régional du *Weather Research and Forecasting* (WRF) avec une résolution de 12 km.

Le logiciel MODFLOW a été utilisé pour simuler et prédire les flux hydrodynamiques des eaux souterraines tout en considérant la variabilité climatique et la dynamique de l'occupation du sol. Les données nécessaires pour la mise en place du modèle sont : les données géologique et hydrogéologique, les données climatique, la recharge de la nappe, les données hydrodynamiques, les données de suivi piézométriques, les données d'exploitation de forage, les données topographique, les données du toit du socle et le modèle numérique de terrain avec 20 m de résolution. Des mesures piézométriques ont été effectuées sur chacun des 55 piézomètres présents sur la zone de modélisation dont le choix de la période d'observation a été porté sur la piézométrie de Mars 2017 où la plupart des piézomètres situés autour de la lagune Aghien ont été suivis.

Certaines des données ci-dessus mentionnées ont permis d'élaborer le modèle conceptuel et de définir les conditions aux limites. On a ensuite procédé au calage en régime permanent qui consiste à minimiser la différence entre la piézométrie mesurée et la piézométrie calculée par ajustement des données d'entrée jusqu'à ce que le modèle reproduise le fonctionnement hydrodynamique de l'ensemble de la nappe d'Abidjan avec un niveau de précision acceptable. Lélément qui permet d'apprécier un tel calage est la racine carrée de la moyenne des écarts normalisés (NRMSE) en pourcentage. Le module PEST de Visual Modflow a permis de calculer les meilleures valeurs des différents paramètres à caler. Par la suite, nous avons procédé à la validation du modèle calé afin qu'il puisse être utilisé pour des simulations. Elle a été effectuée sur des données qui n'ont pas servi au calage, de façon à tester l'aptitude du modèle à des différents scénarii de simulation.Tout ceci est résumé dans la Figure 2 représentée par le diagramme ci-dessous.

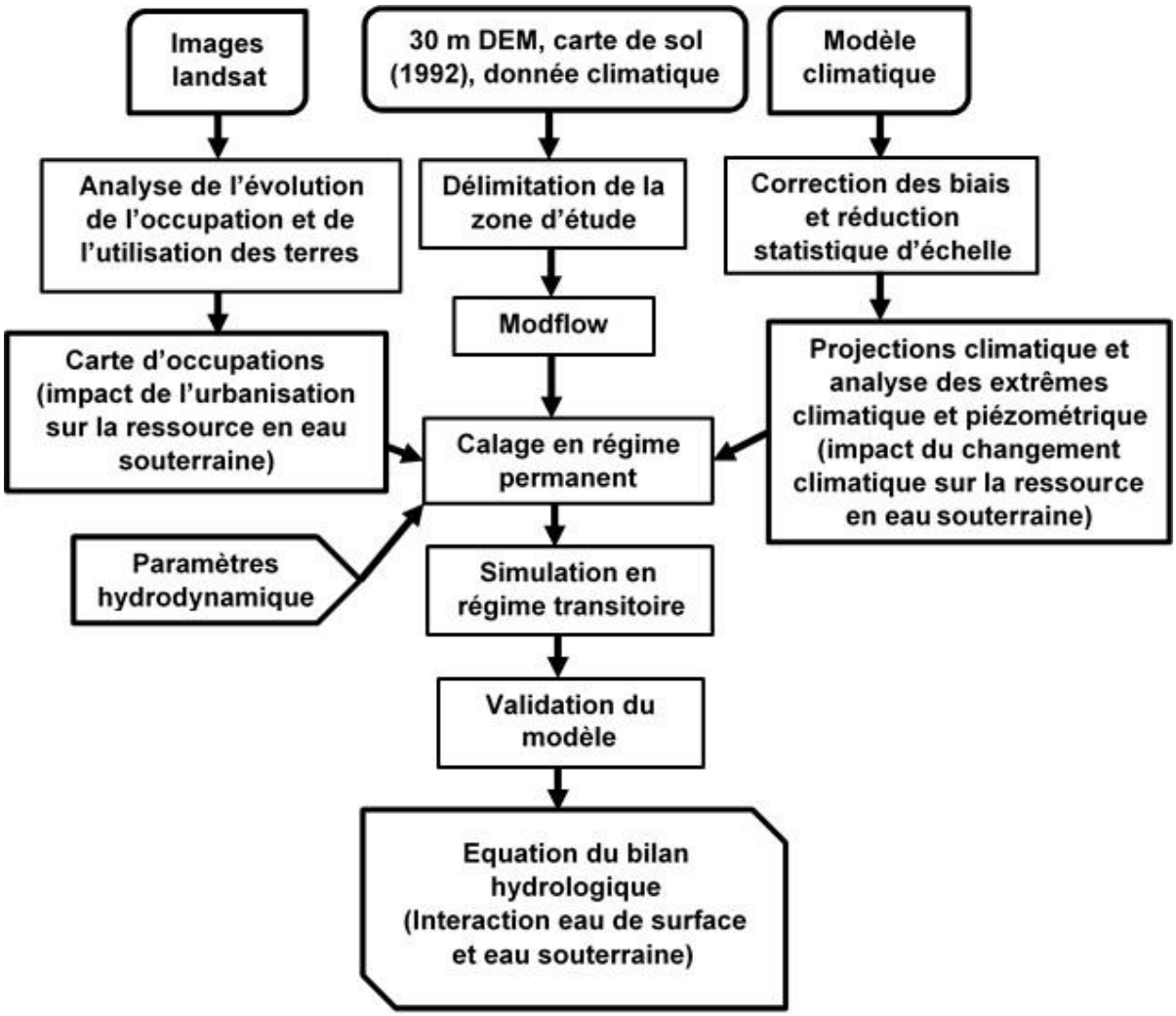

Fig. 2: Diagramme synthétique des travaux de recherche

Résultats et discussion

Les différentes méthodes de traitement appliquées aux données climatiques, hydrologiques, hydrogéologiques et cartographiques ont permis d'obtenir les résultats présentés dans cette section.

La mise en évidence de la dynamique de l'occupation revèle une classification dont la précision globale est respectivement de 98,29 %, 99,90 % et 93,80 % pour les images de 1990, 2000 et 2016. Ces images classifiées indiquent une avancée des zones habitables (39 %) et des terres cultivées (5 %) au détriment des zones forestières de 1990 à 2016. La régression progressive de la forêt s'expliquerait par l'accroissement de la démographie et des activités socio-économiques. La recharge en eau souterraine représente 34 %, 21 % et 26 % de la pluviométrie respectivement en 1990, 2000, et 2016. Alors que la part du ruissèlement pendant ces mêmes années est respectivement de 20 %, 46 % et 14 % de la pluviométrie totale. .. Les résultats liés à l'impact du changement climatique laissent présager un climat plus chaud à l'horizon 2049, avec une augmentation de 1,73 °C de la température annuelle moyenne et une augmentation de

37,32 % de la pluviométrie annuelle moyenne par rapport à la période de référence (1981-2010). La recharge moyenne annuelle future a été déterminée à partir de la température et de la précipitation moyenne annuelle. Cette recharge est en hausse et est comprise entre 482,93 et 1115,78 mm par an. Il faut noter que cette recharge pourrait être revue a la baisse face une urbanisation effrainée et galopante.

Les indicateurs de performance de la modélisation à l'aide du programme informatique traduisent un calage de bonne qualité. Aussi, ces résultats apparaissent tout à fait satisfaisants au regard de la variabilité spatiale des niveaux piézométriques mesurés et des niveaux piézométriques simulés. De plus, l'allure générale de la piézométrie observée est bien reproduite par le modèle, ce qui permet d'obtenir une bonne représentation des directions d'écoulement générales de l'aquifère.

Les scenarios mis en place pour simuler le niveau piézométrique des eaux souterraines révèlent une baisse de la piézométrie qui pourrait avoir un réel impact sur la réserve d'eau de surface en l'occurrence celle de la lagune. Ainsi, le scénario basé sur l'augmentation du débit de pompage révèle une diminution du niveau de l'eau souterraine de l'ordre de 0,1 à 2,8 m autour de la lagune à mesure que l'on augmente le débit. On constate également l'apparition de cône de dépression autour des forages. Cependant, le scenario relatif à la réduction de la recharge de 15 % et 30 % révèlent une diminution plus prononcée du niveau piézométrique allant de 0,2 à 3 m autour de la lagune par rapport au premier scenario. Enfin, la combinaison des deux scenarios met en relief la chute du niveau piézométrique de 0,5 à 4,5 m autour de la lagune avec l'apparition d'un cône de dépression au niveau des forages.

Tous les résultats ci-dessus mentionnés concourent à prédire que la contribution de la réserve d'eau de surface pour satisfaire les besions en eau potable serait un atout mais par à long terme.

Conclusion

En définitive, nous retenons que les paramètres qui ont servi à la réalisation de cette étude à savoir la précipitation, la température, l'occupation du sol, la recharge en eau souterraine, le niveau piézométrique ont fait l'objet d'une analyse minutieuse et il en ressort un développement des zones habitables (39 %) et des terres cultivées (5 %) au détriment des zones forestières, ce qui favoriserait une imperméabilisation des sols, et donc une diminution de l'infiltration des eaux de pluie. Ajouté à cela, il est observé que les projections futures (2020-2049) envisageraient de fortes précipitations. Cela pourrait engendrer de fortess température induisant une augmentation de l'évaporation des eaux de surfaces. Les éléments mentionnés caractérisentl'évidence des effets du changement climatique.

Pour ce qui est de la réserve d'eau souterraine, les scenarios relatifs à l'augmentation du débit de pompage, la réduction de la recharge de 15 % et 30 % révèleraient la chute du niveau piézométrique à l'horizon 2060 allant de 0,1 m à 4 m affectant ainsi l'interaction avec la lagune Aghien.

La finalité de cette étude concoure à estimer l'apport d'eau provenant du souterrain vers la lagune Aghien afin d'avoir une idée plus précise sur le bilan hydrologique de celle-ci. Les projections issues des modèles climatiques et la dynamique de l'occupation des sols peuvent servir de cadre aux gestionnaires de l'eau et aux décideurs pour élaborer des stratégies de planification et d'adaptation des ressources en eau du district autonome d'Abidjan. L'étude recommande à cet effet :

(i) le désengorgement de la ville d'Abidjan en créant des emplois dans les autres villes de Côte d'Ivoire afin de freiner cette urbanisation qui ne cesse de s'amplifier au niveau de la ville d'Abidjan.

(ii) le reboisement à l'échelle locale et la protection des ressources en eau en se conformant aux dispositions prescrites dans le code de l'eau.

(iii) l'intégration de l'adaptation au changement climatique dans tout projet de développement du district autonnome d'Abidjan.

Table of contents

List of Acronyms

AET: Actual EvapoTranspiration

AMC: Antecedent Moisture Condition

AWC: Available Water Content

BMBF: Federal Ministry of Education and Research

BNETD: Technical Research and Planning Institution for Development,

CHIRPS: Climate Hazards Group Infrared Precipitation with Station data

CORDEX: Coordinated Regional Downscaling Experiment

CTT: Cartography and Remote Sensing Center

DEM: Digital Elevation Model

EMS: Earth System Mode

EROS: Earth Resources Observation and Science

ETCCDMI: Expert Team on Climate Change Detection Monitoring Indices

FAO: Food and Agriculture Organization

Feflow: Finite Element subsurface FLOW system

GCM: Global Circulation Models

GDP: Gross domestic product

GFDL-ESM2M: General Fluid Dynamics Laboratory Earth System Model

GHG: Green House Gas

GIS: Geographic Information System

GLOVIS: Global Visualization Viewer

HadGEM: Hadley Centre Global Environment Model

HPP-GMS: Hydrology Pre/Post Processor-Groundwater Modelling System

INS: Institut National de la Statistique

IPCC: Intergovernmental Panel on Climate Change

LULC: Land Use Land Cover

MESRS: Ministry of Higher Education and Scientific Research

MODFLOW: Modular Three-Dimensional Finite-Difference Groundwater Flow Model

NCEP: National Center for Environmental prediction

NEH: National Engineering Handbook

NES: Nash Sutcliffe Efficiency

NRMSE: Normalized Root Mean Square Error

ONEP: National water agency (NWA)

PBIAS: Percent Bias

PET: Potential Evapotranspiration

Phd: Doctor of Philosophy

R^2: coefficient of determination

RCM: Regional Climate Model

RCP: Representative Concentration Pathways

REMP: Rufiji Enironment Management Project

RMS: root mean square

RMSE: Root Mean Square Error

SCS-CN: Soil Conservation Service Curve Num-ber

SDSM-DC: Statistical DownScaling Model -Decision Centric

SODEXAM: Aeronautical and Meteorological Operations and Development center

SOGREAH: Société Grenobloise d'Etudes et d'Aménagements Hydrauliques

UCSB: University of California, Santa Barbara

UNEP: United Nations Environment Programme

USDA: United States Department of Agriculture

USGS: United States geology survey

UTM: Universal Transverse Mercator

WASCAL: West Africa Science Service Center on Climate Change and Adapted Landuse

WGS: World Geodetic System

WPP: World Population Prospects

WRF: Weather Research and Forecasting

WRI: Water Resources Institute

List of figures

List of tables

Chapter 1: General Introduction

In this chapter, we will present the context of the study, problem statement, objectives of the study and literature review which is focus on groundwater recharge related to climate change, land use and land cover change, urbanization and groundwater-surface water interaction.

1.1 Context and problem statement

Without water, there would be no life on earth. It is the most important resources on which all human activities such as agriculture, irrigation, industry, fishery, household, hydropower generation, transportation, and ecosystems are related, but this resources is facing too many issues nowadays. Water is a key point of discussion around the world. The International Dialogue on Water and Climate (2004) noted that water stress will increase significantly in those regions that are already relatively dry such as sub-Saharan Africa, a region which is in a state of high water-related criticality susceptibility (WRI, UNEP 1998).

Climate change has become a global challenge which needs to be addressed. Scientistic research has revealed significant differences in whether pattern on the planet as well as the scale and the speed in which they occur (IPCC 2007). A report of the Intergovernmental Panel on Climate Change has revealed that, based on temperature observations over the past 133 years, (1880 to 2012), the global mean surface temperature has increased by 0.85 °C, along with significant regional differences. The rate of temperature increase has quickened significantly over the past 62 years of observations; the rate of temperature increase from 1951 to 2012 was 0.12°C per ten years. Besides, rapid population growth and its demand has become the challenge of this last century (Txomin *et al*., 2013). There is also an increase in urbanization around the world. In 1990, only 10% of population lived in the towns but today, 55% of the world's population lives in urban areas, a proportion that is expected to increase to 68% by 2050. (UNDESA 2018). Urbanization, which results in the conversion of natural vegetation, forest, agricultural land, wetlands and natural drainages to built-up environments and construction (Danumah 2016) impacts on water resource therefore urbanization may reduce infiltration and hence direct groundwater recharge through impermeabilization of the land surface by roads, buildings, driveways, and parking lots (Foster, Morris and Chilton, 1999; Lerner, 2002; Meyer, 2005)

Groundwater which represent approximately 2/3 of world fresh water resources is the major source of water across much of the world, particularly in rural areas in arid and semi-arid regions (Banton and Bangoy, 1997). Groundwater plays a key role in sustaining many streams, lakes, wetlands, and the entre ecological system (Kollet and Maxwell, 2008). It occurs and

exists beneath the subsurface and the water table in the soils and geologic formations that are fully saturated (Freeze and Cherry, 1999). Groundwater is one of the most essential natural resources of the world. Many major cities and small towns in the world depend on groundwater resource for water supplies, mainly because of its wealth, stable quality and also because it is economically exploitable (Williams 1999). But, the overexploitation of groundwater in the last two decades has led to serious deterioration in the quantity and quality of groundwater resources around the world. In fact, according to (UNEP 2003), about 1,100 million people do not have access to drinking water, and contaminated water is the cause of 5 million deaths every year, with the majority of these in sub-Saharan Africa.

In Cote d'Ivoire, precisely in Abidjan, groundwater supply management is becoming a challenge that the city is facing. In fact, Abidjan's city represent more than 70% of production and consumption of drinking water in Côte d'Ivoire. The Continental aquifer is the only source of drinking water supply in the Abidjan since the independence. This unconfined groundwater plays an important role by garanting water for Abidjan cities population. It is exploited by 77 boreholes and the extraction yield is between 150 and 250 m^3/hour. Daily exploitation is about 312 000 m^3 /day, howevere 461 000 m^3 /day is needed because of the increase in water demand. Therefore, there is lack of water deficit of about 150 000 m^3 /day currently faced by the area. Despite the fact that water resources and hydraulic infrastructure are available, groundwater is facing many issues. Since 1970, decrease of rainfall has led to lack of water in dry season, and there is overexploitation of groundwater due to increase in urbanization. Abidjan aquifer, whose average reserve volume is estimated at 12 500 million m^3 face a loss of 217 million m^3 due to the combined effects of the rainfall decline and the extension of urbanization which results in the impermeabilization of water into the soil leading to low infiltration for groundwater recharge. In fact only 14% of rainfall reach the groundwater due land cover (Sogreah, 1996).

This could not allow this resource to satisfy water demand of Abidjan's city in the future whose population growth rate could reach 13.6% (WPP 2017). However, in concern of anticipation, we think to use surface water and. In this case Aghien lagoon is the one which is involve. Many study have been undertake as part of the project initiated by GéoSciences and Environnement laboratory of Nangui Abrogoua University, HydroSciences Montpellier and LMI Picass'Eau, to study the expected use of Aghien lagoon to supply water such as assess liquid and solid contributions of the tributaries towards Aghien lagoon, impact of urbanization on water quantity in Aghien lagoon tributary watershed and Aghien lagoon and tributaries water quality.
Our work in this thesis, focused on surface water and groundwater interaction in order to estimate groundwater quantity that reaches the lagoon. This part of the groundwater add to the

lagoon reserve will make more or less exhaustive water quantity to supply population from this lagoon

The aim of this study is to evaluate the dynamic of groundwater and assess the influence of climate and land use/land cover change (urbanization) on groundwater recharge in order to satisfy water demand of the population.

1.2 State of arts

1.2.1 Hydrologic cycle

The hydrologic cycle describes the continuous movement of water above, on, and below the surface of the Earth. The water on the Earth's surface (surface water), occurs as streams, lakes, and wetlands, as well as bays and oceans. Surface water also includes the solid forms of water snow and ice. The water below the surface of the Earth primarily is ground water, but it also includes soil water (Schelesinger 1991)

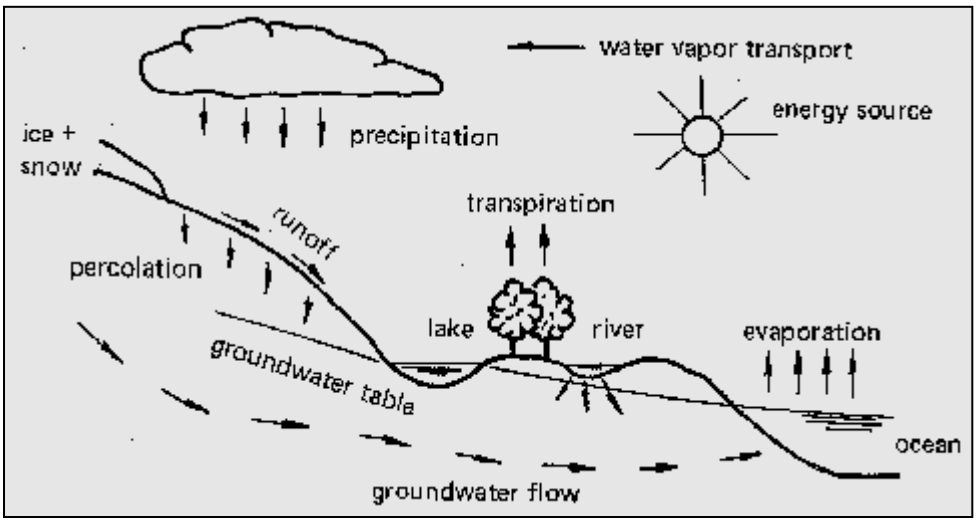

Figure 1: hydrologic cycle

However, for understanding hydrologic processes and managing water resources, the hydrologic cycle needs to be viewed at a wide range of scales and as having a great deal of variability in time and space. Precipitation, which is the source of virtually all freshwater in the hydrologic cycle, falls nearly everywhere, but its distribution is highly variable. Similarly, evaporation and transpiration return water to the atmosphere nearly everywhere, but evaporation and transpiration rates vary considerably according to climatic conditions.

1.2.2 Groundwater recharge

Groundwater recharge is the amount of water percolating and entering in the saturated zone and is closely connected to evapotranspiration and precipitation. In most cases, recharge will be used to define the amount of water reaching an aquifer, or in other words, the storage change

in an aquifer over a specific time. The latter definition actually contains all water flowing into an aquifer, hence not only vertical flow but also horizontal flow from inter-connected aquifers (Ahmed et al. 2007).

When evaluating the recharge in connection with the available water resource, two terms are used: actual recharge and potential recharge. Actual recharge is the amount of water reaching the aquifer under natural conditions. During wet periods, the water table may rise so that there is no available storage left in the aquifer and this causes the aquifer to be completely saturated. During this period the actual recharge will be hampered by the fact that the aquifer is full. The recharge that would have entered the aquifer, if storage had been available, is referred to as rejected recharge.

The term potential recharge is defined as the sum of actual and rejected recharge, or in other words, the excess of rainfall over runoff and actual evapotranspiration. The potential recharge will be limited by both the soil physical parameters and the actual rainfall in the area, but not by the location of the groundwater table. This means that areas with less rainfall will have a smaller potential recharge (Alley, Reilly and Franke, 1999). Although it is commonly stated, that groundwater recharge is reduced with urbanization because of the increase in impervious cover, the reverse is the more common condition urbanization increases ground water recharge. In some cases, groundwater dependent ecosystems are augmented by increased urban recharge (Schueler, 1994; Drouin-Brisebois, 2002; Asquith and Roussel, 2007; Sharp *et al.*, 2009) all indicate little difference in stream baseflows between urbanized and undeveloped watersheds

Recharge is most often determined by looking at the water balance for an area and evaluating the storage change over a specific period. The use of mathematical models like MODFLOW is suitable for evaluating storage changes in groundwater aquifers (Langevin and Guo, 2006). Groundwater recharge is normally computed using the water balance equation, as shown in equation (1).

$$R = P - Q - ET - S \qquad \text{Equation 1}$$

Where R is the groundwater recharge,

P is the rainfall,

Q is the surface runoff, and

S is the change in soil water storage.

All terms of the water balance equation should have the same unit, usually given as a rate (unit depth per unit time) such as mm/month or mm/year. It should be noted that S approaches zero if calculations are made on an annual basis (Fathi et al., 2013).

1.2.3 Land use/land cover change

Land cover is defined as the attributes of the earth's surface and immediate subsurface, including biota, soil, topography, surface and ground water, and human structures (Lambin, Geist and Lepers, 2003). Land use is the human employment of the land cover type (Skole 1994). Natural scientists define land use in terms of human activities such as agriculture, forestry and building construction that modify land surface processes including biogeochemistry, hydrology and biodiversity. Social scientists and land managers characterize land use more broadly to include the social and economic purposes and contexts within which lands are managed (or left unmanaged), such as subsistence versus commercial agriculture, commercial versus residential, or private versus. public land (Ellis and Pontius, 2007).

Several factors natural and anthropogenic such as urbanization, goods, population growth and industrialization affect land and climate. Thus both have been recognized as a driver of the long-term change in land which automatically disturb climate. Therefore, the land use/land cover (LULC) dynamics is an important component to better understand the land patterns induced by human activities and therefore to understand its implications in climate change (Lambin et al. 2001). Also, the understanding of the interactions between land cover and land-use in their spatial and temporal appearances is fundamental to the comprehension of land-use and land cover change (Jansen and Di Gregorio, 2002). The potential for urbanization processes to have an impact on groundwater is a function both of the aquifer's vulnerability to pollution and its susceptibility to the consequences of excessive abstraction. Hydrogeological environments are neither equally vulnerable to pollution (Morris et al. 2003) nor equally susceptible to the consequences of abstraction (Foster, Lawrence and Morris, 1998).

Understanding urban recharge and the effects of urbanization on groundwater recharge is a complex problem. Alterations of the landscape may either increase or decrease groundwater recharge rates. Urbanization may reduce infiltration and hence direct groundwater recharge through impermeablization of the land surface by roads, buildings, driveways, and parking lots (Foster, 1999; Lerner 2002; Meyer, 2005). This reduces direct infiltration of excess rainfall, but also tends to lower evapotranspiration and to increase and accelerate surface run-off (Foster, 1999).

1.2.4 Climate change and climate models

1.2.4.1 Climate change

Climate change according to IPCC (2001) is any significant change in a climate variable such as temperature, rainfall or wind over a longer period of time mostly for a decade or longer. The impact of climate change on groundwater becomes a greater concern and although this issue is currently getting a great deal of attention, its effect on groundwater is still underexposed.

Increased variability in precipitation and more extreme weather events caused by climate change can lead to longer periods of droughts and floods, which directly affects availability and dependency on groundwater. In long periods of droughts there is a higher risk of depletion of aquifers, especially in case of small and shallow aquifers. People in water-scarce areas will increasingly depend on groundwater, because of its buffer capacity. At the same time, indirect climate change impacts such as the intensification of human activities and land use changes increase the demand for groundwater. Strategic use of groundwater for global water and food security in a changing climate is becoming more and more important. This is another reason why groundwater should have a more prominent role in climate debates.

1.2.4.2 Climate models

A climate model is a numerical representation of the climate system based on physical, chemical and biological properties of its components, its interactions and feedback processes. Climate models are systems of differential equations based on the basic laws of physics, fluid motion and chemistry. To run a model, scientists divide the planet into a 3-dimensional grid, apply the basic equations, and evaluate the results. The models calculate winds, heat transfer, radiation, relative humidity, and surface hydrology within each grid and evaluate interactions with neighboring points (IPCC 2007).

1.2.4.2.1 Types of climate models

Climate models are often used to make projections for the future based on certain amounts of emissions (Representative Concentration Pathways, RCPs).Among the many different types of climate models, there are:

- Models that simulate the climate of the whole world (Global Climate / Circulation Model (GCM), Earth System Model (ESM)
- Models that simulate the climate only for a part of the world (Regional Climate Model ,RCM)
- Models with more or less complexity/coupling. Some models only include the atmosphere (Atmospheric models), some models couple the ocean and atmosphere (coupled models). Earth System models couple even more systems.

There are more types of models which are used for specific climate research such as cloud studies on exchange of energy, humidity, etc. between the different air layers.

1.2.4.2.2 Emissions scenarios and RCPs

Emission scenarios are descriptions of how greenhouse gas emissions could evolve on various hypotheses. Emission scenarios are translated into Green House Gas (GHG) concentration scenarios. These are used as direct input in climate models.

Currently 4 Representative Concentration Pathways (RCPs) are used. They are named after a possible range of radiative forcing values in the year 2100 relative to pre-industrial values (+2.6, +4.5, +6.0 and +8.5 W/m^2). The RCPs are consistent with a wide range of possible changes in future anthropogenic (i.e.human) GHG emissions, and aim to represent their atmospheric concentrations:

- RCP2.6 corresponds to very ambitous climate policy, which probably leads to a temperature change of about 2 degrees Celcius compared to the pre-industrial era.
- RCP8.5 represents a scenario where few measures are taken and few technological breakthroughs are used.

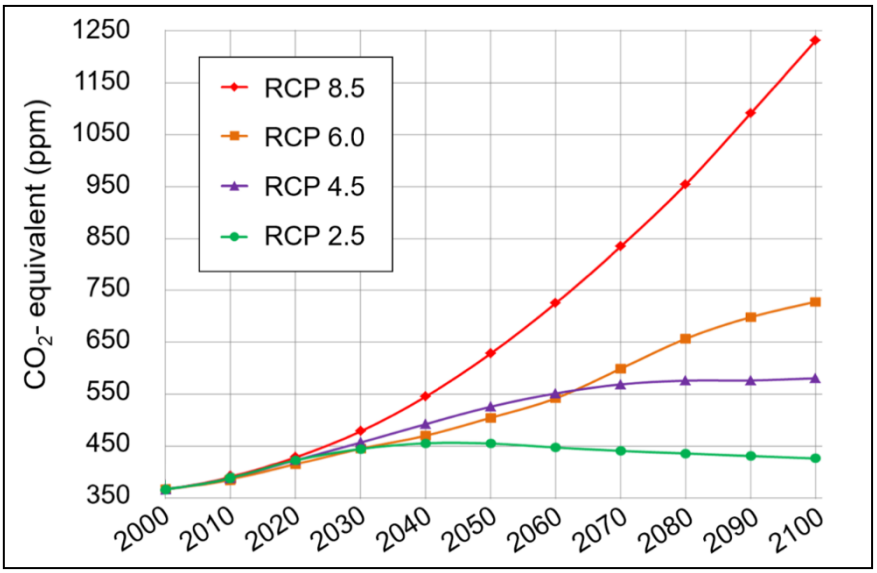

Figure 2: representative concentration pathways (RCPs) from the fifth assessment report by the international panel of climate change (IPCC AR5 Greenhouse gas concentration pathways)

1.2.4.2.3 Global and regional climate models

A Global Climate Model (GCM) is a numerical model representing physical processes in the atmosphere, ocean, cryosphere and land surface simulating the response of the global climate system to increasing GHG concentrations. GCMs depict the climate using a 3D grid over the globe. Different GCMs may simulate quite different responses to the same GHG emission scenarios, simply because of the way certain processes and feedbacks are modelled. Regional Climate Models (RCMs) do a similar job as GCMs, but for a limited area of the Earth. Because they cover a smaller area, RCMs can generally be run more quickly (less computational power required) and at a higher spatial resolution than GCMs.

RCMs use information from GCMs at their boundaries *(*nested regional climate modelling technique*)*. The driving data at the boundaries are derived from GCMs and can include GHG and aerosol forcing. 'Regional' in RCMs refers to regions as large as Europe or a large part

of Europe. Currently many RCMs for Europe have a spatial resolution of about 25 x 25 km but also many simulations at 12 by 12 km are available. RCMs are used as a downscaling technique (from a coarser resolution of global models to higher resolution)

1.2.4.2.4 Climate model bias

Climate model bias are the differences in statistics of the observations for the reference period and the climate model simulation for the same period. It is determined by comparing the climate model output for a past period with observational data for that same period. This is illustrated in the figure below.

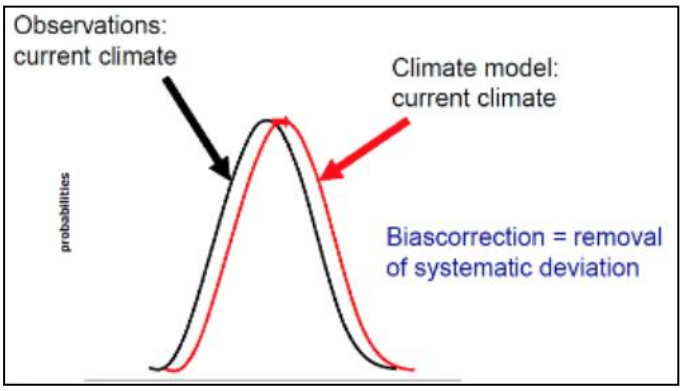

Figure 3: Schematic representation of climate model bias: the systematic difference between model output and observations

1.2.5 Groundwater modelling

Groundwater modelling is a way to represent a system in another form to investigate the response of the system under certain conditions, or to predict the behaviour of the system in the future. Futher, it is a powerful tool for water resources management, groundwater protection and remediation. Decision makers use models to predict the behaviour of a groundwater system prior to implementation of a project or to implement a remediation scheme. Clearly, it is a simple and cheap solution compared to project establishment in reality. It is also a complex task due to the fact that it requires a lot of sensitive data such as recharge rates and its infiltration distribution, difficult boundary conditions, uncertainty of soil properties, the existence of many extraction wells, and spreading of pollutants (Ghodoosipour 2013). Models are most frequently constructed to simulate the response of hydraulic heads of Groundwater to changes inpumpage or recharge (Zhou and Li 2011).

Groundwater models are important in the context of investigating groundwater system response to the external natural and man-made changes, understanding the hydrogeological system characteristics and the interrelationship with the environment,

1.2.6 Surface water and ground water interaction

The interaction of groundwater and surface water involves many physical, chemical and biological processes that take place in a variety of physiographic and climatic setting for many decades studies of the interaction of groundwater and surface water were directed primarily at large alluvial stream and aquifer systems. Interest in the relation of groundwater to surface water has increased in recent years as a result of widespread concerns related to water supply; contamination of ground water, lakes and streams by toxic substances (commonly where not expected) acidification of surface water caused by atmospheric deposition of sulfate an nitrate eutrophication of lakes; loss of wetlands due to developments and others changes in aquatic environments. As a result, studies of the interaction of ground water and surface water have expanded to include many other setting, including headwater streams, lakes wetland and coastal areas. Practically surface water and groundwater interaction is the interplay between water and on beneath of the land surface. This interaction includes the flow of surface water into the groundwater system and the flow of groundwater into the surface water system. The flow of surface water into the groundwater system is defined as infiltration, which includes the flow of water into rock or soil from rainfall at the land surface and the flow of water from a surface stream into its streambed (Wilson and Moore, 1998). This flow may also include the flow of water from a lake or any other surface water body into the ground. Water flowing in the other direction, from groundwater to surface water, includes spring flow and base flow to surface streams and lakes (baseflow, in this context, is the seepage of groundwater into a stream).

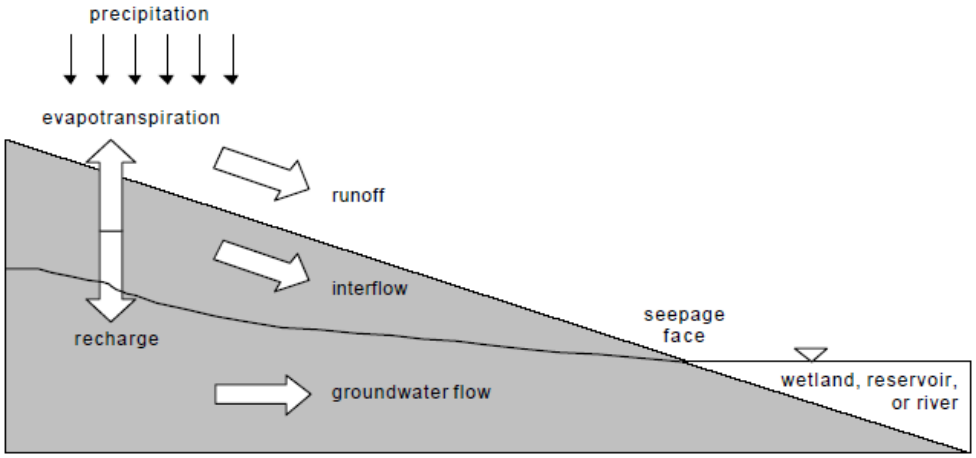

Figure 4: Typical interaction of groundwater and surface water

1.3 Research questions

- What is the influence of urbanization on groundwater recharge from 1990 to 2016?
- How will climate change under RCP4.5 scenario affect rainfall, temperature, piezometric level (recharge) in the future 2020-2049?
- How can we estimate interaction between surface water and ground water?

- Will this resources add to the contribution of groundwater be able to satisfy water demand of Abidjan's population in the future (2050)?

1.4 Thesis objectives

1.4.1 Main objective

The aim of the study was to give an overview of groundwater dynamic in interaction with surface water and assess the influence of climate and land use/land cover change (urbanization) on groundwater recharge in order to satisfy water demand of Abidjan's population.

1.4.2 Specific objectives

The specific objectives of the study are to:

- Assess groundwater recharge under the changing LULC in the Continental Terminal catchment,
- Evaluate the impact of the Representative Concentration Pathways (RCP4.5) climate change scenario on rainfall, temperature and recharge in the near future 2020-2049, and
- Model and analyse locally impact of climate and LULC change on groundwater balance (surface water and groundwater interaction) using the MOFLOW model.

1.5 Novelty

Many studies on water resources have been undertaken on the Abidjan Aquifer in order to better exploit this resources. Despite all those studies, Abidjan's population still suffer from water scarcity. Therefore, the government wanted to use Aghien lagoon water in addition oti groundwater to supply Abidjan's city population. Although some studies have been conducted to estimate water balance of this lagoon. However, the contribution of groundwater have not been consider as one of the water balance components. The novelty in this work is to find out the contribution of groundwater in surface water (Aghien lagoon) in order to improve water balance.

1.6 Scope of the Thesis

This study focusses on groundwater recharge regarding effect of climate and land cover change in the Continental Terminal catchment using groundwater balance method. Climate change projections and the impacts on climate extremes and water resources for the study area were also studied. Groundwater and surface water interaction were assessed by simulated groundwater hydrodynamic

1.7 Expected results and benefits

At the end of this work, the obtained results are listed as follow:

-A better understanding of hydrogeological functioning of groundwater and particularly the interaction with surface water in Abidjan

-Impact assessment of urbanization on groundwater recharge

-Improved prediction of future water availability of the basin in order to help stakeholders in planning for water resources management.

1.8 Outline of the Thesis

This thesis is subdivided into eigth chapters. **Chapter 1** present a general introduction which highlight the study background, the research problem, the literature of previous and related researches and the objectives that guided the study, the novelty, the scope of the study and expected outcomes are discussed. **Chapter 2** provides a detailed description of the study area including location, climate, vegetation, hydrography, geology and the topography. **Chapter 3** describes the various data collected, the tools and methods used in analyzing the data. It also describes Modflow model and input data preparation, the model setup, calibration and validation. **Chapter 4** deals with the results and discussion on Influence of Land Use Land Cover (LULC) on groundwater recharge. In **chapter 5**, Impact of climate change on groundwater recharge are presented. **Chapter 6** talks about groundwater modelling especially surface water and groundwater interaction, finaly and in **chapter 7**, conclusions and recommendations from the study are provided.

Chapter 2: Study area

This chapter discusses about the study location. It presents the study area and give detail on location, topography, climate, vegetation, soil and land use. The water resources, demography, environmental, social and economic activities of the catchment are also described.

2.1 Location

The Continental Terminal Aquifer knows by Abidjan's Aquifers (Figure 5) is part of the sedimentary zone. Located in the south-eastern part of Ivory Coast between Latitudes of 5°10 and 5°38 North and Longitudes of 3°45 and 4°21 West in geographic coordinate system (WGS 84, zone 30 N).

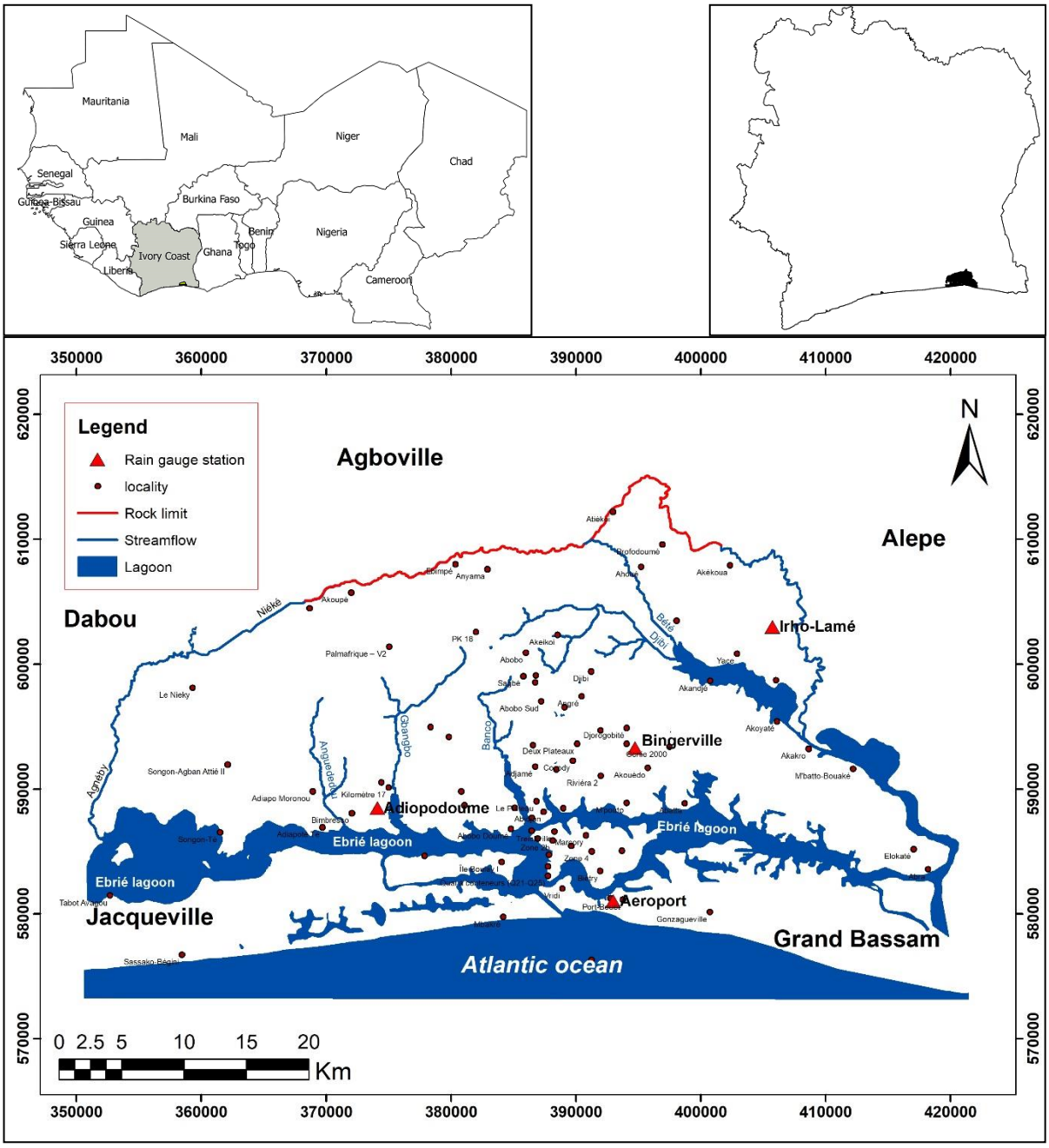

Figure 5: Location of the study area

It has an area of about 1160 km^2 and is located in Abidjan district with an estimated population of 4 707 404 (INS, 2014). The rapid population growth caused an overflow of its administration limit. It is limited in the south by the Atlantic Ocean; in the southwest by Jacqueville; in the west by Dabou; in the north by Agboville, in the south-east by Grand-Bassam and in the east by the Alepe.

2.2 Relief and Geomorphology

The autonomous district of Abidjan is home for three (03) major geomorphological units (Tastet, 1979): (i) Two-level Highlands (40 to 50 m and 100-120 m), represented by the mounds of the Continental Terminal, north of the Ebrié lagoon;(ii) deep valleys ranging from 12 to 40 meters, cutting into the highlands of the Tertiary as evidenced by the Banco and Gbangbo ravines. These valleys act as the drains of the northern part of the city, like the various talwegs. Therefore, any flow goes to all the most saggy part, that is to say towards the lagoon; (iii) Plateaus of medium and low altitude ranging from 8 to 12 m outcrop along the shoreline of the Quaternary. The plains and lagoons in the South are all the more collapsed.

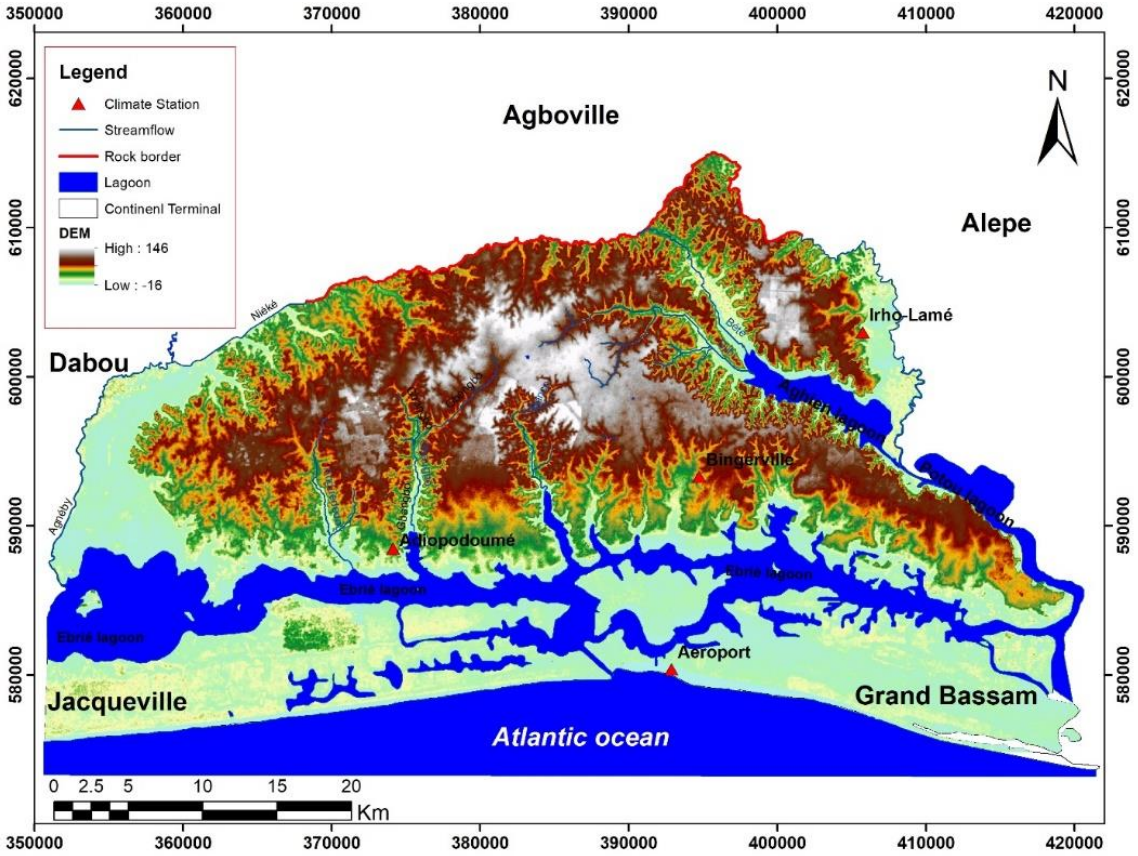

Figure 6: Elevation map of the Continental Terminal hydrogeological basin

2.3 Vegetation

The study area belongs to the forest zone of Côte d'Ivoire. The tropical rainforest, pre-lagoon savannas, mangroves and swamp forests constitute the vegetal landscapes. The original vegetation of the Abidjan region consisted mainly of Turraeanthus Africanus, which grow on rather poor clay soils. That forest was completely destroyed to extend the city of Abidjan and clearing forest for agriculture. Today, only a few hectares of this forest remains in the Banco National Park and a few small forest fragments. Pre-lagoon savannas are among the inclusive savannas. Their ecological uniqueness lies in the fact that they are all located on sandy soils from the Continental Terminal (Tastet, 1979). Mangroves forests or on salty hydromorphic soils from alluvium, are rather small. They are found on the flat banks of estuaries and lagoons. They are much exploited for their wood and bark (BNETD 2008). Swamp forests occupy the coastal strip

2.4 Climate

Abidjan, is subject to a moderate transitional equatorial climate attenuated or Attiean climate or sub-equatorial climate divided into four (4) seasons in the annual cycle: long dry season from December to May, long rainy season from May to July, short dry season from August to September and short rainy season from October to November (Tapsoba, 1995).

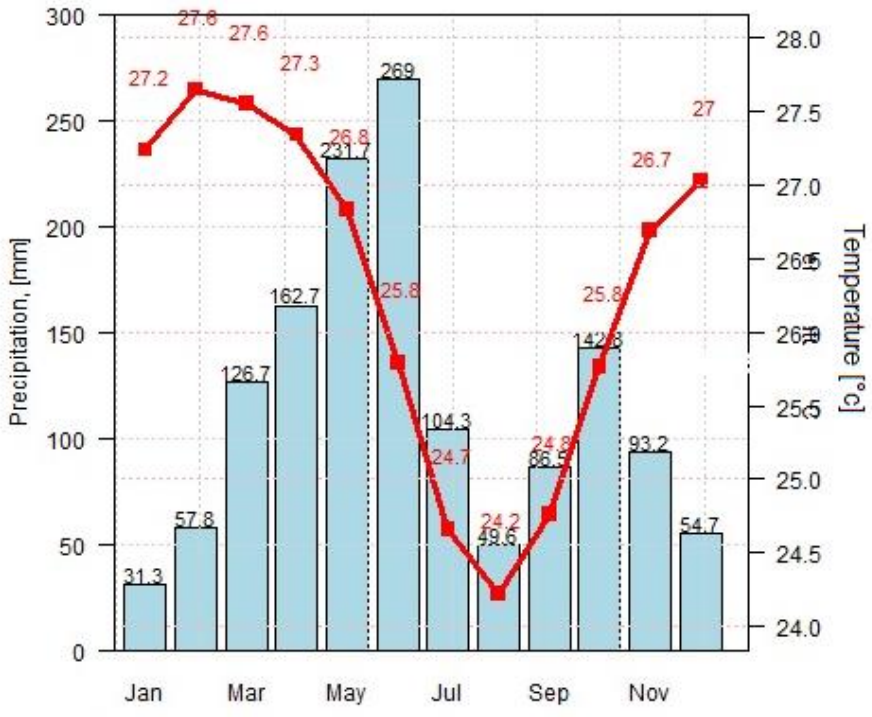

Figure 7: Ombrothermic diagram of Abidjan (1982-2018)

Overall, the annual rainfall ranges from 1718.38 mm to 1169.42 mm (1982-2018), and the temperature varying between higher maxima at 29.54 ° C and lower minima at 23.84 ° C. The

area is characterized by low thermal variability and a monsoon wind (south-west) experienced every month of the year.

Figure 7 summarize the seasonal evolution of the rainfall and temperature parameters over the study area. Average temperatures (in red) and rainfall (in blue sticks). It was noted that temperatures were low during the months of high rainfall and low rainfall.

2.4.1 Temperature

Figure 8 represents the seasonal evolution of the temperature from 1982 to 2018. The analysis show that the minimum temperature presents a wave over the year with maxima in March and April (on average 25.84° C for April) and the month of August is the coolest month (average of 22.66 ° C). The maximum temperatures also follow the trend of the minimum ones with maxima in february (29.54°C, warmer months) and the minimum in August too with Temperature of 26.48°C. Mean Temperature follows the same trend like the maximun ones with maxima in same month (27.64°C) and the minimun in august (24.22°C) therefore February and August represent extremes month temperature (27.64 ° C-24.22C)

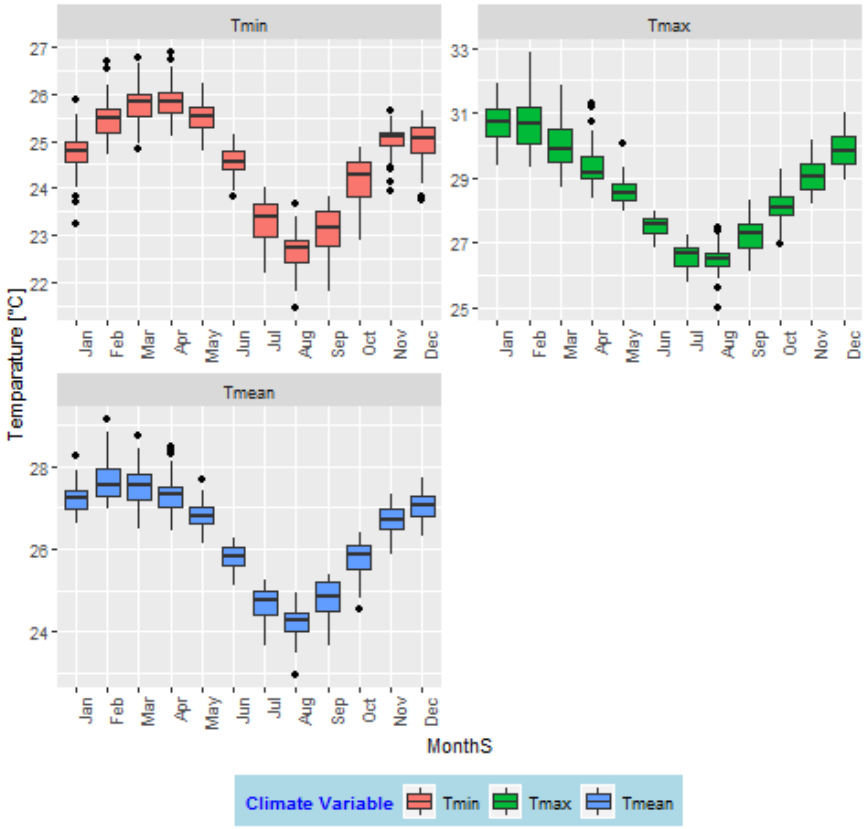

Figure 8: Temperature regime

2.4.2 Precipitation

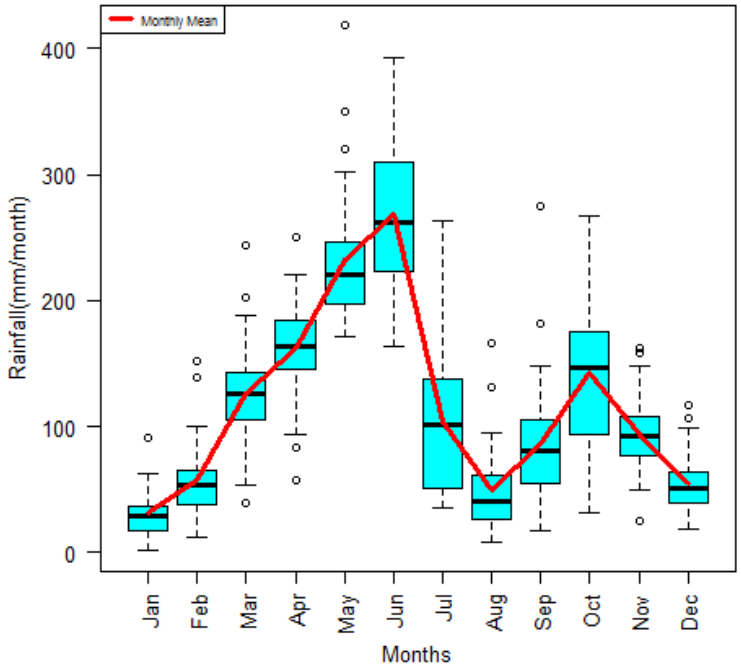

Figure 9: Variability of average monthly rainfall of Abidjan (1982-2018)

The rainfall regime is bimodal. The average monthly rainfall has a high variability over the year. This graph shows two rainy season. The first period from May to July with a peak of 269 mm in June, corresponds to the long rainy season and the second period from October to November corresponds to the short rainy season with a peak of 142.8 mm in October. The average annual precipitation over the 1982-2018 period in Abidjan is 1410.07 mm / year. Dry season is from December to April for the long dry season and from August to September for the small dry season.

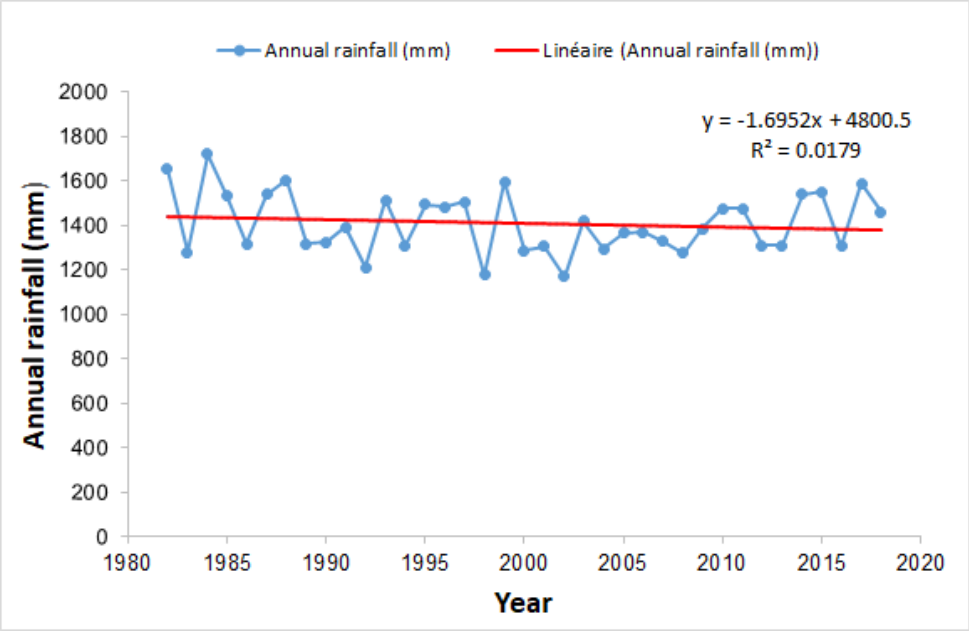

Figure 10: Mean annual rainfall of Aeroport synoptique station 1982 to 2018

In Figure 10 the trend refer to the rainfall is not stationary over the study period. There is a slight decrease in internal rainfall.

2.5 Hydrography

The district of Abidjan is watered by an extensive lagoon system composed of lagoons Ebrié (parallel to the Atlantic Ocean and intersecting the coast), Aghien and Potou and by numerous rivers that flow into the lagoons and feed the groundwater of Abidjan. They include:

- Agneby and Mé, flowing North-South into the Ebrié lagoon and they are the largest river system of the region.
- Banco, Gbangbo and Anguédédou, small rivers flowing North-South.
- Djibi and Bete, flowing Northwest - Southeast (NW-SE) into the Aghien lagoon

This hydrological system is characterized by relatively varying river runoff ratios due to low slopes and vegetation density, and higher for other rivers due to deforestation of those areas.

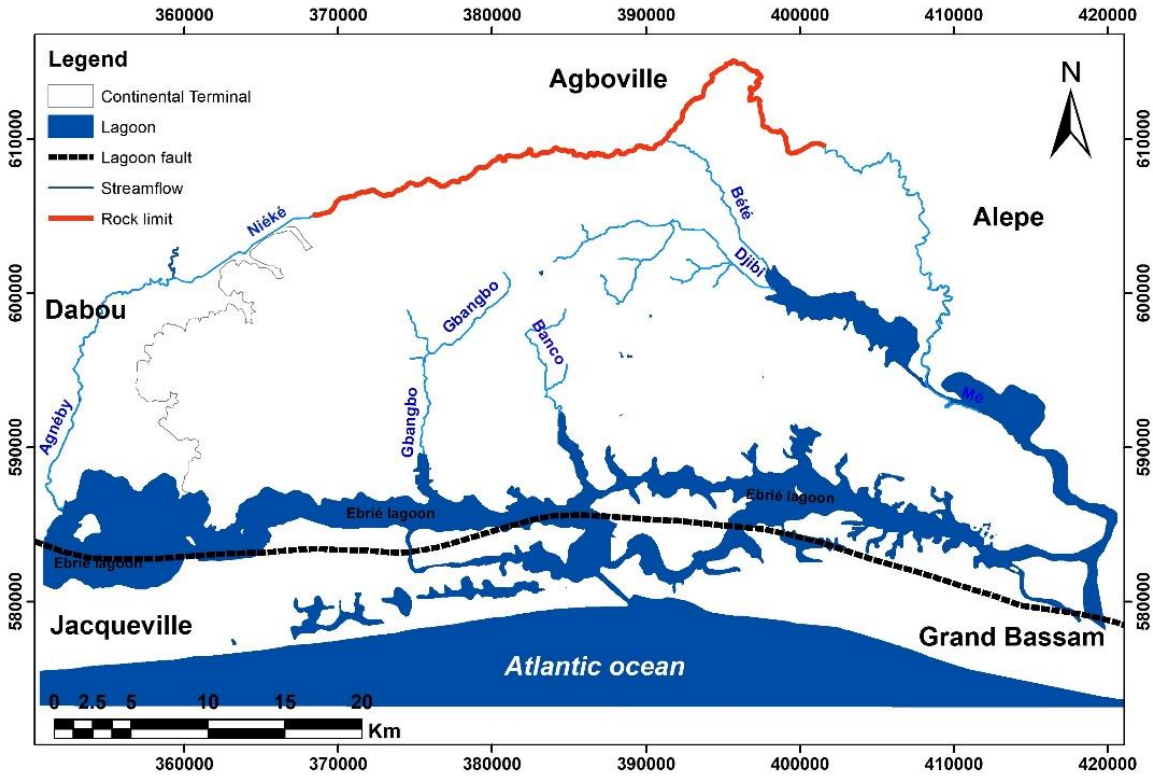

Figure 11: Hydrography of the study area

2.6 Soil and land use

2.6.1 Soil

The soils of the study area belong to the class of highly desaturated lateritic soils, depleted-modal, on tertiary sands (Continental Terminal) (Papon and Lemarchand 1973). However, the iron formations (levels gravel, fragments of armor and ironstone), classified in depleted soils are more or less reworked frequent in west of Abidjan in northern and southern border. Also, the sedimentary soil of Abidjan developed on Neogene collection consists of more or less clay

sands classified in the group of waterlogged soils. Hydromorphic soils in turn are at the estuary and near the main river. Depending on the importance of organic accumulation, two subclasses of waterlogged soils have been distinguished:

-Mineral hydromorphic soils that grow on alluvial river terraces and valley bottoms, periodically inundated by floods and ancient sands of the coastal band where the oscillations of water cover the entire profile (Humo-ferruginous layer). These soils are characterized by the presence of patches of waterlogging in the topsoil or in the underlying horizon depth pseudo-clay (mottled horizon grey rust and yellow ocher) reflecting alternating oxidizing and reducing conditions clay or (more or less mottled bluish gray horizon) reflecting reducing conditions can develop.

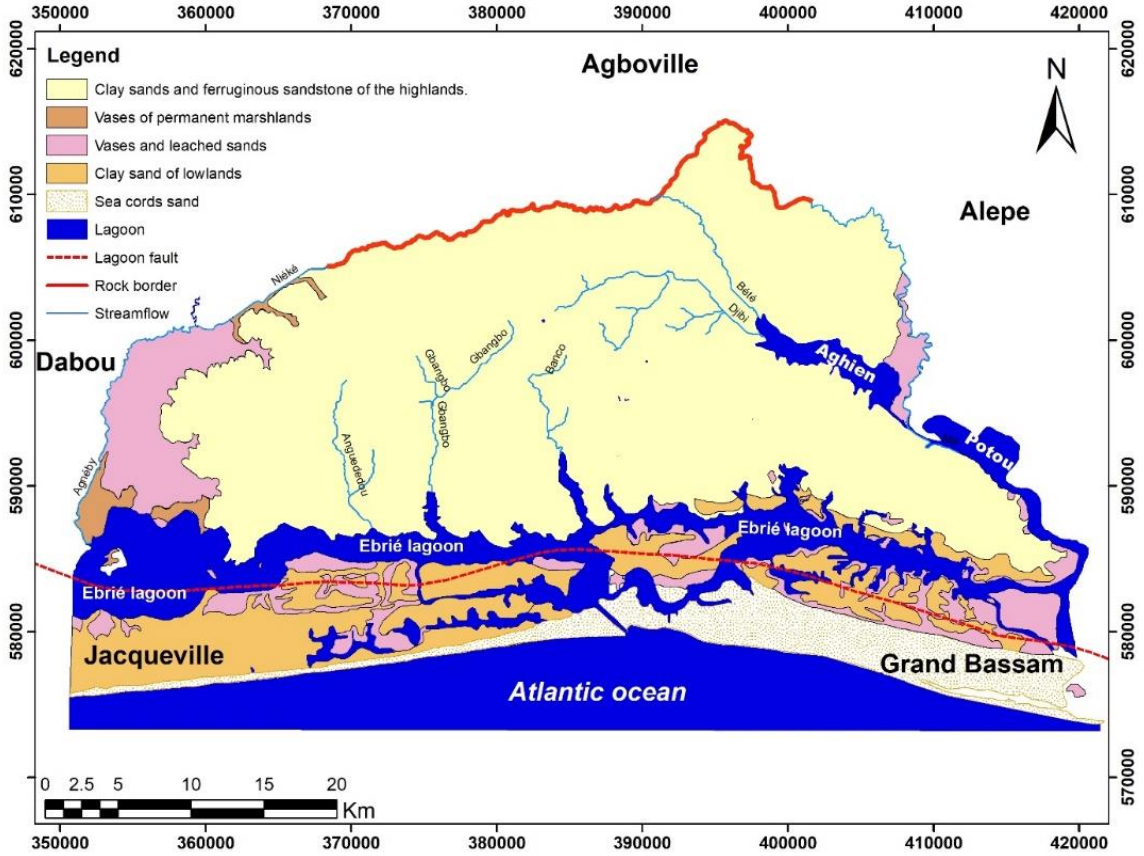

Figure 12: Soil map (Roose and Cheroux 1966)

According to (Roose and Cheroux, 1966) the pseudo- clay soils (to stains and concretions) and which most often clay (leached or all) grow in low funds and small valleys of colluvial-alluvial material. In floodplain soils pseudo- clay are more common and are associated with poorly developed soils and waterlogged modal input of alluvial material.

-Organic hydromorphic soils that are represented in areas of swamp forest or grass

origin, are permanently waterlogged throughout the year. These soils located on plateaus and moderate slopes (less than 3%) include two series: one series sandy and sandy loam series, the two sets are not separated on the sketch, only the depleted soil subgroup is modal noted. Soil slopes are more clayey in the top of the slope and very sandy in the lower slope. Fertility traits of these soils are medium, with soil depth, although its physicochemical properties are very low when it falls below a few centimetres of the topsoil.

2.6.2 Land use

The LULC of Abidjan is dominated by residence area and the ratio of a developed area and an undeveloped area is about 1 to 3. The developed area is divided into 60% of a residential area, 16% of an institutional and utility area, 6% of a commercial and industrial area, and 18% of other areas.(JICA Study Team,2013)

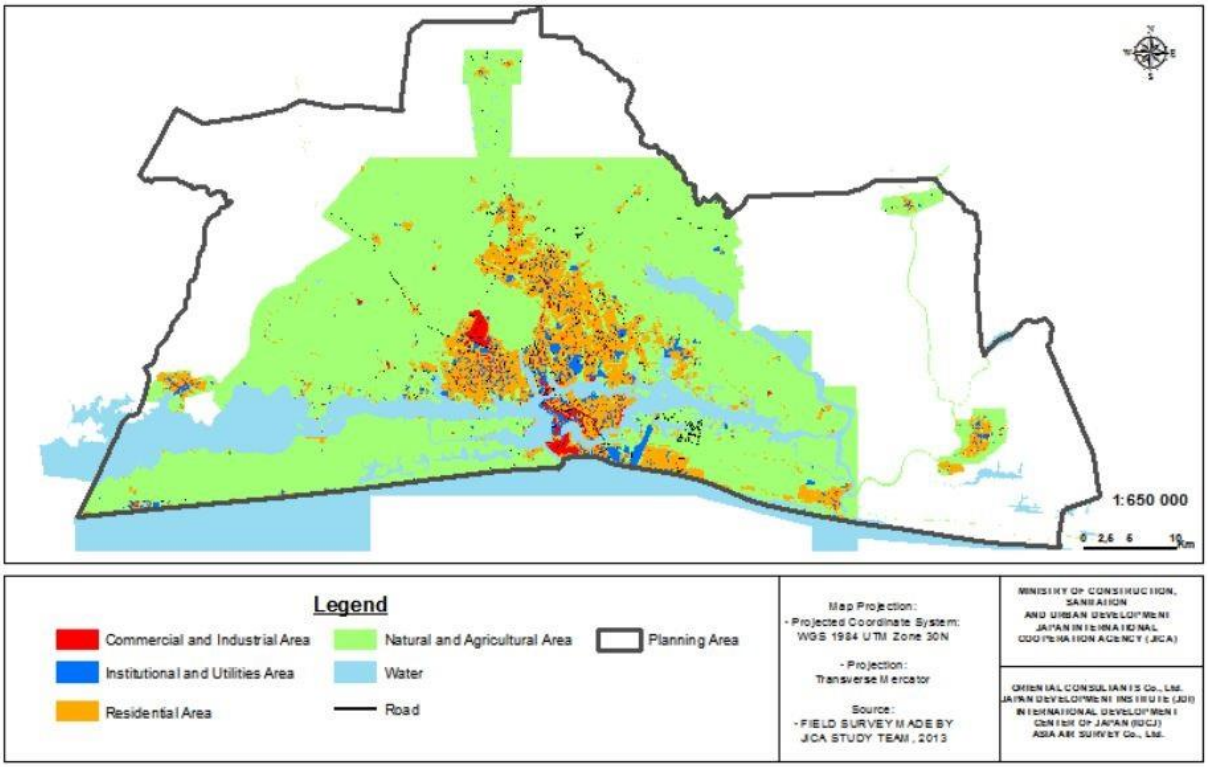

Figure 13: Land use (Source: JICA Study Team, 2013*)*

2.7 Geology, hydrogeology and Hydrodynamic characteristics of Continental Terminal

2.7.1 Geology

2.7.1.1 Regional geology

The West African geology consists of a vast Precambrian craton (formed since about 1600 Ma) surrounded by mobile zones that experienced major tectonic events in the Upper Precambrian and Paleozoic, resulting in the formation of chains such as the Pan-African chains of the Rokelides, Pharusides and Dahomeyides; the Caledonian Hercynian Mauritanide chain; the

Hercynian chain of the Moroccan Meseta; the Anti-Atlas chains; and the Ougarta chains (Dakoure 2003) The western part of the craton consists of the Guinea Rise, also called the Man shield, which occupies the southern half of the West African craton. The Pan African belt of the Rokelides on the boundary of this part is associated with marginal tectonic events due to the reactivation of the Archaean rocks. The North of the craton is occupied by the sediments of the great Taoudeni Basin formed from the Infracambrian to the Lower Palaeozoic, which is obscured in the east by continental Tertiary to Quaternary deposits and in the west by the Mauritanide belt, which forms the eastern boundary of the Mesozoic-Tertiary sediment of the Senegal Basin. The southwest, falling in the Bove Basin, is occupied by Lower Palaeozoic sediments which interrupt the continuity of the Rokelide belt with the Mauritanide belt. In the southwestern and eastern parts of Taoudeni Basin and Bove Basin, repectively, Mesozoic dolerite sills occur. In the eastern part, the craton underlies Infracambrian to Lower Palaeozoic sediments of the Volta Basin and the Pan African rocks of the Togo-Benin-Nigeria swell which are joined to each other by the intensely thrustfaulted rocks of the Togo belt. The Mesozoic Tertiary Iullmedden Basin, which separated to the block of the narrow Cretaceous Bida Basin and Benue Trough by the Togo-Benin-Nigeria swell, is limited in the north by the Pan African rocks in the Adrar des Iforas and the Air, and the Pan African rocks of the Gourma lie on its western boundary. The Chad Basin located at the extreme east is mainly occupied by Quaternary sediments. Some granite intrusions of Palaeozoic to Jurassic and Tertiary ages occur in Niger, Nigeria and Cameroun. Smaller narrower basins of Cretaceous age located along the southern coast of West Africa are filled with sediments (Spudis 2005). The main geological units of West Africa are presented by Figure 14: Main geological units of West Africa (Spudis 2005)

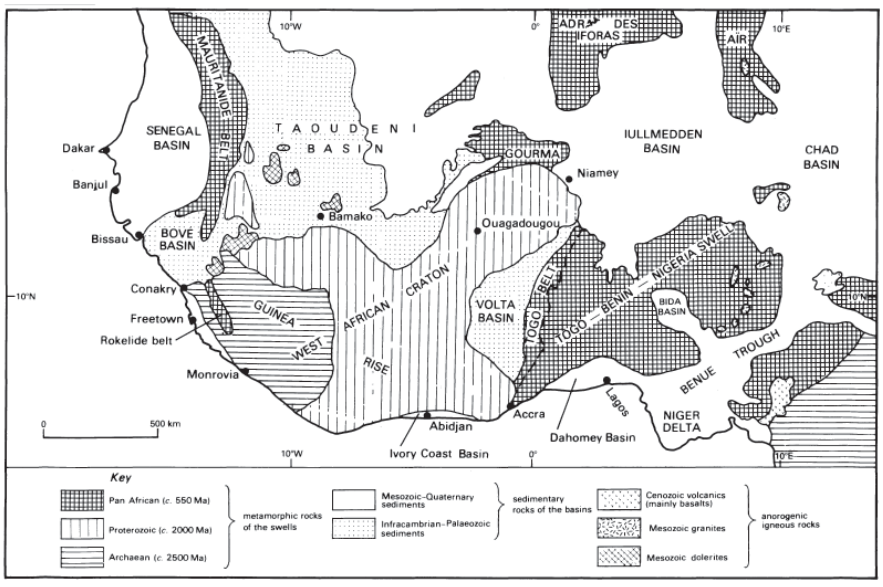

Figure 14: Main geological units of West Africa (Spudis 2005)

2.7.1.2 Geology of the study area

The study of the structure and evolution of the earth's crust shows that the study area has a simple geology which is part of Ivorian coastal sedimentary basin. Regarding a litho-stratigraphic, the sedimentary basin presents significant lateral and vertical facies variations. The stratigraphic column is constituted from top to bottom by several formations types with characteristics and ages different. It includes an emergent part " on shore " and a submerged part " off shore ".

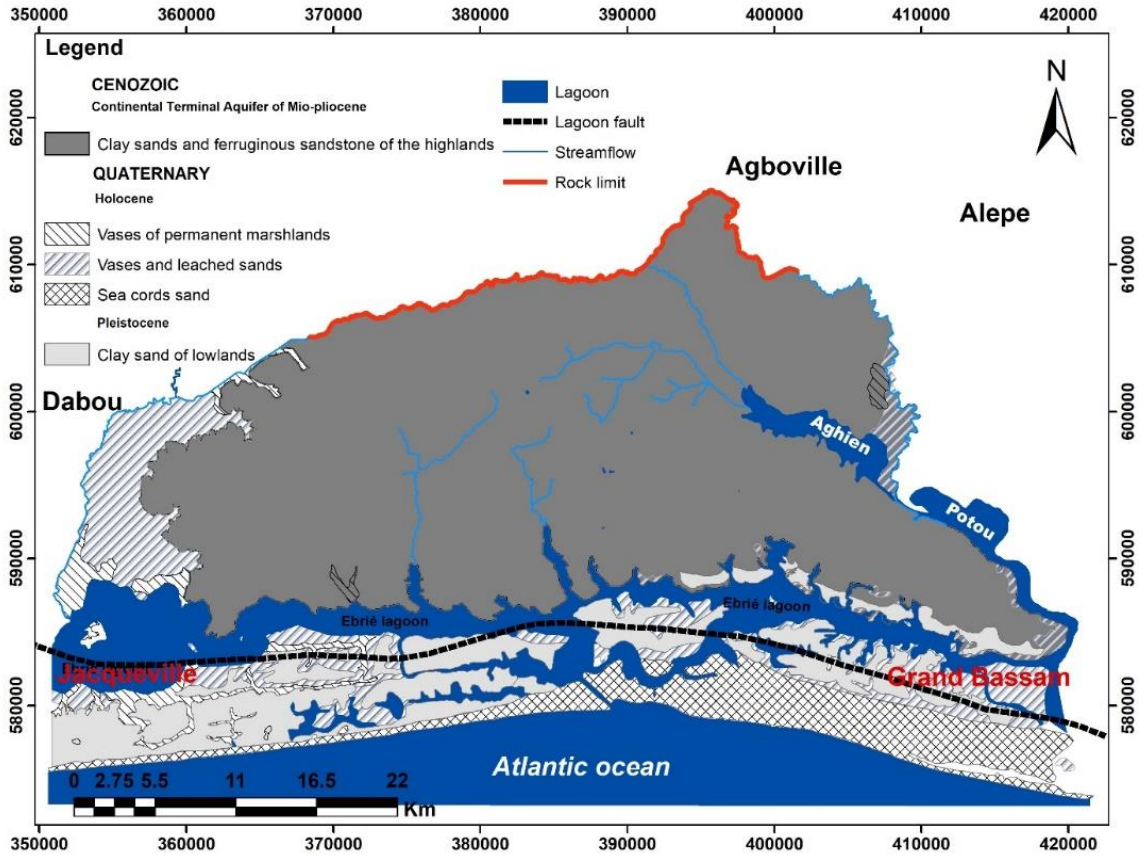

Figure 15: Geology map modify by (Delor et al. 1992)

The study area highlight different type of formation:

- The Quaternary that we will see in the part attributed to Quaternary formations;
- The Continental Terminal (CT);
- Ancient formations of late Cretaceous, Paleocene and Eocene ages

The Quaternary age formations are located in the south of "lagoon fault" and in the fluvio-lagoon depressions. These formations consist mainly of sands and gravelly sands, vases or clays, muddy sands and sandy or silty vases.

The lithology of the formations that make up the Mio-Pliocene is characterized by coarse sands, variegated clays, ferruginous sandstones and low-level iron ores. These materials are derived from the disintegration of the base. The Continental Terminal is also marked by lenticular

stratification. At its northern limit, the base of the Continental Terminal rests in discordant bevel on the Precambrian basement.

From the Upper Jurassic to the Upper Cretaceous, the formations encountered are essentially characterized by sands, conglomerates, clays, marls, sandstones and fluvial sands and sandstone sometimes dolomitic limestones. Paleogene and Eocene are composed of glauconous clays, sands and small calcareous beds.

The Continental Terminal belong to Moi-pliocene age formations and it is characterized by lenticular stratification of coarse sand, variegated clay, ferruginous sandstone and iron ore which cover all the sedimentary basin as higthland with the exception of quaternary littoral. Its depth varie from 0 to 160m and it's around 125m in Abidjan (Figure 16)

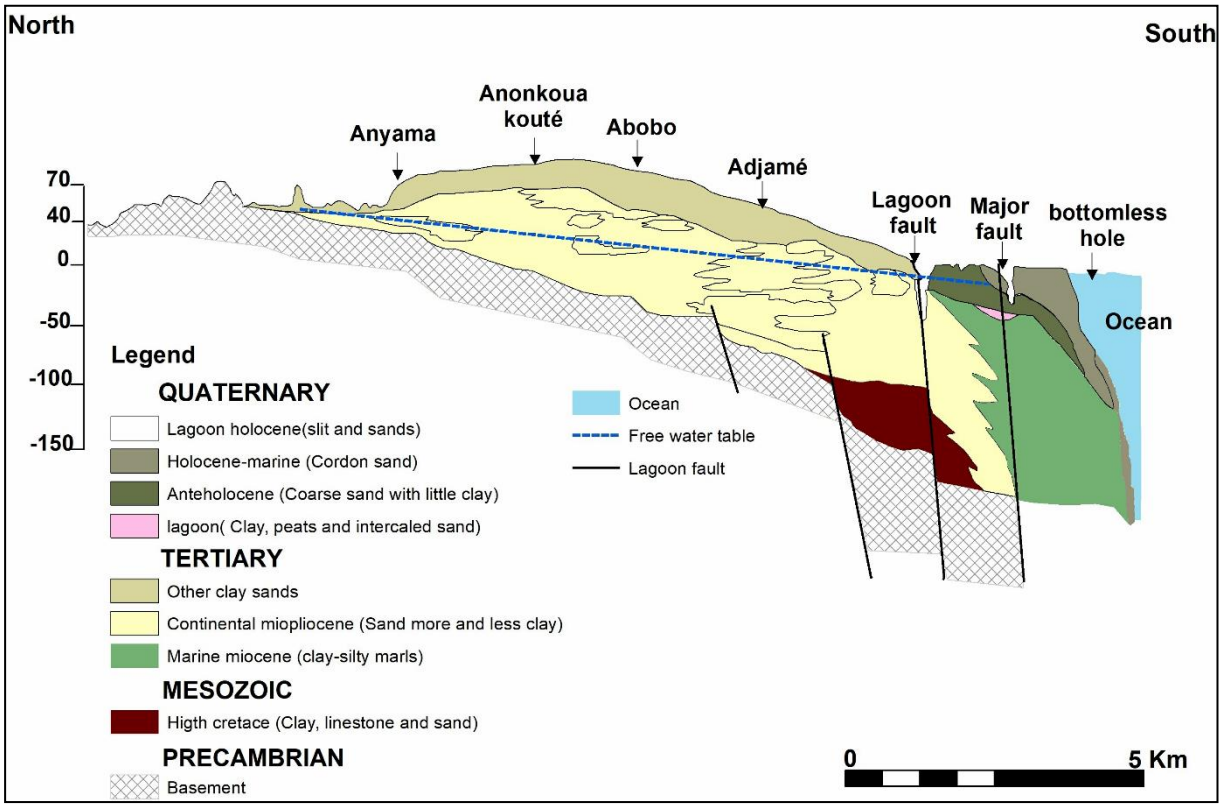

Figure 16 Geological formations of the coastal sedimentary basin in Abidjan (Jourda, 1987 transform by Koffi (2017))

2.7.2 Hydrogeology

The coastal sedimentary basin in Abidjan is composed of three aquifers: the Quaternary aquifer, the Continental Terminal aquifer, and the Maastrichtian aquifer. The Continental Terminal aquifer covers the entire surface of the coastal sedimentary basin in the form of high plateaus, with the exception of the Quaternary littoral area (Loroux 1978).This aquifer is unconfined, and includes four levels from top to bottom. The formations encountered are discontinuous lateritic cuirass and locally sandy clays or clayey sands, coarse fluvial sands, mixed clayey sand and

black clay, and gravelly sands; however, most formations are clayey sands interspersed with variegated clay (Loroux, 1978; Tastet; 1979; Aghui and Biemi, 1984)

2.8 Hydrodynamic characteristics

Previous studies undertook by Aghui and Biemi, (1984); Jourda, (1987); Sogreah, (1996); KOUADIO, (1997); Kouame, (2007) show the hydrodynamic characteristics of the Continental Terminal aquifer

- Hydraulic Conductivity (K): 14.10^{-2} to 20.10^{-2} m^2s^{-1}
- Specific Storage (Ss) :0.05 and 0.2
- Discharge : $7m^3/h$ – $338m^3/h$
- Permeability is about 10^{-3}m/s in fine sand coarse and come donw localy from 10^{-5} to 10^{-6} ms^1 according to the size
- Hydraulic gradient is from 1,66 ‰ to 1,92 ‰ respectivly around Banco river and Gbangbo river and increase in the north part
- Piezometric data reveal that Continental Terminal groundwater flow direction is from the North to the South

2.9 Continental Terminal modeling studies

Several modeling studies have been done on the Continental Terminal, for instance:

- Kouamé et al., 2013 used Modflow V.3. to predict the evolution of Abidjan aquifer level from 2005 to 2030 using scenario to increase water production at stations provided by SODECI to face of high demand in drinking water. The study is based on old data from the last century.
- Kouassi, 2013 with HPP GMS V4.50, this work was undertaken to assess the transmissivity field on Abidjan aquifer.
- Artelia, 2014 with visual Modflow, determined the discharge limit to protect the Abidjan Aquifer.
- Kouakou, 2013. The aim of his study was to model the Perchloroethylene dissolved in the saturated zone and unsaturated zone of Abidjan Aquifer with FEFLOW

2.10 Demography, environmental, social and economic activities

2.10.1 Demographics and Environmental

The Autonomous District of Abidjan enjoys a population of 4,707, 404 habitants including 2 334 392 males and 2 373 012 females (GPHS, 2014). This population consists of almost all the communities of Ivorian origin such as the Ebrié, the Agni, the Alladian, the Attie, the Baoule, Bete, Dida, the Malinke, the Yacouba, Senoufo, the Wè, etc. and nationals of foreign

countries, including Burkinabes, Beninese, Ghanaians, Guineans, Malians, Mauritanians, Nigerians, Nigerians, Senegalese, Togolese, Lebanese, etc. and including 97.37% in the 10 municipalities of central Abidjan city, the rest spreading over the other four municipalities, namely Anyama, Bingerville Songon and Brofodoumé (GPHS, 2014).

This population supports a high proportion of Ivorians (77.6%), against a relatively large number of foreigners (22.4%), mainly from the West African subregion. Its density, much higher than the country average is 2221 inhabitants per km² against 70.3 inhabitants per km² nationally. The population is distributed as follows in the 13 municipalities of the District of Abidjan.

The crisis situation experienced by Cote d'Ivoire from 2002 to 2011 has had serious repercussions on the population of the study area. Indeed, the crisis led to a vast movement of population from northern, central and western regions to the southern part of the country especially in Abidjan District where the population grew as a consequence of migration creating a framework for environmental unhealthy and unsuitable lives for the majority of the population.

2.10.2 Social and economic activities

Abidjan's district economic weight is largely dominant in Côte d'Ivoire and accounts for 40% of the country's GDP, (i.e. 9.52) billion, with major concentration of business in secondary and tertiary sectors (primary sector is predominant in the sub-prefectures):

-Secondary industry: The industrial sector is dominated by agro-food, textiles, plastics and chemical industries, electricity, building materials. The food industry includes mainly oil palm manufacture, processing of bergamot and Seville oranges, processing of rubber, the production of beverages from pineapples, oranges and mangoes and especially roasting coffee, Robusta variety, as well as packaging and processing of cocoa. Abidjan is also the first African tuna port and three plants package tuna primarily for the European market. This activity generates about 3,000 salaried jobs and is an important source of foreign exchange. The chemical industry is dominated by offshore exploitation of oil and gas products.

-Tertiary industry: The service sector consists of international commercial banks, representations of international financial institutions and more than thirty insurance companies.

2.11 Conclusion

The study area location, relief and geomorphology, vegetation, climate, hydrography, soil and land use, geology, hydrogeology, and demography and environmental, social and economic activities have been described and discussed.in this chapter. The study area is characterized by a bi-modal rainfall regime with four (4) seasons in the annual cycle: long dry season from

December to May, long rainy season from May to July, short dry season from August to September and short rainy season from October to November. Mean temperature range between 27.64°C and 24.22°C and high evapotranspiration. The area belong to the coastal sedimentary basin from cretaceous period to quaternary and the aquifers are under good recharge condition the land use is dominate by residential area follow by institutional, commercial and industrial area. Besides the population is growing very fast and therefore urbanization is increasing which can impact LULC and to affect grounwater recharge

Chapter 3: Data, materials and methods

This chapter describes the various data collected, the tools and materials used and the methodology used in data collection and analysis. In This section we are going to highlight firstly on land use and land cover data collection, classification, then data collection on climatic data. Finally hydrodynamic and piezometric data used to perform the model have been collected. The flowchart (below) give an overview of the methodology used in this work and consists to understood interaction between groundwater and surface water regarding the impact of urbanization sprawl on groundwater recharge

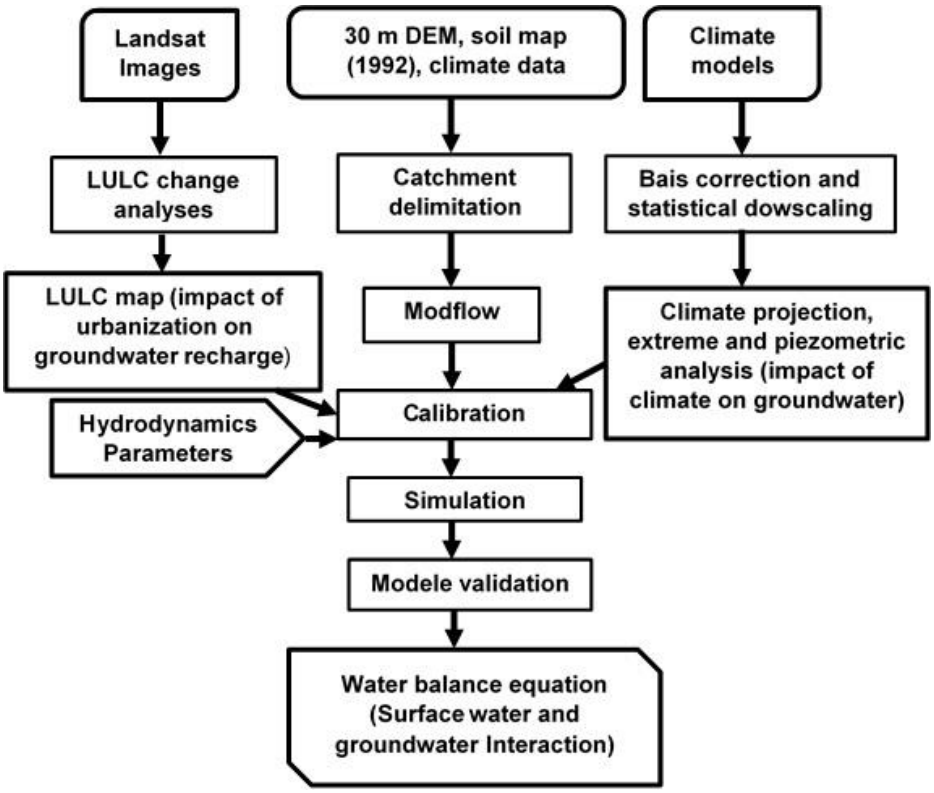

Figure 17: Overview of the methodology used in this study

3.1 Data

3.1.1 Climate data

3.1.1.1. Precipitation and air temperature data

Climate data collected on the field is from four climatic station, with daily rainfall from 1960 to 2017 and monthly air temperature from1960 to 2012. Table I shows the characteristics of the climate stations used in this study. The climate data were provided by SODEXAM (Aeronautical and Meteorological Operations and Development center) and

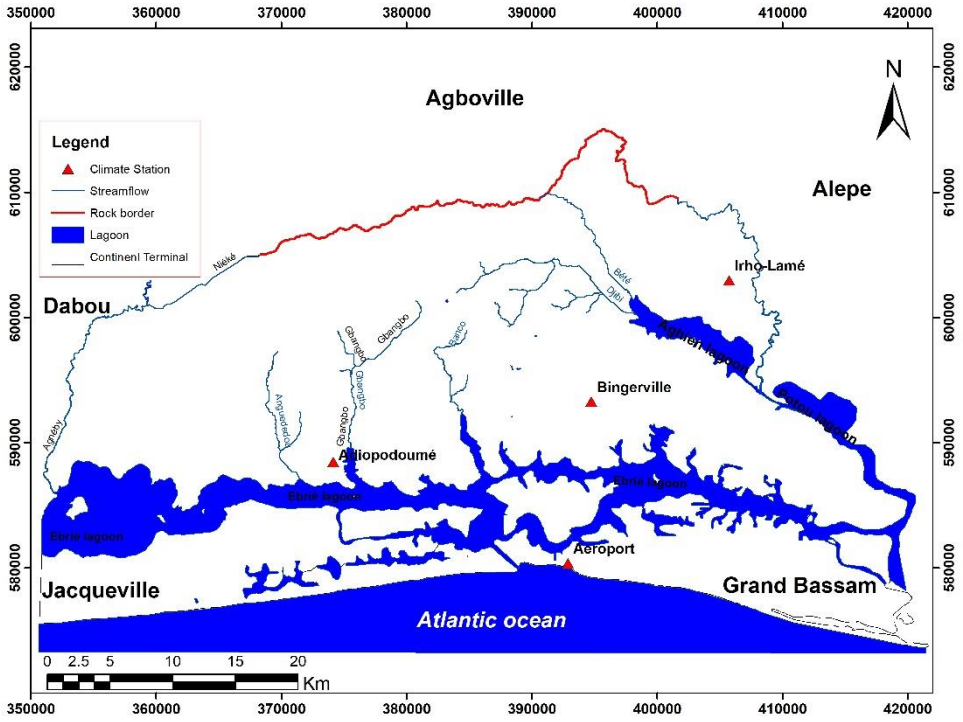

Figure 18: Climate station of the study area

NCAR (National Center of Agronomical Research). The Airport synoptic station of Abidjan is able to record all the climatic data such as precipitation, maximum and minimum temperature, relative humidity, the wind, solar radiation, etc. In our case, only precipitation and temperature were required as climate data. Other climate data used in this study were provided by WRF model

Table I: Characteristics of the selected stations

Type of data	Scale /resolution	Station	Period	Source of data
Rainfall (mm)	Daily	Aeroport	1960-2017	SODEXAM NCAR
		Bingerville	1960-2017	
		Irho-Lamé	1983-2017	
		Adiopodoumé	1971-2017	
Temperature (°C)	Monthly	Aeroport	1960-2012	SODEXAM NCAR
		Bingerville	1960-2012	
		Irho-Lamé	1983-2012	
		Adiopodoumé	1971-2012	

3.1.2 Landsat images

The 30m resolution Landsat Images for the years 1990, 2000, and 2016 covering a period of 26 years, were downloaded for two scenes (Table II) based on availability and seasonal compatibility from the United States Geological Survey (USGS) GLOVIS website (USGS 2017). A cloud cover criterion of less than 10% was used. In all cases, end of growing/harvest season (February and March) images were used to reduce the confusion between natural vegetation and agricultural lands, and to minimize interference due to cloud cover (Zoungrana

et al. 2015; Ruelland et al. 2008). All images downloaded were already geometrically corrected and georeferenced to the Universal Transverse Mercator (UTM) projection WGS84 zone 30 north.

Table II: General characteristics of Landsat image

Date of acquisition	Platform (sensor)	Scene path & row (p, r)	No. of bands
2016-03-24	Landsat_8 (OLI /TIRS)	p195r056, p196r056	11
2000-02-02	Landsat_7(ETM+)	p195r056, p196r056	8
1990-02-11	Landsat_4	p195r056, p196r056	7

OLI: Operational Land Imager, ETM+: Enhanced thematic mapper, Bands used: 5, 4, 3 & 2

3.1.3 Hydrogeological data

Data was collected on monitoring wells, pumping test and borehole lithological logs of wells drilled in the study area. Furthermore, topographical and geological maps were obtained from ONEP and CTT

3.1.3.1. Pumping test data

In the field area, historical and new pumping test data carried out in 1999-2000 for the old one and 2016-2017 for the new one were collected which were used to compute hydrodynamic parameter. These data were also used for groundwater modeling.

3.1.3.2. Monitoring well

A distribution of the wells locations with regards to their spatial positions is shown in figure… An overall of 55 boreholes were monitoring during the field work. Among them this 9 news piezometer were made in 2016 and 2017. The piezometrtic measurements relate to the period from January 2010 to April 2018 with a monthly measurement frequency.

3.1.3.3. Borehole lithological logs

Lithological log data obtained during the field survey were extract from technical and geological drilling sheets of former and new borehole realized on the study area and were used to propose a diagram of the geometry of the Aquifer.

3.1.3.4 Topographic data

The information on the topography of the basin is deducted from the shuttle radar topographic mission with 20 m resolution were downloaded from USGS Earth Resources Observation and Science (EROS) center database. They were used as input of the modflow model.

3.1.4 Station and gridded climate data

Historical daily rainfall, maximum and minimum temperature station data within the study are over the period 1981-2005 were obtained from the West African Science Service Center on Climate Change (WASCAL) research Center. Due to the limited spatial distribution of climate stations within the catchment, additional seventeen gridded daily precipitation data (Figure 19) from the Climate Hazards Group Infrared Precipitation with Station data (CHIRPS) for the period 1982-2018 were also used. The CHIRPS precipitation dataset is a product of the US Geological Survey (USGS) and the Climate Hazards Group at the University of California, Santa Barbara (UCSB). The data which is available on daily timescale at a 5km spatial resolution (Funk *et al.*, 2015) was freely downloaded from (http://chg.geog.ucsb.edu/data/chirps). Quality control was checked for four stations (Irho lame, Bingerville, Adiopodoumé and Aeroport) using Microsoft excel and Rclimdex package.

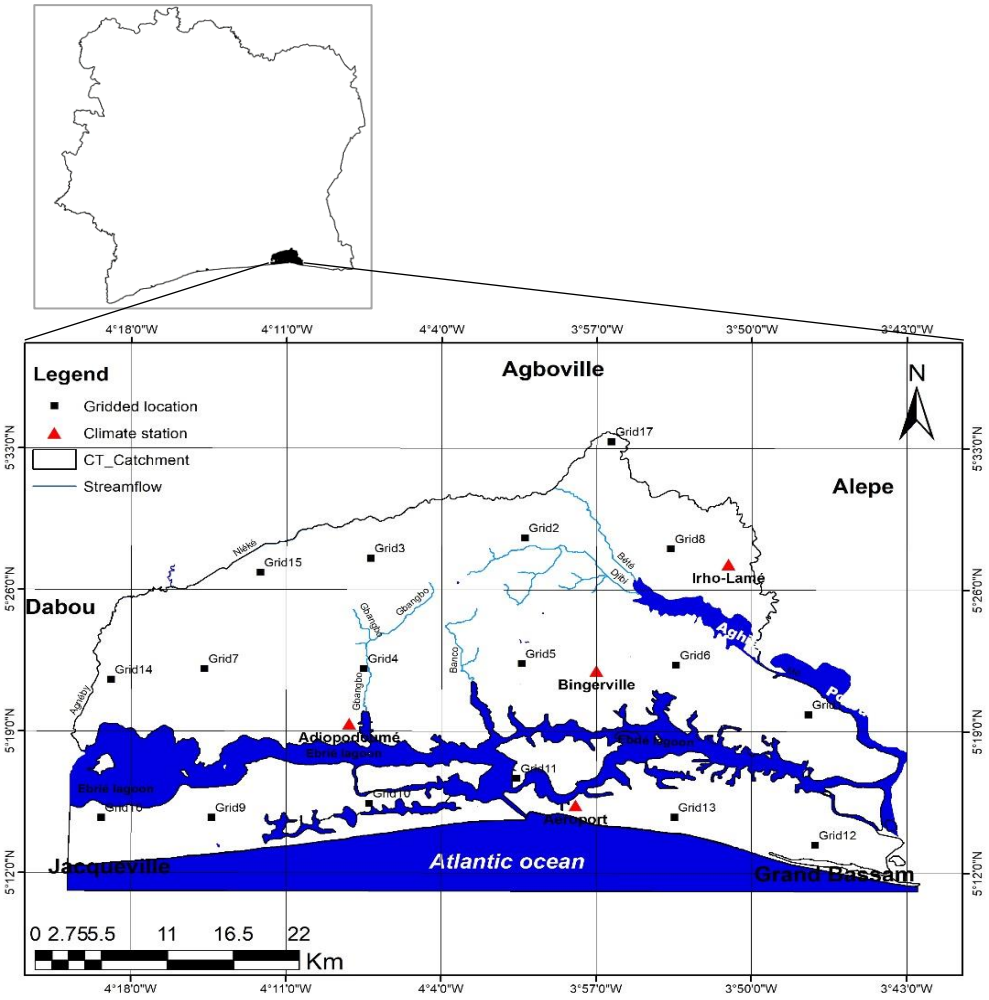

Figure 19: Climate station and gridded precipitation locations within a 12km grid

3.1.5 Regional climate models datasets

Regional Climate Models (RCMs) datasets (Table III) within the CORDEX-Africa experiment and West African Science Service Center on Climate Change and Adapted Land Use regional

climate simulations (WASCAL-WRF) were obtained from both CORDEX-Africa (https://climate4impact.eu/impactportal/data) and WASCAL geoportal (Heinzeller et al. 2016). The two CORDEX-Africa RCMs have been selected based on their ability to simulate the basic climatological features in West Africa (Kim et al. 2013). The recently developed 12km RCMs (WRF-HadGEM2 and WRF-GFDL)simulation over West Africa only were downscaled from the General Fluid Dynamics Laboratory Earth System Model (GFDL-ESM2M) and the Hadley Global Environment Model (HadGEM2-ES) using the Weather Research and Forecasting Model (Heinzeller et al. 2017). A detailed technical description and parameterization of the 12km WRF models can be found at Heinzeller *et al*. (2017). The climate change scenario datasets used in this study consist of daily rainfall, minimum and maximum temperature for the RCM historical (1981-2011) and future (2020-2049) for RCP 4.5 which represents moderate future emission. It is worth mentioning that this study considered only RCP4.5 scenario because the WRF-HadGEM2 and WRF-GFDL models are driven by only RCP4.5 scenario with no other RCPs. The data for the study catchment was extracted from these simulations by raster package in R programming using the catchment shape file. The study catchment was found to be well captured by only a single grid box for CORDEX RCMs and two grid boxes for the 12km WRF simulations owing to its small size.

Table III: Description of the Regional Climate Models

GCM	RCM	INSTITUTION	RESOLUTION
ICHEC-EC-EARTH	REMO2009	Max Planck Institute- Computational methods in systems and control theory (MPI-CSC), Germany	50km
HadGEM2-ES	WRF-HadGEM2	WASCAL / KIT/IMK-IFU	12km
GFDL-ESM2M	WRF-GFDL	WASCAL / KIT IMK-IFU	12km

3.1.6 Population data

According to RGPH (2014), Abidjan's population was estimated to 4 707 404 in 2014, with 2.67% of growth rate (INS.2014).This population data was used to assess climate change and population growth on groundwater resources.

3.1.7 Piezometric data

In addition to the 55 piezometers monitored by ONEP, 13 piezometers were measured during the rainy and the dry season (Table IV and Table V) in order to performe piezometric network

Table IV: Information about piezometer not followed (rainy season)

Localisation	Longitude (m)	Latitude (m)	Hm (m)	Land level (m)	Date	Deep (m)	Hydraulic heads (m)
Zone-Ouest	381529	593623	0.25	87	07/09/2017	81.28	5.97
Andokoi	381614	593548	0.18	87	07/09/2017	67.81	19.37
Niangon Nord	376193	594020	0.95	30	07/09/2017	13.2	17.75
Rivera centre	392951	595311	0.25	70	05/09/2017	53.85	16.4
Bingerville	402072	592967	0.25	98	05/09/2017	90.09	8.16
Bingerville-jardin botanique	401677	593022	0.38	101	05/09/2017	98.16	3.22
Ayama-Hotel kedjenou	383416	604671	0.51	103	31/08/2017	48.7	54.81
Djorogobite (Forage gros debit sodeci)	394218	598132	0.67	101	31/08/2017	85.42	16.25
Agneby village	359524	590131	0.7	14	07/09/2017	6.13	8.57
Bettesso	359277	592881	0.55	25	07/09/2017	9.93	15.62
Adonkoi II	364540	597854	0.28	27	07/09/2017	4.65	22.63
Abata village	398527	588757	0.15	7	05/09/2017	3.6	3.55
EPP Carrière	398691	592745	0.42	40	15/09/2017	30.48	9.94

Table V: Information about piezometer not followed (dry season)

Localisation	Longitude (m)	Latitude (m)	Hm (m)	Land level (m)	Date	Deep (m)	Hydraulic heads (m)
Zone-Ouest	381529	593623	0.25	87	19/04/2018	80.1	7.15
Andokoi	381614	593548	0.18	87	19/04/2018	67.52	19.66
Niangon Nord	376193	594020	0.95	30	19/04/2018	13.2	17.75
Rivera centre	392951	595311	0.25	70	19/04/2018	52.8	17.45
Bingerville	402072	592967	0.25	98	19/04/2018	89.26	8.99
Bingerville-jardin botanique	401677	593022	0.38	101	19/04/2018	89.34	12.04
Ayama-Hotel kedjenou	383416	604671	0.51	103	19/04/2018	47.6	55.91
Djorogobite (Forage gros debit sodeci)	394218	598132	0.67	101	19/04/2018	84.02	17.65
Agneby village	359524	590131	0.7	14	19/04/2018	6.36	8.34
Bettesso	359277	592881	0.55	25	19/04/2018	10.23	15.32
Adonkoi II	364540	597854	0.28	27	19/04/2018	4.66	22.62
Abata village	398527	588757	0.15	7	19/04/2018	3.58	3.57
EPP Carrière	398691	592745	0.42	40	15/09/2017	29.73	10.69

3.2 Groundwater recharge estimation and land use-land cover mapping

3.2.1 Groundwater recharge

Groundwater recharge refers to the entry of water from the unsaturated zone into the saturated zone below the water table surface, together with the associated flow away from the water table within the saturated zone (Freeze and Cherry 1979). Recharge occurs when water flows past the groundwater level and infiltrates into the saturated zone. It is an extremely important water component of the circulation cycle in nature.

There are several methods such as geological, hydrogeological, geophysical and remote sensing techniques, which can be applied to determine groundwater recharge potential zone (Mukherjee 1996). Many factors affect the occurrence and movement of groundwater in a region, including topography, lithology, geological structures, depth of weathering, extent of fractures, primary porosity, secondary porosity, slope, drainage patterns, landform, land use/land cover, and climate (Jha et al. 2007) Groundwater recharge is not easy to estimate mainly in the urban area,

3.2.1.1 Water balance method

In this study, Groundwater recharge will be estimated using the water balance method by considering monthly water infiltration. Further water balance is another name for the principle of mass conservation in which changes of total water volume, inflow (precipitation) and outflow (evaporation, transpiration, surface and subsurface runoff) on a given area are balanced. However, the estimation of water flux between water balance components is still an interesting and demanding hydrological challenge and the effects of land use change on water balance and estimating runoff in unstudied watersheds are continuous themes of scientific and expert ecohydrological studies (Zhang et al. 2008; Todini 2007; Alemaw and Chaoka 2003) There are various research and applied problems where the calculation of water balance is used: for the estimate of a regional water balance, for the assessment of the impact of human activity and climatic variations on basin runoff, in planning and allocation of fresh water resources, in engineering applications such as bridge management systems, etc. An understanding of water balance in relation to climatic and morphological basin features gives us insight into complex processes which are conducted regarding different spatial and temporal relations (Zhang et al. 2008). The predictions of more frequent and longer drought periods and of greater intensity of floods clearly define the need for a more detailed knowledge of existing and of future watershed conditions. For such knowledge the calculation of water balance is essential and may also provide reliable information in defining strategies for climate change mitigation measures on the watershed.

In this study, recharge is estimated using monthly mean area precipitation (1982-2018) based on the Thornthwaite flowchart (Annex1). This method has been used in 1996 by SOGREAH on the Abidjan aquifer.

It allows us to calculate the monthly infiltration rate from (Equation 2) (Thorntwaite and Mather 1955; 1957).

$$P = AET + R + I + \Delta S \qquad \text{Equation 2}$$

With P (mm) = total rainfall

AET (mm) = actual evapotranspiration

R (mm) = runoff

I= infiltration

ΔS= water stock variation in the available water content (AWC)

3.2.1.1.1 Actual evapotranspiration (AET)

AET is the amount of water which is actually evaporated and depends on many parameters such as: precipitation, temperature, insolation, wind, vegetation, nature of the soil, useful soil reserve (Pidwirny 2006). To estimate this parameter, Thornthwaite method was used. It is a widely used empirical method for estimating evapotranspiration and the only variable used is monthly temperature. It is link to potential evapotranspiration which is describe below

3.2.1.1.2 Potential Evapotranspiration (PET)

The most common approach for estimating evapotranspiration is the Penman-Monteith Equation which represents the evapotranspiration from a vegetated surface (Dingman 2008). However, the lack of sufficient data available in our case required another simpler approach. The potential evapotranspiration can be obtained at a monthly time step from the Standard Thornthwaite method (Thornthwaite 1948) which only uses the parameters temperature and average daylight. The Standard Thornthwaite method starts by calculating an annual heat index (*I*) from the sum of all the monthly indices, (*i*):

$$i = \left(\frac{T}{5}\right)^{1.514} \qquad \text{Equation 3}$$

where T is the monthly mean temperature. The annual heat index is then given by:

$$I = \sum_{n=1}^{12} i_n \qquad \text{Equation 4}$$

where n is the number of months. The potential evapotranspiration is then calculated with the following relationship:

Equation 5

$$PET' = C\left(\frac{10T}{I}\right)^{\alpha}$$

where *C* is a constant (16) and *a* is function of *I*:

$$\alpha = 67.5 \cdot 10^{-8}\mathrm{I}^{-3} - 77.1 \cdot 10^{-6}\mathrm{I}^{2} - 0.0179\,\mathrm{I} + 0.492$$ Equation 6

Last, *PET'* needs to be calibrated for the specific month by weighing with the average hours of daylight (*d*) and the number of days in the respective month (*N*):

$$PET = PET'\frac{d}{12}\cdot\frac{N}{30}$$ Equation 7

The Standard Thornthwaite method was developed for a temperate climate, but is still widely used over the world (Xu and Singh 2001). Usually these calculations yield underestimations of the evapotranspiration and should be calibrated from Penman-Monteith calculations for more detailed results(REMP 2003). However, this was not possible in this current study where the Standard Thornthwaite method was used to estimate monthly potential evapotranspiration values for sedimentary basin of the Continental Terminal.

3.2.1.1.3 Surface runoff determination

Out of many methods for runoff estimation, the Natural Resources Conservation Service Curve Number (NRCS-CN) (formerly called as SCS-CN) method developed by the U. S. Department of Agriculture (USDA) still remains the most popular, fruitful and recurrently used method. The major reasons for this popularity may be attributed to ease of use, less number of input parameters, easy to modify, robustness of model results, and acceptability among both researcher and practitioner community. The SCS-CN method is based on the principle of the water balance (Equation 8) and two fundamental hypotheses. (i) The ratio of direct runoff to potential maximum runoff is equal to the ratio of infiltration to potential maximum retention (Equation 10). The initial abstraction is proportional to the potential maximum retention (Equation 9).

$$P = I_a + F + Q$$ Equation 8

$$\frac{Q}{P - I_a} = \frac{F}{S}$$ Equation 9

$$I_a = \lambda S$$ Equation 10

Where, *P* is the total precipitation (mm), *Ia* is the initial abstraction before runoff (mm), *F* is the cumulative infiltration after runoff begins (mm), *Q* is direct runoff (mm), *S* is the potential maximum retention (mm), and λ is the initial abstraction (ratio) coefficient. SCS (2004) introduced general equation (Equation 11) by combining (Equation 8) and (Equation 9).

$$R = \begin{cases} 0, & for\ P \leq I_a \\ \dfrac{(P - I_a)^2}{(P - I_A + S)}, & for\ P > I_a \end{cases}$$ Equation 11

Where;

R = runoff (mm)

P = rainfall (mm)

Ia = Initial abstraction (surface storage, interception, and infiltration, mm)

S = potential maximum retention (mm)

The potential maximum retention *S* (mm) can vary in the range of $0 \leq S \leq \infty$, and it directly linked to *CN*. Parameter *S* is mapped to the *CN* using (Equation 12) as:

$$S = \frac{25400}{CN} - 254$$ Equation 12

The CN which is a function of LULC, soil type, hydrologic soil group and antecedent moisture condition (AMC) is a key factor of the SCS-CN method, and it can vary from 0 to 100. Three AMCs were defined as dry (lower limit of moisture or upper limit of *S*), moderate (normal or average soil moisture condition), and wet (upper limit of moisture or lower limit of *S*), and denoted as AMC I, AMC II, and AMC III, respectively (Mishra and Singh, 2003). Higher AMC and *CN* value would indicate the more runoff potential and vice versa, therefore, median CN obtained from array of CN values would commonly be adopted for the watershed (Hawkins et al. 1985; Schneider and McCuen 2005; Hjelmfelt 1991). The CN is usually calculated from available tables in the National Engineering Handbook, Section 4 (NEH-4) as well available curves; however, this procedure is very tedious, laborious, and time consuming. Further, large errors can be expected in surface runoff estimation where, the validity of the hand book tables for CN was not verified. It faces problems of ambiguous calculation associated to the soils outside the classified hydrological soil groups. The SCS-CN method does not adequately model all of the important physical processes of runoff generation. Thus, it would benefit to larger research and practitioner community to modify the SCS-CN method to encompass these processes.

The SCS-CN method assimilates the convolution of runoff generation into CN. However, lumped conceptual approach and simplicity of a single parameter introduces great uncertainty to estimate runoff in practical applications. In last four decades, extensive research work has been conducted to overcome existing demerits of the SCS-CN method. It does not adequately model the impact of land use changes, morphometric parameters, and long term evapotranspiration loss. In spite of many modifications done in the SCS-CN method, a need of its further improvement has always been expected to satisfy unresolved challenges. To modify

the existing SCS-CN method towards better runoff prediction is reliable and feasible solution to cope problems of poor hydrologic analysis. Recent modifications in determination of *CN* are reported by slope adjustment procedure (Sharpley and Williams, 1990; Mingbin *et al.*, 2006), asymptotic determination of CNs from measured rainfall-runoff data (Hawkins 1993; Hawkins et al. 2009; Bonta et al. 2007; Hjelmfelt et al. 2001; Kowalik and Wałęga 2015), two-CN system approach (Soulis and Valiantzas, 2012), determination of CN by incorporating ET for continuous hydrological simulation (Kannan et al., 2008; Jajarmizadeh et al., 2012), composite CN-generation using RS variables sensing variables like vegetation, impervious surface, and soil (Fan et al., 2013). For complex watersheds with high temporal and spatial variability in soil and land use, the SCS-CN model integrated into the RS/GIS system (Zhan and Huang, 2004; Geetha et al., 2007; Viji et al., 2015). In conventional CN determination procedure, the impact of land use change, long memory characteristics and variance heterogeneity of watershed due to accumulation of soil moisture does not address. It also does not take into account the effect of slope, stream length and other morphometric parameters which are highly influenced on runoff generation. Further, it does not incorporate long-term losses such as evaporation and evapotranspiration. Therefore, it is necessary to modify the CN to improve performance of the SCS-CN method.

3.2.1.1.3.1 CN Determination for different AMC

AMC indicates watershed wetness and the moisture content of soil prior to a storm. The AMC is explained variation in *CN* at different time step. Based on rainfall magnitude of previous five days and season (dormant season and growing season), three AMC levels (AMC I, AMC II & AMC III) were documented by SCS (Table VI) AMC I, AMC II and AMC III were defined as dry (lower limit of moisture or upper limit of S), moderate (normal or average soil moisture condition), and wet (upper limit of moisture or lower limit of S) respectively. SCS-CN manual provides the average condition of a watershed AMC II (CNII) value (USDA, 1985). The CN value of AMC I (CNI) and AMC III (CNIII) can be adjusted by applying the (Equation 13) and (Equation 14) (Chow et al., 2002) respectively:

Table VI: Antecedent Moisture Condition classes for CN determination

AMC-class	Dormant season (mm)	Growing season (mm)	Condition
I	<13	<36	Dry soil but not the wilting point
II	13-28	36-53	Average condition
III	>28	>53	Saturated soils, heavy rainfall or light rainfall

$$CN_I = \frac{4.2\ CN\ II}{(10 - 0.058\ CN\ II)}$$ Equation 13

$$CN_{III} = \frac{23\ CN\ II}{(10 + 0.13\ CN\ II)}$$ Equation 14

3.2.1.2 Water table fluctuation (WTF)

The recharge estimation using piezometric level fluctuation method is based on the principle that the increase of ground water level within the unconfined aquifer is due to the recharge (Healy and Cook 2002 ;Yin et al. 2011). However pumping or evapotranspiration mainly challenge this hypothesis. According to Delin et al. (2007), there are some three other assumptions using this technique: (i) in shallow unconfined aquifers, groundwater recharge and discharge are directly linked to the rise and fall in groundwater levels ; (ii) during the period of fluctuation in groundwater table, the value of specific yield (Sy) of aquifer is known and invariable ; and (iii) “the pre-recharge water level recession can be extrapolated to determine water level rise”. Some of the difficulties arising from this technique are the identification of the cause of water level fluctuation because the fluctuations are not always due to recharge and discharge; and also the calculation of specific yield (Healy and Cook ,2002). According to Crosbie et al. (2005), rainfall is not the only parameter that causes the rising of the water table. Groundwater level rise is mainly influenced by river stage; the increased gas pressures in the vadose zone can also be a cause (Heliotis and DeWitt 1987). The second case occurs generally when trapping air in the vadose zone between the wetting front and the water table due to the events of high intensity of rainfall, and other causes of water table fluctuations are due to earth tides, pumping, and lateral flow (Crosbie *et al.,* 2005).

Crosbie *et al.* (2005) suggested removing an eventual cause of rising water table different from rainfall before estimated recharge to avoid overestimation.

The analysis method of aquifer fluctuations is probably the largest used method to estimate the recharge. It has been used in several studies (Meinzer and Stearns 1929; Rasmussen and Andreasen 1959;Gerhart 1986; Hall and Risser 1993)

The groundwater recharge rate (R) can be estimated by applying this mathematical equation:

$$R = S_y \times \frac{dh}{dt} \approx S_y \times \frac{\Delta H}{\Delta t} \qquad \text{Equation 15}$$

Where Sy is specific yield of the groundwater aquifer material, *h* is the height of the water table and *t* is time (Healy and Cook 2002).

The WTF method Application involves two steps: estimating the water-level rise ΔH (tj) and estimating specific yield Sy. According to Meinzer (1923). The water-level rise Δh is the difference between the top of the rise of water level and the lowest point at the time of top of the extrapolated antecedent recession curve (Healy and Cook 2002). The recession curve is the trace that the well hydrograph would have followed without the presence of any rising of precipitation (Healy and Cook 2002; Delin *et a l.*, 2007)

In the Continetal Terminal Aquifer, this method was applied by (Kouassi 2013; Berthe et al. 2015). In this case, effective porosity were used rather than specific yield because we are facing an unconfined aquifer (Castany 1998). The study were base on the prevoius on the study area showing that the specific yield is between 0.1 to 0.21 (Geomines 1982) also the study undertook by Sogreha (1996) reveal that the specific yield is 0.1 at North Riviera catching field and 0.14 computed in the borehole F2 located in the east zone

3.2.2.. Land use-land cover mapping

3.2.2.1 Data processing and analysis

Landsat images were selected based on time coverage, and amount of clouds. The study area is covered by two (2) different Landsat scenes 196-56 and 195-56. Landsat TM and ETM+ images for the years 1990, 2000 and 2016 were downloaded from the United States Geological Survey's (USGS).The two (2) images were done using the Environment for Visualization Images (ENVI) 5.3. All image data were geometrically corrected to the Universal Transverse Mercator (UTM) WGS84, Zone 30 North local projection type. In addition, image enhancement, mosaicking and sub-setting were also done. Furthermore, preliminary image interpretations were conducted using false color composites of red, green and blue. These processes were done on the Earth Resources Data Analysis System (ERDAS) Imagine 2015. Figure 20 below illustrates the process work flow used for this study.

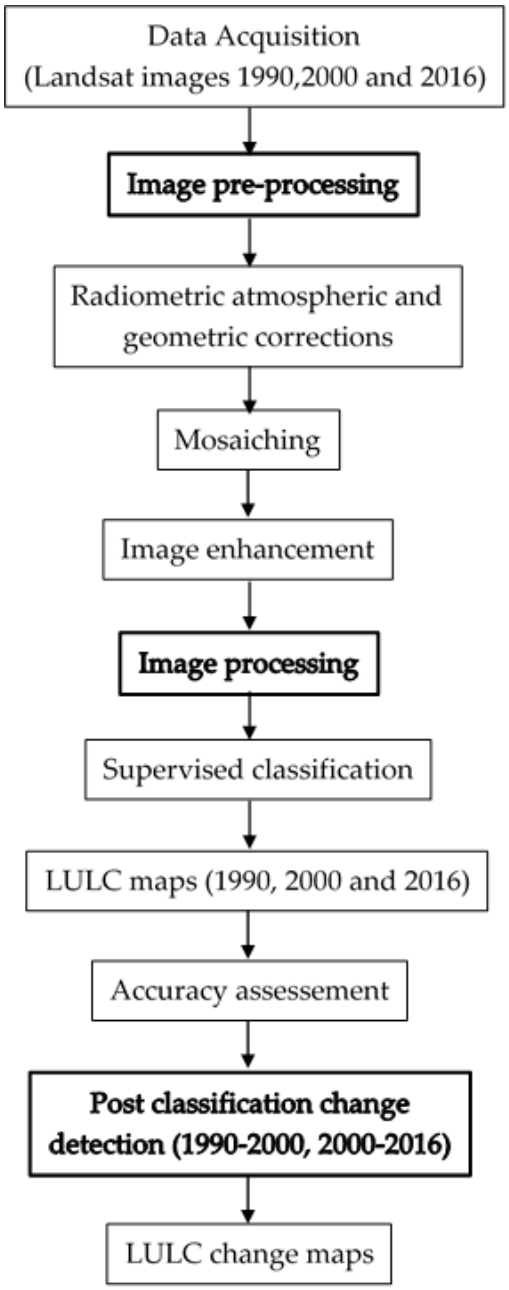

Figure 20: Flow chart of methodology for LULC change

3.2.2.2 Classification and validation

Classification is the process of assigning pixels to informational classes of interest (Campbell and Wynne 2011). The classification process involves spectral or pattern recognition in order to create a cluster of classes from multispectral images. The three Landsat data were classified to reveal changes in LULC between 1990,

2000 and 2016. Supervised classification was carried out for each satellite image separately using the maximum likelihood algorithm based on the collected training data site. For each LULC class, the maximum training and validation samples were implemented. The number of region of interest built in each classification was more than 3000 respectively. Hence, more than 100 ground truth points were randomly selected for all identified LULC classes collected

from the field for validation and accuracy assessment for 2016 years. The same classification algorithm was used to classify images of the others years. However, for these periods, validation of classification was relied essentially on sites where there was no change (identified from the current image and the oldest ones), using existing land use maps in that period or near. Also, historical LULC information was recorded to derive knowledge of the LULC changes that have occurred on the surveyed sites between 1990 and 2000 from the national center of mapping and remote sensing. Sample from spot image from 1990 with 10 m resolution too was recorded. Accuracy assessment was performed independently for each image period using ENVI post classification assessment.

3.2.2.3 Post-classification

Classification accuracy is the degree to which image classification agrees with ground reference data (Campbell and Wynne 2011). Classification accuracy can be assessed to provide an overall measure of the quality of a map, to form the basis of an evaluation of different algorithms or to help gain an understanding of errors (Congalton *et al.* 1998, Foody 2002). A classification error results when there is a discrepancy between the classified data and the ground reference or 'truth' (Foody 2008).

Several measures of determining classification accuracy can be derived from the error matrix (Congalton 2001, Foody 2002, Foody 2008) depending on the intentions of the user. It is recommended that the raw confusion matrix be presented and that it must not be normalised (Foody2002), so that accuracy measures can be computed as appropriate by users (Congalton and Green1999). According to Congalton and Green, some of the accuracy statistics, which can be measured from the error matrix, are Overall Accuracy (OA), Producer's Accuracy (PA), User's Accuracy (UA), Kappa Index of Agreement (KIA) and Conditional Kappa (CK). In this study, Image classification accuracies were determined by applying statistical analysis for validation based on confusion matrix and Kappa. Overall accuracy, producer's accuracy and user's accuracy were also determined. The confusion matrix provides information on the correct and incorrect prediction made by a classification algorithm by comparing a classified map with ground information. 2016 classified image was validated using the ground truth data collected during the field campaign. However, because there was no sufficient past land cover information and no aerial photography at these specific period, a different approach was used to assess the reliability of the 1990 and 2002 images classification based on areas with no change, maps , sampling within high resolution image (spot) as GCT and historic land cover information from years nearly close. From visual observation and all these information recorded, areas with similar characteristics and spectral signature between these old images have been selected. This allows classification for these previous dates and enhances the

accuracy of the classification process. At the end of the classification process, all files have been saved as Geotiff before further GIS analysis.

3.2.2.3.1 Accuracy assessment

The aim of accuracy assessment is to quantitatively determine how effectively pixels were grouped into the correct feature classes in the area under investigation. Accuracy assessment of the classified image of the year 1990, 2000 and 2016 were performed. An error or confusion matrix which is one of the most widely used accuracy assessment method (Congalton and Green, 2009) was generated for all the LULC classes. The error of omission or producer's accuracy (Equation 16), error of commission or user's accuracy (Equation 18), overall accuracy (Equation 19) and the Kappa value (Equation 17) were determined for each classified LULC map.

$$\text{Producer accuracy} = \frac{\text{number of correctly classified classes in the column}}{\text{total number of items verified in that column}} \quad \text{Equation 16}$$

$$\text{User's accuracy} = \frac{\text{Number of correctly classified classes in the row}}{\text{total number of items verified in that row}} \quad \text{Equation 18}$$

$$\text{Overall accuracy} = \frac{\sum(\text{correctly classified classes along diagonal})}{\sum(Row\ total\ or\ column\ total)} \quad \text{Equation 19}$$

$$\text{Kappa (K)} = \frac{N\sum_{i=1}^{r} x_{ij} - \sum_{i=1}^{r}(x_{i+} \times x_{+i})}{N^2 - \sum_{i=1}^{r}(x_{i+} \times x_{+i})} \quad \text{Equation 17}$$

where r is the number of rows in the matrix, $x_{ij}$is the number of observations in row i and column i,x_{i+} and x_{+i} are the marginal totals of row i and column i, respectively, and N is the total number of observations.

3.3 Climate change impact study

3.3.1 Data quality control and CHIRPS validation

The main focus of this validation work is to assess the performance of the CHIRPS over the study area, therefore the validation were done at monthly and annual time-scales by the comparing the extracted point-based CHIRPS data for the Aeroport, Bingerville, Irho lamé and Adiopodoumé locations with the Aeroport, Bingerville, Irho lamé and Adiopodoumé stations data. The performance of the CHIRPS precipitation data was assessed using several statistical indicators such as Pearson correlation coefficient (r), percentage bias (PBIAS), standard deviation, the root mean square error (RMSE) and Nash-Sutcliff coefficient (NSE)

3.3.2 Climate projections

Compared to climate predictions, climate projections depend only insignificantly on initial states. In their context, boundary conditions are of much greater importance. Boundary

conditions refer to external factors of influence. In addition to natural factors, such as the varying solar constant and volcanic eruptions, the climate is also significantly influenced by anthropogenic interferences, such as greenhouse gas emissions and land-use changes. As a basis for climate projections, the changes expected to occur during the coming decades and centuries are evaluated in the form of scenarios. Based on the assumptions made, climate projections provide information about the future state of the climate.

The scenarios used are referred to as Representative Concentration Pathways (RCPs) and represent very widely varying socio-economic pathways of development and the related different impacts on the Earth's radiation and energy budget. The different impacts are a result of the underlying scenarios considering the wide range of potential changes in greenhouse gas emissions. Currently, the focus is on four scenarios up to 2100 which have been developed in preparation of the IPCC Fifth Assessment Report: RCP2.6 (mitigation scenario), RCP4.5, RCP6.0 and RCP8.5 (business-as-usual scenario). They form the basis for assessing the range of future climate changes.

The numbers of the scenario names relate to the additional radiative forcing level expected at the end of the 21st century, i.e. the additional amount of energy (e.g. 8.5 watts per square metre (W/m2) in the RCP8.5 scenario) in the climate system in 2100 compared to the years 1861–1880. Climate projection activities are co-ordinated worldwide as part of the Coupled Model Intercomparison Project (CMIP) initiative set up by the World Climate Research Programme (WCRP).

In order to assess the reliability of a climate model, it is important to simulate the state of the climate over past time periods for which comprehensive sets of observation data are available. The criteria for such evaluation include, among others, the satisfactory reconstruction of averages over the studied period, of the frequency distributions of the data values, of the minimum and maximum values (magnitude and frequency of occurrence) or of the annual variation cycle, the spatial occurrence patterns and the changed signal observed during the studied period. Another essential criterion is whether a climate model is able to provide a realistic reproduction of the so-called climate sensitivity, which is usually understood as the atmospheric warming following a doubling of the carbon dioxide concentration in the atmosphere.

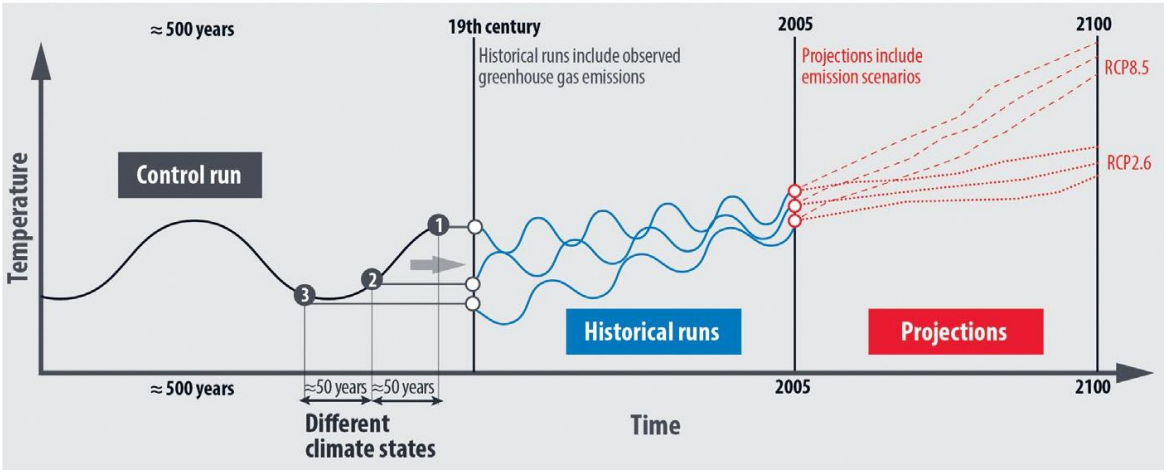

Figure 21: Schematic representation of climate projection

3.3.3 Statistical Downscaling

Statistical downscaling is an approache to generate high-resolution regional climate models based on the large-scale information from either reanalysis data or global climate models.

The Statistical downscaling model (SDSM) (Wilby et al. 2002) which is a hybrids tatistical downscaling method incorporating a weather generator and a multiple linear regression technique, is used in this study.The primary principle of SDSM is to establish the statistical relationship between the predictands and predictors and then determine the required parameters for the weather generator at each individual grid point. If the relationships betweena certain predictand and predictors are statistically significant, the SDSM can regress the predictands

The SDSM-DC version 5.2 was used to generate daily rainfall and temperature scenario datasets for the study area through the following process: (1) quality control (2) predictor variable selection (3) model set-up and calibration (4) weather generation, and (5) generation of future climate scenario. Reanalyzed atmospheric dataset acquired from National Center for Environmental prediction (NCEP) at 275km resolution for the Continental Terminal was used together with the observed rainfall and temperature data for the SDSM model calibration at the monthly scale. The large-scale predictor variables were screened further to select the best predictors for temperature and rainfall required for the weather generator. The rainfall and temperature time series were considered as conditional and unconditional variable respectively based on its normal distribution. Correlation analysis was done at 0.05 significance level based on partial correlation (partial r) value and P-value for the model calibration period of 1982 to 2011. The calibrated SDSM-DC model was used to generate 20 ensemble mean of downscaled daily rainfall and temperature for each station and gridded location using the weather generator. After comparing results of simulated and observed rainfall and temperature, the calibrated SDSM-DC model was used to generate future (2020-2049) climate change scenario (RCP 4.5) datasets based on projections from multi-model mean of the 5th Coupled Model

Intercomparison Project (CMIP5) of the World Climate Research Program (WCRP). The CMIP5 scenarios run which consist of an ensemble mean of forty-one (41) GCMs projects mean daily rainfall and temperature of 2.57mm and 29.44 ^{o}C respectively for the catchment by 2020-2049. The 2020-2049 RCP4.5 data was generated using mean addition/change factors based on the evaluation of mean annual rainfall, minimum and maximum temperature changes between the historical (1982-2011) and future (2020-2049) period.

3.3.4 Recharge estimation with thornthwaite model

The climate RCM data available were only precipitation and temperature, the recharge estimation has been done using the Thornthwaite model (McCabe and Markstrom 2007) developed by the U.S. Geological Survey which used temperature in degrees Celsius and monthly total precipitation in millimeters as input data. The Thornthwaite model is based on the monthly waterbalance model that is driven by graphical user interface. The water-balance model calculates the water amount of the various components of the hydrological cycle (Figure 22) using a monthly accounting procedure. Seven other "input parameters (runoff factor, direct runoff factor, soil-moisture storage capacity, the latitude of the location, rain temperature threshold, snow temperature threshold, and maximum snow-melt rate of the snow storage)", incorporated in the model, were changed during the model calibration process McCabe and Markstrom, (2007). The model was calibrated to fit the groundwater recharge previously simulated using EARTH model in the past. To calibrate this model, monthly precipitation and temperature from RCP4.5 from 1982 to 2011 were used as input data, direct runoff was set to zero because local scale surface runoff infiltrates on the way to the river system. There is no direct runoff contribution to the discharge of the basin. The soil moisture storage capacity was calibrated to be 100 mm. All other parameters were unchanged. After calibration, the model was applied to simulate groundwater recharge from 2020 to 2049, as well as potential evapotranspiration, actual evapotranspiration, soil moisture storage and runoff.

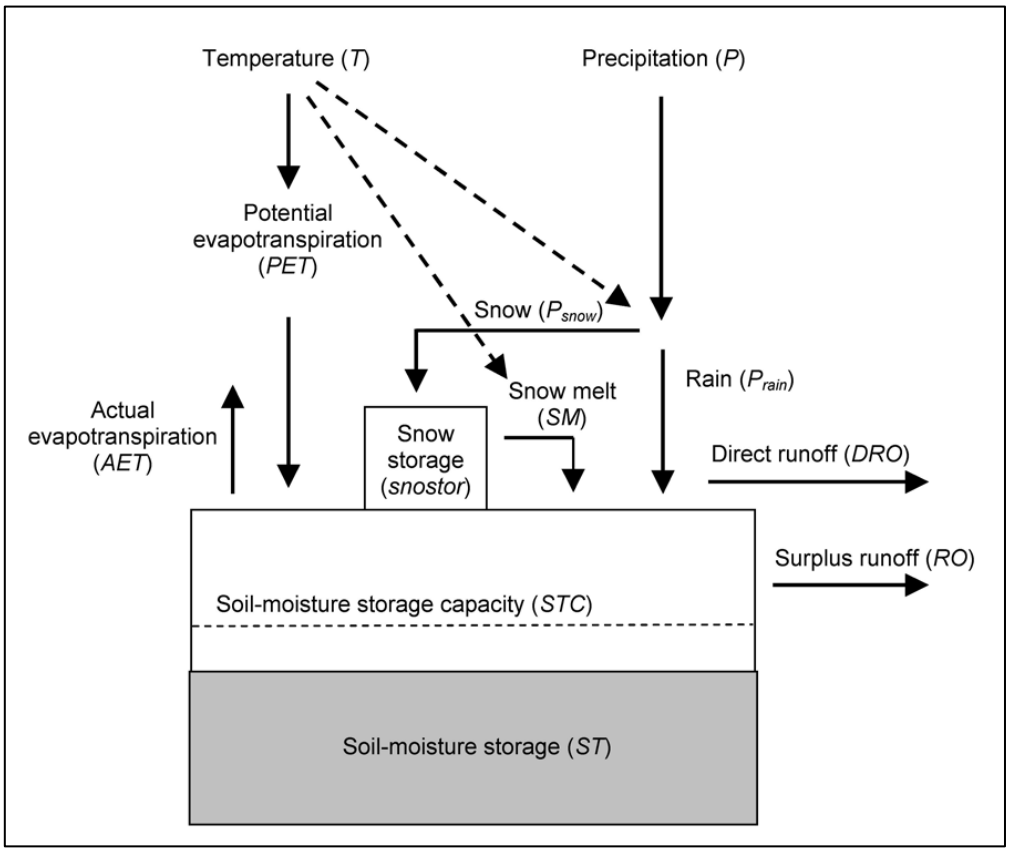

Figure 22: Diagram of the water-balance model.

3.4 Groundwater modelling

Models simplify reality, and are, therefore, imperfect. The famous statistician George Box insisted, all models are wrong, but some are useful (Box and Draper 1987). Applicability of any model and its usage depends on the objectives of that model. Though they are imperfect, models are very useful in hydrogeology. It is a challenge to the modeller to represent the real word problem in a simplified form without compromising the accuracy or making invalid assumptions. Generally, groundwater model is applied in order to estimate the groundwater dynamic (quantity), and/or identify the elements responsible for groundwater pollution (quality). In this study, quantification of the groundwater dynamic was taking into account, as it presents a real problem for every aquifer and difficult to estimate.

All process-based models of groundwater flow are derived from two basic principles: conservation of mass, which states that water is not created or destroyed; and Darcy's law, which states that groundwater flows from high to low potential energy. Groundwater modeling can also be used to predict the future groundwater flow systems by using groundwater models as a predictive tool or as a generic tool to investigate groundwater flow process. As we can notice, groundwater plays an important role in terms of mitigation and adaptation face to climate change nowday; therefore, its modeling can be a powerful tool for water resources

management, groundwater protection and remediation. Groundwater models can be classified into three types: physical, analogue or mathematical models

-Physical models include laboratory tanks andcolumns packed with porous material (usually sand) in which groundwater heads and flows are measured directly. For example, in pioneering work (Darcy 1856) measured head in sand-packed columns of various diameters and lengths to show that flow in porous media is linearly related to the head gradient. Physical models are mostly used at the laboratory scale (Mamer and Lowry 2013; Illman, Berg, and Yeh 2012; Fujinawa et al. 2009; Sawyer, Cardenas, and Buttles 2012)

-Analog models are laboratory models that rely on the flow of electric current electric analog models;(Skibitzke 1961) or viscous fluids (Hele-Shaw or parallel plate models; (Collins and Gelhar 1971) to represent groundwater flow. Analog models of groundwater flow,especially electric analog models, were important in the 1960s before digital computers were widely available (Bredehoeft and Konikow 2012).

-Mathematical model solutions may be either analytical or numerical (Kouli et al. 2009; Baalousha 2009). Analytical methods were first used in hydrogeology to solve the equations (determination of transmissivity), as they are not able to solve complicated equations, then, their application is limited (Simmons et al. 2010) Though the analytical methods are limited by application, they are often very useful because they can serve as verification of solutions of more complex systems obtain by numerical methods (Essink 2000; 2001). In addition, they can provide exact solutions to the governing differential groundwater equations for simple boundary conditions (Shelton 2011). When the partial differential equation become very complex, the use of numerical methods is recommended because they might treat more complicated problems than analytical solutions (Baalousha, 2009). Numerical models are actually more effective and easy to use due to the rapid development of computer processors. They are generally used to simulate problems which cannot be accurately described using analytical models(Mandle 2002). Unlike numerical solutions, analytical solutions give a continuous output at any point in the problem domain. The most numerical methods widely used for solving mathematical model equations are the finite difference and finite element methods (Baalousha, 2009). Only the finite difference methods were applied in this study because they are easy to understand and program (Kinzelbach 1986). The finite difference methods are also used in many computer codes such that MODFLOW and produces reasonably good results. Basically, the finite difference method consists of substituting differential expressions by quotients of differences (Bundschuh and Arriaga, 2010). Therefore, the partial differential equation solution is performed by means of a system of algebraic equations that can be solved using different techniques because the numerators of these quotients are the

differences that include the values of the unknowns (Bundschuh and Arriaga 2010). Furthermore, the finite difference method consists of discretizing the problem area into regular elements that are identified with discrete points or nodes (Essink, 2000). The use of finite difference methods, although widely used, introduces some disadvantages (Baalousha, 2009). For example, they do not fit properly to an irregular model boundary, and output accuracy of the finite difference methods is not good in the case of solute transport modeling (Baalousha, 2009). Groundwater models can be simple, like one-dimensional analytical solutions or spreadsheet models (Olsthoorn 1985) or very sophisticated three-dimensional models. It is always recommended to start with a simple model, as long as the model concept satisfies modelling objectives, and then the model complexity can be increased (Hill 2006). Regardless of the complexity of the model being used, the model development is the same. The stepwise methodology of groundwater modelling is shown in Figure 23. The first step in modelling is identification of model objectives. Data collection and processing is a key issue in the modelling process. The most essential and fundamental step in modelling, however, is model conceptualization. Calibration, verification and sensitivity analysis can be conducted after model completion and the first run. The following sections explain in detail each step in groundwater modelling.

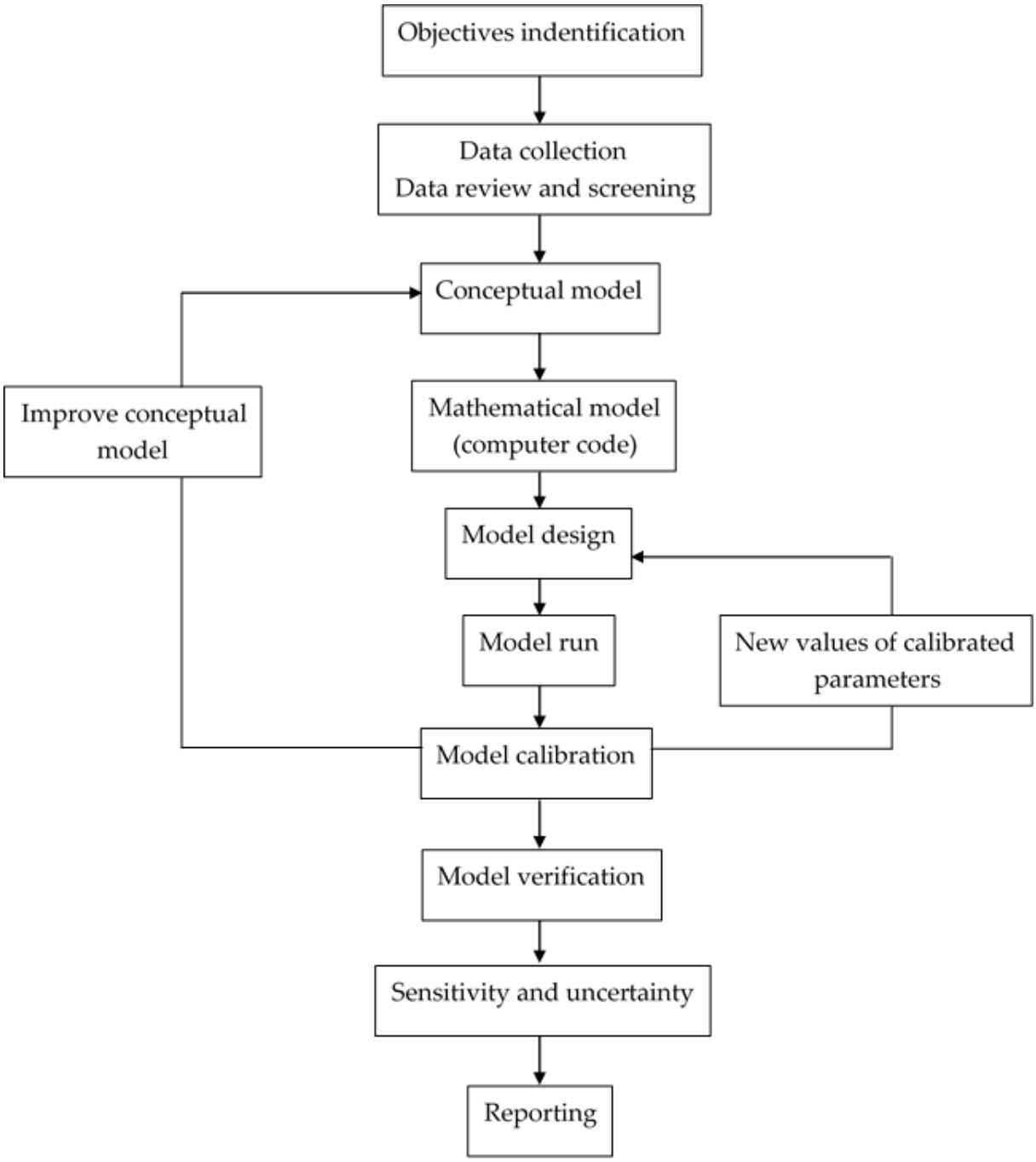

Figure 23: Stepwise methodology of groundwater modelling. modified from (Anderson and Woessner 1992)

3.4.1. Modeling process

3.4.1.1. Conceptual model

To solve any site-specific groundwater problem, the hydrogeologist must assemble and analyze relevant field data and articulate important aspects of the groundwater system. The synthesis of what is known about the site is a conceptual model (Kresic and Mikszewski 2013). A conceptual model is a descriptive representation of a groundwater system that incorporates an interpretation of the geological and hydrological conditions. Information about water balance is also included in the conceptual model. It is the most important part of groundwater modelling

and it is the next step in modelling after identification of objectives. Building a conceptual model requires good information on geology, hydrology, boundary conditions, and hydraulic parameters. A good conceptual model should describe reality in a simple way that satisfies modelling objectives and management requirements (Bear and Verruijt 1987). It should summarise our understanding of water flow or contaminant transport. Development of conceptual model is the most important part of modeling process because theoretically, the numerical model accuracy depends on a good conceptual model (Anderson and Woessner, 1992). This was proved by Council (1999), who affirms that model conceptualization should be re-examined when the model cannot be calibrated to match the calibration data. Furthermore, the conceptual model involves the understanding of aquifer characteristics and their quantification in time and space. A good conceptual model is a simple way to summarize the understanding of groundwater flow behavior. It requires necessary information on geology, hydrology, boundary conditions, and hydraulic parameters. The conceptual model is the basis of the mathematical model and plays an important role for selecting a type of computer code to be used in modeling as well as the design and priority of site characterization activities (Council 1999). The conceptuel model was simplified in this study to facilitate groundwater flow modeling. This simplification involved all important features and processes such as geological data, pumping test data, groundwater levels, rainfall data, topography, groundwater exploitation, *etc.*

A conceptual model in hydrogeology is a representation of the hydrogeological units and the flow system of groundwater which need deep information to be done such as, topography data, surface-water bodies, hydraulic head data, hydraulic conductivity data and groundwater recharge and discharge (Mandle, 2002). Besides, setting up a conceptual model requires three steps: defining hydrostratigraphic units; preparing a water budget; and defining the flow system according Anderson and Woessner (1992).

In many case, it is very difficult to find all information especilly in the current study where the field information collected was not sufficient but represented the essential data, which could allow reproducing as best as possible the natural groundwater system in the study area. Since the study was focused on regional groundwater flow system that does not require excessive details (Wilson 2005). Hydrological logs of boreholes data collected from National water agency (NWA) were used to characterize the lithology of the study area. The study area geology is domonated by lenticular stratification, coarse sand of variegated clays, ironstone and irone, however, for simplification, the aquifer of the study area was set as a single numerical layer under unconfined condition based on birrimians schists which constitutes the impervious base (Tastet, 1979; Sogreah, 1996). The top the aquifer is constituted by the topography which varies

from 0 to 140 m in elevation (Figure 24 and Figure 25). The bottom of the aquifer is located at the contact of fine sands with the granitic bedrock whose elevations varies between +30 and -150 m according Substratum elevation map (Aghui and biemi, 1984) showing in Figure 24 and Figure 26

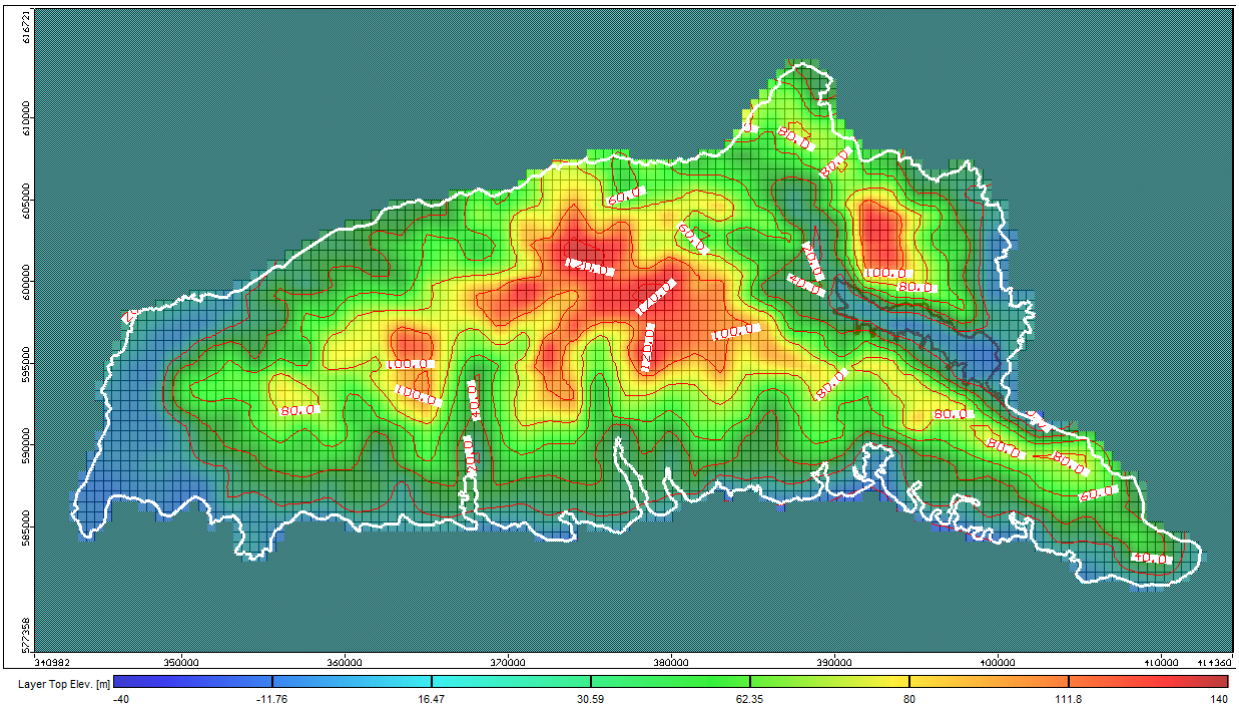

Figure 24: Top the aquifer

Figure 25: Aghien lagoon and high altitude (hills)

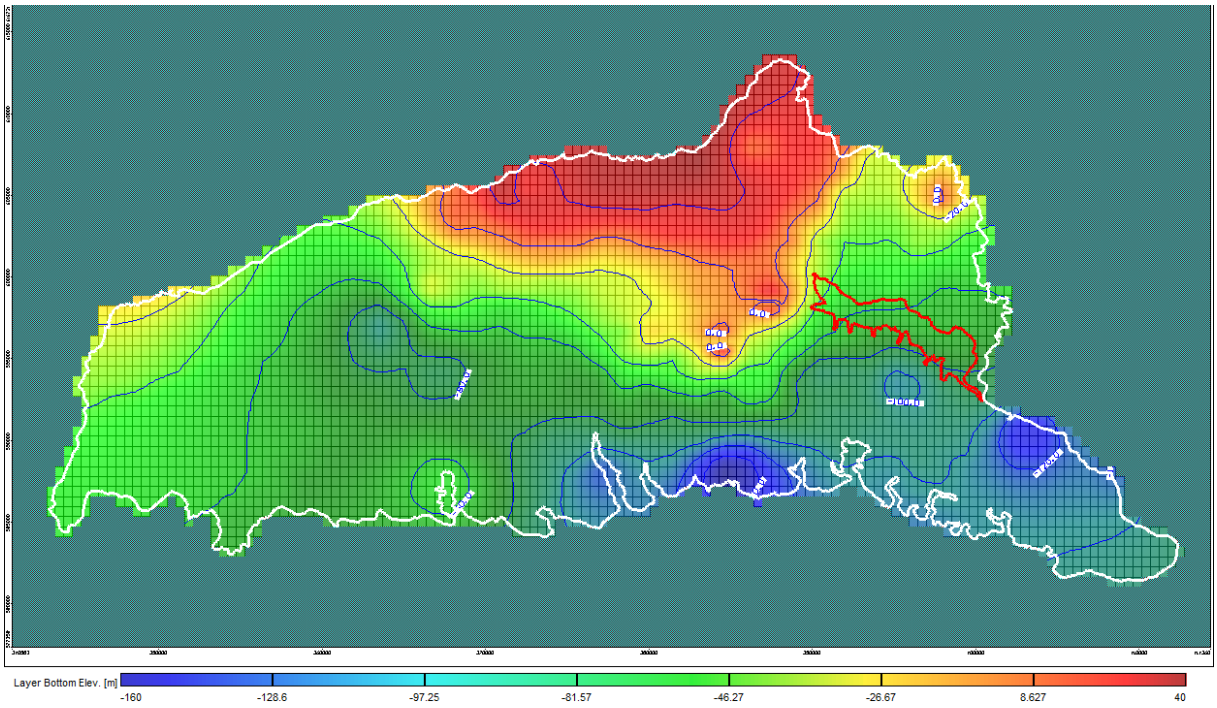

Figure 26: The bottom of the aquifer

The thickness of the aquifer varies between 20 m in the North and 160 m in the South (Jourda, 1987).The model is one layered (Figure 27) constitute by coarse sand fine sand (Sogreah, 1996).

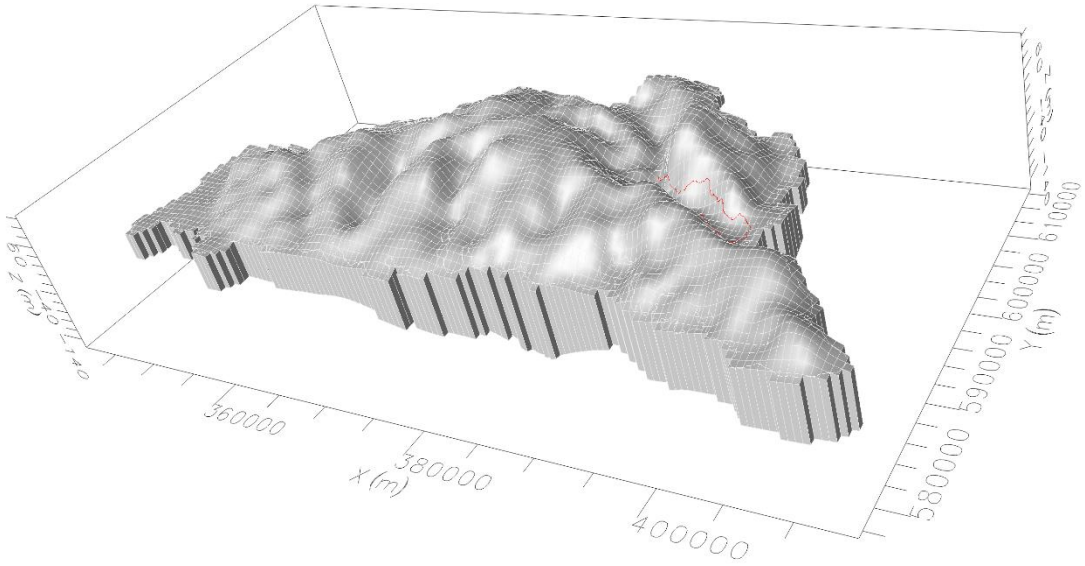

Figure 27: Model geomertry in 3D

The pumping test data was investigated to estimate the value of hydraulic conductivity based on Cooper-Jacob method (Cooper and Jacob, 1946). Hydraulic conductivity is a one of the important parameter use in groundwater modeling flow occording to Jeffrey (1997). Its variability (increase or decrease) affects directly groundwater flow rates estimation (Healy and Scanlon 2010; Moore 2002).

The hydraulic conductivity obtained form pumping test was adjusted during the calibration process to simulate the groundwater level. Calibrated values are between 1.10^{-5} and 3.10^{-4} m/s

(Figure 28), which is relevant according to the lithology facies of the aquifer and the pumping test results

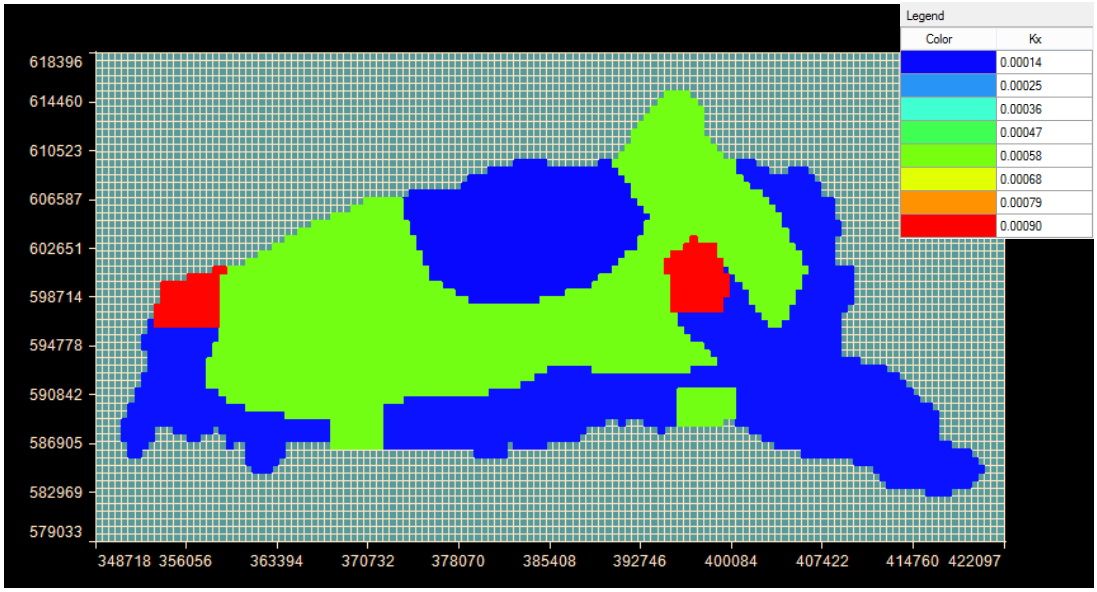

Figure 28: Permeability values distribution

Groundwater recharge is essential in groundwater modeling study and it is one of the most difficult hydrological component to be quantified (Wheater 2010). Groundwater recharge are estimated using water table fluctuation and mass balance method. The results from theses methods were adjusted as well during the calibration process and shows that the highest recharge value are located in the northeast part of the study area which is about 500 mm/year and the lowest recharge value is 5 mm/year distributed along the slopes of the aghien lagoon (Figure 29), this low recharge rate can be justified by the high runoff in this area, drained by the lagoon. It should be noted that evapotranspiration has been removed directly from the recharge.

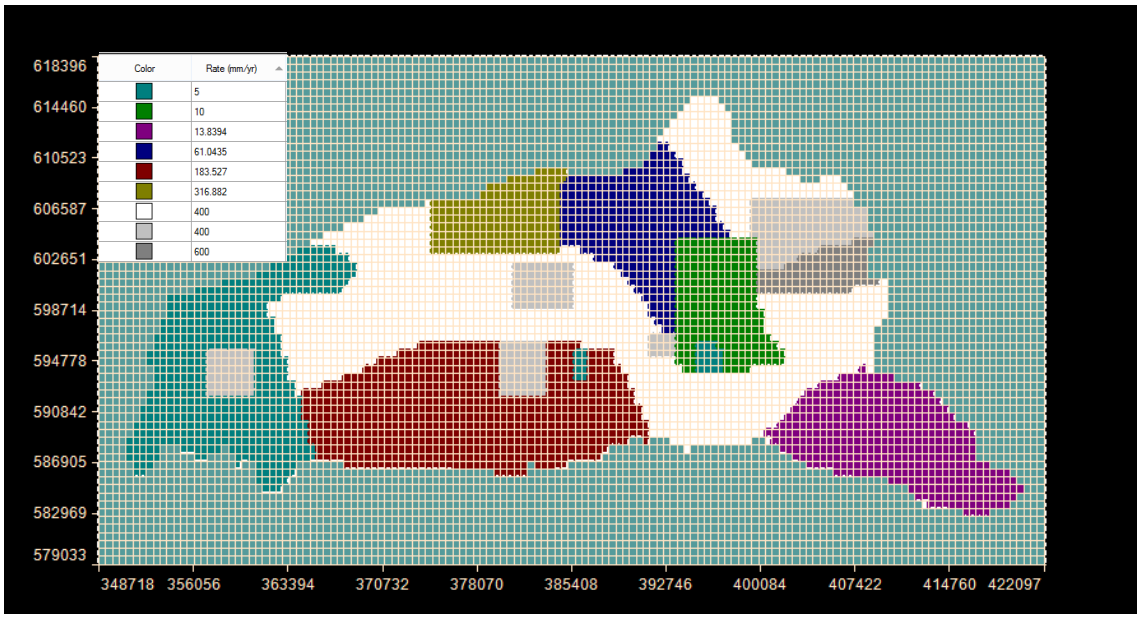

Figure 29: Recharge values distribution

3.4.1.2 Model software selection

Groundwater flow modelling procedure begins with a proper understanding of the hydrogeological setting or physical system and the problem to be investigated. Once the system is well understood, the next step is to translate the physical system into a set of solvable mathematical equations. This has resulted in the familiar groundwater flow and transport equations in common use today. However, the choice of a numerical method depends on the convenience and expertise of the modeller and the nature of the data available. There are numerous groundwater flow models available, but the widely used, since the 1990s, over time and space is MODFLOW (Harbaugh 2005), and was selected in this study. MODFLOW is a modular three-dimensional finite-difference groundwater model that was developed by the United States Geological Survey (USGS), and first published in 1984 (McDonald and Harbaugh 1988). The model code is written in FORTRAN and divides input data into modules known as packages (Ahern 2005). MODFLOW uses groundwater flow equation that is the combination of continuity equation and Darcy's law (Harbaugh, 2005). In a porous medium, the partial-differential equation (Equation 20) is used to simulate the movement of the three-dimensional groundwater flow (Harbaugh, 2005):

$$\frac{\partial}{\partial x}\left(K_{xx}\frac{\partial h}{\partial x}\right)+\frac{\partial}{\partial y}\left(K_{yy}\frac{\partial h}{\partial y}\right)+\frac{\partial}{\partial z}\left(K_{zz}\frac{\partial h}{\partial z}\right)-W=S_S\frac{\partial h}{\partial t} \qquad \text{Equation 20}$$

Where K_{xx} , K_{yy} , K_{zz} are the hydraulic conductivities in the x, y and z directions respectively which are assumed to be parallel to the axes of hydraulic conductivity (LT^{-1}) h is the potentiometric head (L), W is a volumetric flux per unit volume and represents sources and/or sinks of water (T^{-1}), S_s is the specific storage of the porous material (L^{-1}) and t is the time (T). Equation (14) describes groundwater flow under transient or non-equilibrium conditions in a heterogeneous and anisotropic medium when the principal axes of hydraulic conductivity are aligned parallel to the coordinate directions.

Under steady state conditions, the time variable nature of the hydraulic head on the right-hand side of Equation 20 becomes negligible when sinks are not considered significant enough to cause such changes. As such, (Equation 20) is reduced to (Equation 21)

$$\frac{\partial}{\partial x}\left(K_{xx}\frac{\partial h}{\partial x}\right)+\frac{\partial}{\partial y}\left(K_{yy}\frac{\partial h}{\partial y}\right)+\frac{\partial}{\partial z}\left(K_{zz}\frac{\partial h}{\partial z}\right)=0 \qquad \text{Equation 21}$$

Equation 20 and Equation 21 are both derived from the law of conservation of mass and the continuity equation for heterogeneous anisotropic media. Two main approaches are used to solve equations (14) and (15). These are the finite element approach and the finite difference approach. In either case, a system of nodal points is superimposed over the problem domain (Wang and Anderson 1982) and the aquifer sub-divided into a grid to analyse the flows

associated within a single zone of the aquifer (Igboekwe and Achi 2011). This governing equation 15 can be solved either analytically or numerically. Dependent on their approaches, assumptions and capability, both methods (analytic and numeric) may be used to solve the equation (Belay 2009). MODFLOW is known as one of the best tools to describe and predict groundwater flow system. It is able to simulate both, steady state and transient flow conditions in unconfined aquifers, confined aquifers and variably confined/unconfined aquifers (Kim *et al.*, 2008).

MODFLW (McDonald and Harbaugh 1988) was used as calculation program broadly because of its simple methods, modular program structure and separate package to resolve special hydrogeological problems. For example, the popular software of GMS, Visual MODFLOW and PMWIN were all developed based on MODFLOW program. Combing with GIS technology they provided good visualization interface for user and played a significant role in the groundwater evaluation and management of many countries. From now on, many 2-D or 3-D groundwater flow quantity and quality models have been constructed successfully to resolve many groundwater flow problems.

3.4.1.3 Model set up

Building a conceptual model requires good information on geology, hydrology, boundary conditions, and hydraulic parameters. Setting up conceptual model is a more complex and time-consuming process and should describe reality in a simple way that satisfies modelling objectives and management requirements (Bear and Verruijt 1987). To simulate groundwater flow, we need to applied finite element method. In this study, MODFLOW was choosen to simulate groundwater flow. The modular design of the MODFLOW model allows for the addition of new packages to both expand the capacity of the model and improve the accuracy. A number of additional packages have been developed, ranging from the simulation of the effect of artificial recharge to the interaction between surface water and groundwater.

3.4.1.3.1 Model discretization

A groundwater flow model in the study are was built using Visual Modflow Flex 6.1. The Continental Terminal with an area of 1160 km^2 is assumed to be a rectangular shape. The grid cells were designated as “inactive” outside the model domain and as “active” inside the model domain. (Figure 30) The model was divided into 64 rows and 139 columns with the size of each cell being 500 × 500 m. The model includes one layers to represent the hydrogeological condition and data on the porous aquifers at the study site. The simulation period was from January 2010 to 31 December 2017, with 120 stress periods defined for the simulation. Two time steps were defined for each stress period. Groundwater levels observed in 2017 were used as the initial conditions of the model.

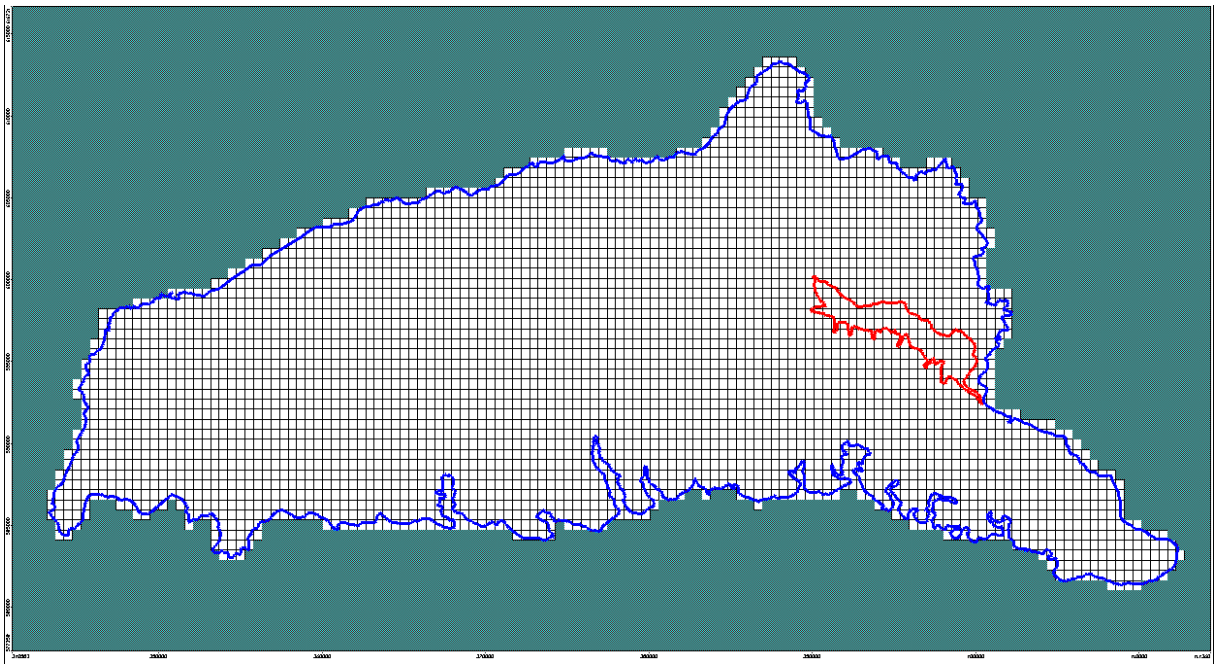

Figure 30: Map showing grid over entire coverage area.

3.4.1.3.2 Aquifer geometry

All relevant features or data, such as topography, digital elevation model (DEM), borehole data, geological structure, drainage density, groundwater flow, and boundary conditions of the aquifer system are very important for setting up the model (Chenini and Ben Mammou 2011; Yao et al. 2015). However, aquifer geometry determination is critical in numerical modeling because it influences model calibration results (Middlemis 2001) .The DEM was used as the aquifer top and the rock as a basement. The thickness changed from the south to the north

3.4.1.3.3 Aquifer properties

Aquifer properties are the most important part of the modeling groundwater flow system. The hydraulic properties of an aquifer, including transmissivity, hydraulic conductivity and storativity, determine water movement through the aquifer as well as storage in the aquifer. Different methods such as Theis, Jacob and Theim are commonly used to determine the aquifer properties from pumping test data (Singhal and Gupta 2010). In this study, the horizontal hydraulic conductivity value was calibrated until a good correlation between simulated and observed heads was obtained.

3.4.1.3.4 Boundary conditions

Boundary conditions are a key component of a mathematical model and strongly influence the flow directions calculated by a steady-state numerical model and most transient models. Boundaries include hydraulic features such as groundwater divides and physical features such as bodies of surface water and relatively impermeable rock. Boundary conditions can be classified into three main types:

- Specified head (also called Dirichlet or type I boundary). It can be expressed in a mathematical form as: h (x,y,z,t) = constant
- Specified flow (also called a Neumann or type II boundary). In a mathematical form it is: ∇h (x,y,z,t) = constant
- Head-dependent flow (also called a Cauchy or type III boundary). Its mathematical form is: ∇h (x,y,z,t) + a*h = constant (where "a" is a constant).

It is preferable to use physical boundaries when possible (e.g., impermeable boundaries, lakes, rivers) as the model boundaries because they can be readily identified and conceptualised

Selection of boundary conditions is critical to the development of an accurate model (Franke et al. 1987). In Modflow, two categories of cells (constant-head and no-flow cells) can be used to simulate boundary conditions. "Constant-head cells are those for which the head is specified for each time and the head value does not vary as a result of solving the flow equations. No-flow cells are those for which there is no flow into or out of the cell (Harbaugh, 2005). The value 1 was set to constant-head cells inside the basin and the value -1 was assigned to no-flow cells outside the basin.

In this study hydraulic boundaries conditions expected are very clear due to the existence of very dense hydrogrqphic network in the area which acts as a nutural boundary. The boundary conditions are:

-Constant head limits in areas where water bodies are present,

-River condition at Aghien cells

-Non flow limit in noth where the basement outcrops

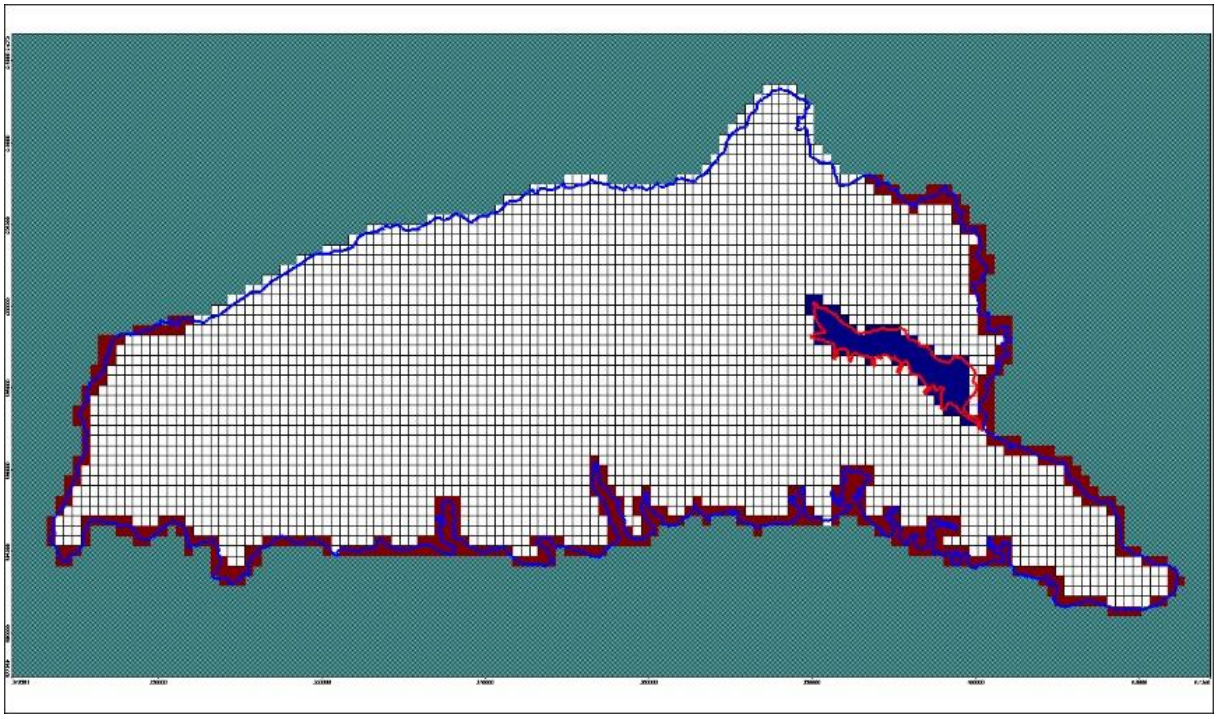

Figure 31: Boundary conditions

The River boundary condition is used to simulate the influence of a surface water body on the groundwater flow. Surface water bodies such as rivers, streams, lakes and swamps may either contribute water to the groundwater system, or act as groundwater discharge zones, depending on the hydraulic gradient between the surface water body and the groundwater system. The Modflow River Package simulates the surface water/groundwater interaction via a seepage layer separating the surface water body from the groundwater system (see following figure). The Modflow River Package input file requires the following information for each grid cell containing a River boundary;

- River Stage: The free water surface elevation of the surface water body. This elevation may change with time.
- Riverbed Bottom: The elevation of the bottom of the seepage layer (bedding material) of the surface water body.
- Conductance: A numerical parameter representing the resistance to flow between the surface water body and the groundwater caused by the seepage layer (riverbed).

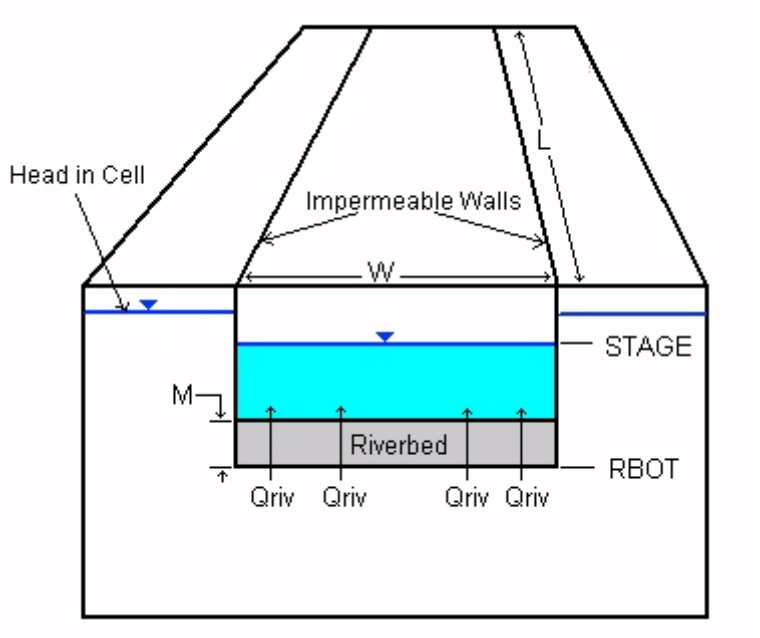

Figure 32: Schematic of river boundary

3.4.2. Hydrogeological characterization and numerical simulation models

Lithological log data obtained during the field survey were carefully studied and compared with the known geology and hydrogeology of the study area to ensure coherency and accuracy. The data captured information on the borehole IDs, their spatial positions (longitudes and latitudes in degree decimals) and locations, well depths, top and bottom elevations, hydrogeological unit descriptions and lithology types. A total of fifty five wells were logged showing rock types such as clay, mudstone, intercalations of mudstone, laterite, and sandstone. A distribution of the

wells locations with regards to their spatial positions is shown in Figure 33.Drill depth of boreholes in the study area is recorded between 50 m to 191 m.

The longitudes and the latitudes of the boreholes were converted to Universal Transverse Mercator (UTM) in units of metres. Also, elevations and descriptions on the well logs were imported into MODFLOW for lithological and hydrostratigraphy modelling. Static water level values obtained from the monitoring well data were averaged for the period 2010 to 2017 and processed into appropriate formats for steady state simulation in MODFLOW. Hydraulic head data was obtained by subtracting the averaged static water levels from the reference elevations of the boreholes.

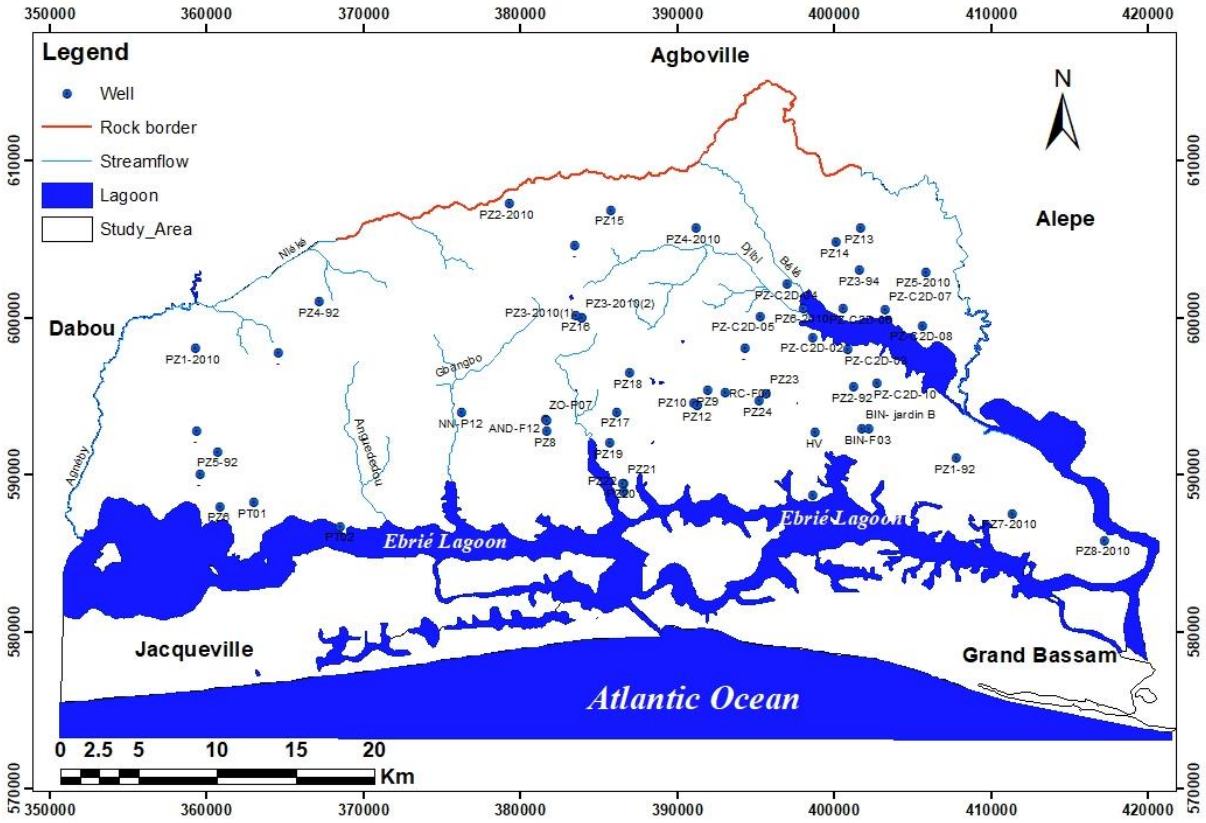

Figure 33: Map showing the borehole locations in the Continetal Terminal

3.4.3 Numerical simulation of flow

The most commonly used numerical model to simulate surface water–groundwater interactions is Modflow (Furman 2008; Barlow and Harbaugh 2006). However, there are also a number of more sophisticated models that include a more realistic physical coupling between surface water and groundwater.

Numerous streamflow packages with different levels of complexity have been developed for Modflow. We limit our discussion to streamflow packages developed by the USGS because of their availability and their widespread acceptance. The first streamflow package was the River Package RIV (McDonald and Harbaugh 1988). In the River Package, rivers are conceptualized

as head dependent flux boundaries. Follow-up packages to the River Package are the Stream Package STR1 (Prudic 1989), the Streamflow Routing Package SFR1 (Prudic et al. 2004), and the Streamflow Routing 2 Package SFR2 (Niswonger and Prudic 2006). Several conceptual assumptions of the River Package are the same in all streamflow packages. In all of Modflow's streamflow packages, the flow from a river to the aquifer is calculated differently for hydraulically connected and disconnected systems. In Modflow terminology, the groundwater is hydraulically connected if the water table is above the elevation of the base of the streambed sediments. In this case, the exchange volumetric flux $Q_{MF}[L^3T^{-1}]$between the river and the groundwater is calculated using

$$Q_{MF} = \frac{K_c L_w}{h_c}(h_{riv} - h) = C_{riv}(h_{riv} - h) \qquad \text{Equation 22}$$

where $K_c[LT^{-1}]]$ is the hydraulic conductivity of the clogging layer, L is the length of the river within a cell [L], w is the width of the river [L], h_c [L] is the thickness of the clogging layer, h_{riv} is the hydraulic head of the river [L], h is the groundwater head, and C_{riv} $[L^2T^{-1}]$ is the conductance of the clogging layer (McDonald and Harbaugh,1988). The hydraulic conductance is a lumped parameter summarizing the geometry of the river and the clogging layer as well as its hydraulic conductivity.

If the water table h is below the elevation of the streambed bottom $Z_a(h < Z_a)$, the surface water groundwater system is considered hydraulically disconnected in MODFLOW. In this case, the volumetric infiltration flux Q_{MF} from the river to the aquifer is calculated using

$$Q_{MF} = C_{riv}(h_{riv} - Z_a) \qquad \text{Equation 23}$$

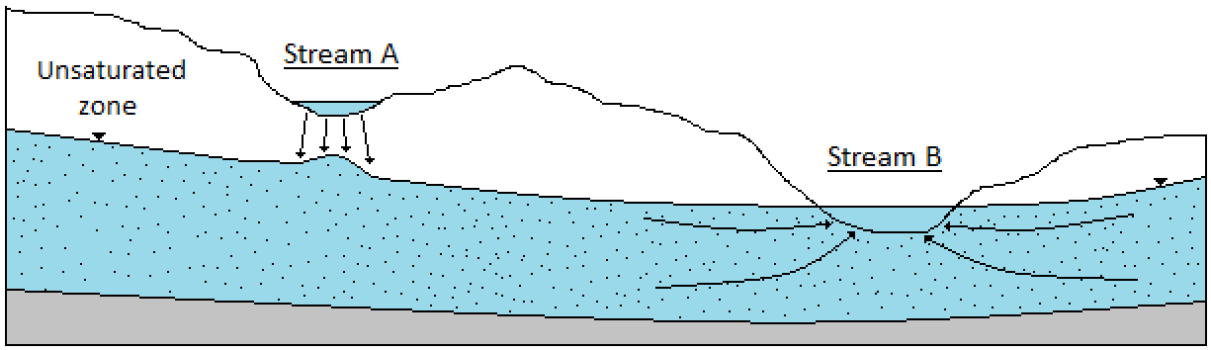

Figure 34: Landscape division of surface water-groundwater interaction type. Stream A is a disconnected losing stream with the river stage positioned above the regional groundwater table, while Stream B is a gaining stream with the river stage positioned below the regional groundwater table.

3.4.4. Calibration of the model

Model results may differ from field measurements after the first run of a model. This is expected because modelling is just a simplification of reality and approximations and computational errors are inevitable. The process of model calibration is aimed at fine-tuning the model results to match the measurements in the field. In a groundwater flow models, the resulting groundwater head is forced to match the head at measured points. This process requires changing model parameters (i.e. hydraulic conductivity or groundwater recharge) to achieve the best match.The calibration process is important to make the model predictive and it can also be used for inverse modelling.

To illustrate the calibration process of a groundwater flow model, consider the groundwater head measurements $(h_{ob})_i$at the observation point i. The simulated head at thesame point is $(h_{sim})_i$. The root mean square error of the residual is given by:

$$RMSE = \left[\frac{1}{n}\sum_{i=1}^{n}(h_{ob} - h_{sim})^2\right]^{1/2} \qquad \text{Equation 24}$$

Calibration involves an optimization process to minimize the RMSE given in (Equation 24) to get a well-calibrated model, proper site characterisation and sample data are required. Otherwise, the calibrated model will only be valid for a set of conditions and not for any condition. Calibration can be manually done or automatically. Software like PEST (Doherty et al. 1994) and UCODE (Poeter and Hill 1998) can be used for automatic calibration.

3.4.4 Model Verification and Validation

The term “validation” is not completely true when are in groundwater modelling domain. (Oreskes et al. 1994) asserted it is impossible to validate a numerical model because modelling is only approximation of reality Model verification and validation is the next step after calibration. The objective of model validation is to check if the calibrated model works well on any dataset. Because the calibration process involves changing different parameters (i. e. hydraulic conductivity, recharge, pumping rate etc.) different sets of values for these parameters may produce the same solution. (Reilly and Harbaugh 2004) concluded that good calibration did not lead to good prediction. The validation process determines if the resulting model is applicable for any dataset. Modellers usually split the available measurement data into two groups; one for calibration and the other for validation.

3.4.5 Sensitivity Analysis

Sensitivity analysis is important for calibration, optimisation, risk assessment and data collection. In regional groundwater models, there are a large number of uncertain parameter. Coping with these uncertainties is time-consuming and requires considerable effort.

Sensitivity analysis indicates which parameter or parameters have greater influence on the output. Parameters with high influence on model output should get the most attention in the calibration process and data collection. In addition, the design of sampling location, and sensitivity analysis can be used to solve optimisation problems. The most common method of sensitivity analysis is the use of finite difference approximations to estimate the rate of change in model output as a result of change in a certain parameter. The Parameter Estimation Package "PEST" uses this method (Doherty et.al. 1994).

Some other more efficient methods of sensitivity analysis have been used. Automatic differentiation has been used for sensitivity analysis in groundwater models and it produces precise output compared to finite difference approximations (Baalousha 2007)

3.4.6 Uncertainty Analysis

Uncertainty in groundwater modelling is inevitable for a number of reasons. One source of uncertainty is the aquifer heterogeneity. Field data has uncertainty. Mathematical modelling implies many assumptions and estimations, which increase the uncertainty of the model output (Baalousha and Köngeter 2006).

There are different approaches to incorporate uncertainty in groundwater modelling. The most famous approach is stochastic modelling using the Monte Carlo or Quasi Monte Carlo method (Liou and Der Yeh 1997; Kunstmanna and Kastensb 2006). The problem with stochastic models is that they require a lot of computations, and thus they are time consuming. Some modifications have been done on stochastic models to make them more deterministic, which reduces computational and time requirements. Latin Hypercube Sampling is a modified form of Monte Carlo Simulation, which considerably reduces the time requirements (Y. Zhang and Pinder 2003).

3.4.7 Common Mistakes in Modelling

A major mistake in modelling is conceptualisation. If the conceptual model is incorrect, the model output will be incorrect regardless of data accuracy and modelling approach. A good mathematical model will not resurrect an incorrect conceptual model (Zheng and Bennett 2002) . In all models, it is necessary to identify a certain reference elevation for all head so that the model algorithm can converge to a unique solution (Franke et al. 1987).

Boundary conditions should be treated with care, especially in a steady state simulation. Sometimes boundary conditions change during simulation and become invalid. A model with hydraulic boundary conditions will be invalid if stresses inside or outside the model domain cause the hydraulic boundaries to shift or change. Therefore, boundary conditions should be monitored at all times to ensure they are valid.

Model parameterisation is a common mistake in modelling. Theoretical values of hydraulic properties or groundwater recharge should never substitute field data and field investigation. Assumptions like isotropy and homogeneity should not be used without support from field investigation.

Selection of the model code is important to obtain a good solution. Different codes involve different mathematical settings that suit a certain problem. The selected code should consider characteristics of the area of interest and the objectives of modelling.

Models can be well calibrated and match well with the measured values, but have an incorrect mass balance. This can be a result of an improper conceptual model.

3.5 Piezometry characterization

Grandwater flow direction and recharge are importante in aquifer characterization when it is about groundwater flow understanding. Hydrogeoelogy model setup requiere hydraulic head meserment in different site of the study area, piezometer map is necessary to be done using the hydraulic head and allow to identify the area where grandwater flow is changing (Atteia 2011) and recharge zone. In fact these zone are important to identify especially the recharge zone because it determine groundwater renewed zone and make it continuing in many years.

3.5.1 Hydraulic head

Hydraulic head is the mechanical energy that causes groundwater to flow. It can be calculated in two ways: the sum of pressure head (hp) and elevation head (z), or h= (hp+hz) and the difference between the land surface and depth of water or h= land elevation –depth to water. Where the pressure head (hp) is the height that water rises in a piezometer (a well that is open only at the top and bottom of its casing), the elevation head (z) is the elevation of the bottom of the piezometer or measuring point in feet above sea level.

3.5.1.1 Piezometer network

Piezometers (55) had been monitore since 2010 by ONEP. All the piezometers are regulary followed on bimonthly basis with some interruption observed during the crisis period. These piezometers were carried out on different project. Some of them have been build in 1992 and others in 2010 and the most recent in 2016 and 2017. We also have a piezometric data monitoring from 1977 to 1992. Most of the piezometers are not functional except filtisac piezometer (Pz 18)

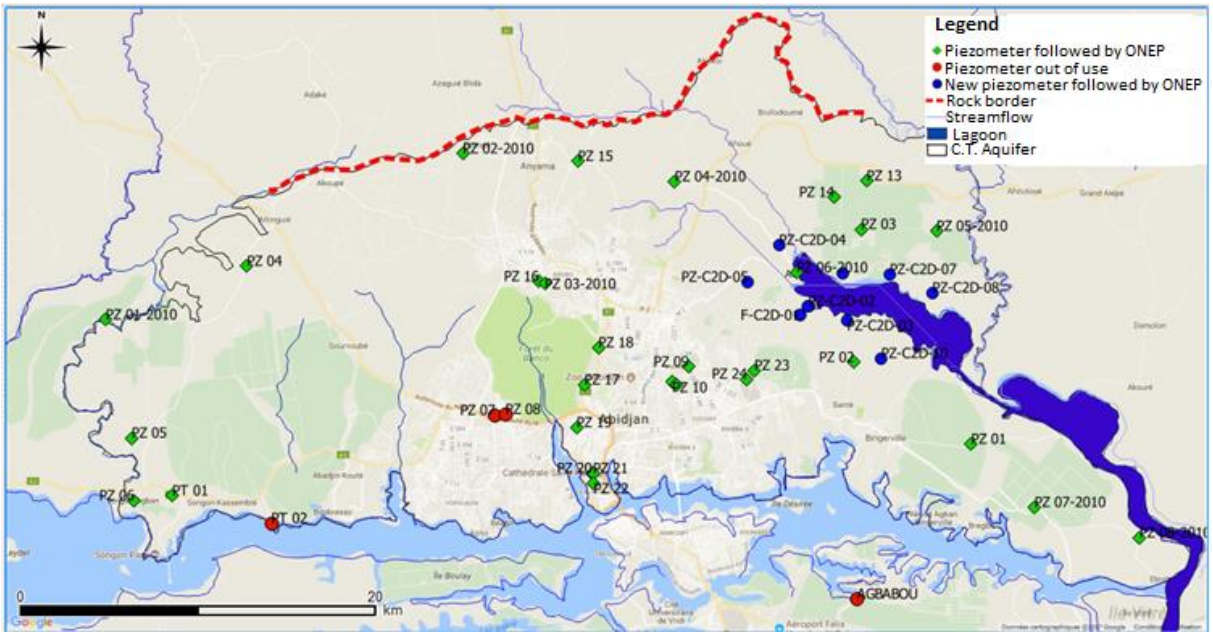

Figure 35: Piezometers location on the study area

Table VII: Piezometers used during the study

N°	Denomination	Longitude (m)	Latitude (m)	hydraulic heads
1	PZ22	386530	588970	-1.71
2	PZ8-2010	417108	585881	-1.05
3	PZ1-92	407686	591111	1.2
4	PZ7-2010	411233	587587	1.2
5	PZ21	386497	589515	1.38
6	PZ20	386442	589515	2.106
7	PZ23	395555	595231	2.794
8	PZ6	360805	588045	2.8
9	BIN- jardin B	401677	593022	3.22
10	PZ19	385593	592071	3.24
11	-	398527	588757	3.55
12	PZ1-2010	359233	598123	3.82
13	PZ2-92	401136	595676	4.55
14	PZ17	386054	594054	5.06
15	PZ6-2010	397921	600679	5.33
16	PT02	368471	586761	5.75
17	ZO-P07	381529	593623	5.97
18	PZ11	391209	594468	6.037
19	PZ9	391880	595437	6.38
20	PZ-C2D-10	402652	595894	6.65
21	PT01	362927	588312	6.7
22	PZ10	390933	594597	6.72
23	PZ-C2D-03	400739	598030	6.94
24	BIN-F03	402072	592967	8.16
25	PZ-C2D-04	396940	602212	8.44
26	-	359524	590131	8.57
27	PZ12	391214	594465	8.78
28	PZ24	395128	594757	9.58

29	HV	398691	592745	9.94
30	PZ-C2D-08	405521	599544	10.06
31	-	394218	598132	10.15
32	PZ-C2D-02	398575	598809	10.67
33	PZ5-92	360667	591534	10.915
34	PZ-C2D-07	403137	600572	11.93
35	PZ5-2010	405758	602977	12.43
36	PZ-C2D-06	400487	600624	13.2
37	PZ-C2D-05	395201	600157	14.87
38	-	359277	592881	15.62
39	PZ3-94	401531	603088	16.08
40	RC-F01	392951	595311	16.4
41	PZ18	386849	596529	16.43
42	PZ8	381617	592816	17.23
43	NN-P12	376193	594020	17.75
44	AND-F12	381614	593548	19.37
45	PZ14	400031	604870	20.53
46	PZ4-92	367143	601090	20.64
47	PZ13	401589	605782	21.1
48	-	364540	597854	22.63
49	PZ3-2010(1)	383813	600083	29.08
50	PZ3-2010(2)	383813	600083	29.08
51	PZ16	383488	600206	32.35
52	PZ4-2010	391104	605756	40.05
53	PZ15	385690	606903	51.19
54	-	383416	604671	54.81
55	PZ2-2010	379234	607334	62.92

3.5.1.2 Manual measurement

For the manual reading, we carry out each two months a field work aquipped with a water level meter multifunction which is able to measure groundwater level, hydraulic conductivity and the pH.

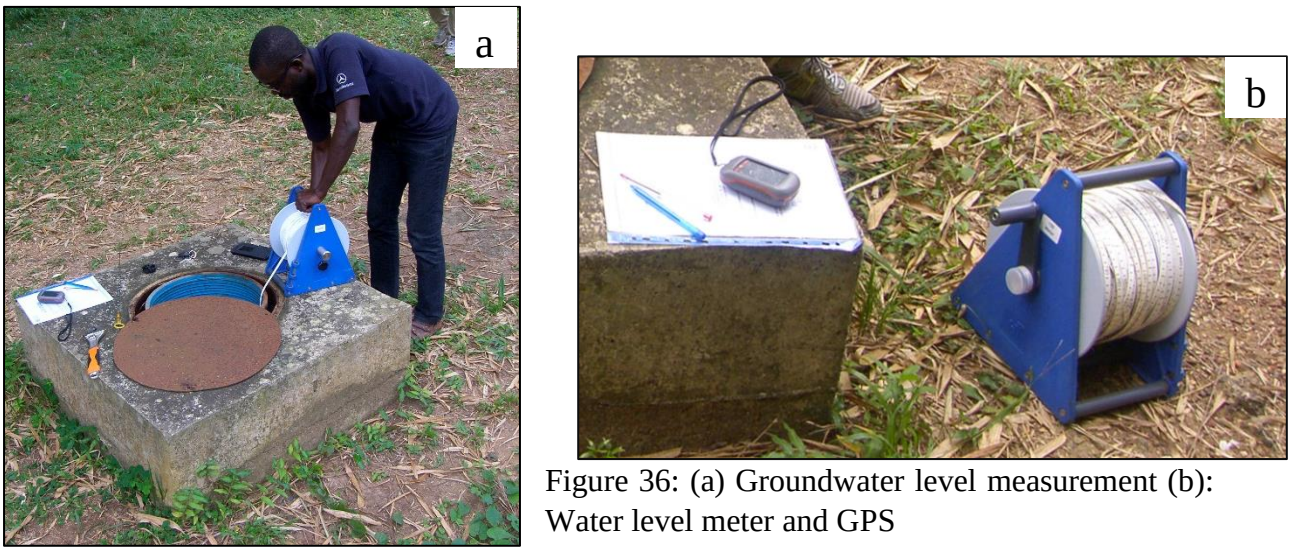

Figure 36: (a) Groundwater level measurement (b): Water level meter and GPS

3.5.1.3 Automatic measurement

Thalimedes measures water levels using an electronic sensor, and then stores this data in the logger's non-volatile memory. The records are retrieved using: (a) a laptop PC, or (b) the OTT VOTA data retrieval unit. Thalimedes can either be used as a stand-alone device, or attached to an existing strip chart recorders. Thalimedes is a float-operated shaft encoder with integrated datalogger. Changes in water level are transferred via a float-cable-counterweight system to a pulley on the encoder unit. The rotation caused by this action is converted into an electrical signal, which is then transferred to the datalogger and saved as a measurement. This mechanism is illustrated in Figure 37.

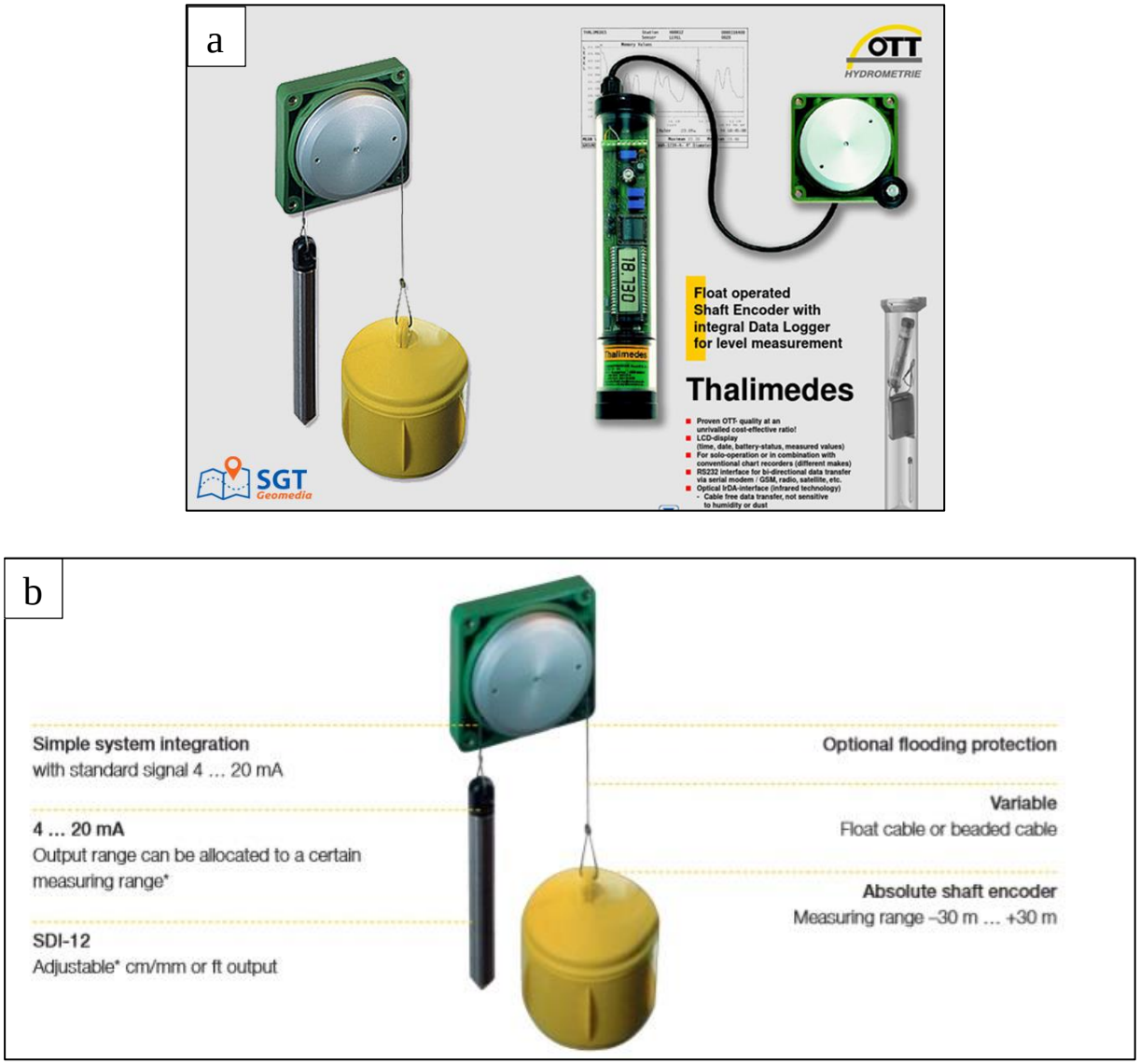

Figure 37: (a): Datalogger (b): Thalimedes setup

3.5.2 Data process and Analyse

Data acquired manually and automatically are processed before their analysis

3.5.2.1 Manual data

Piezometric levels were obtained from the depths of water measured manually from Equation 25

$$PL = Gl - Wl + Ag$$ Equation 25

With PL (m) =Piezometer Level; Gl (m) =Ground level; Wl (m) =Water level in the piezometer and Ag (m) = Above ground

3.5.2.2 Automatic data

Automatic acquisition data are corrected before being used. Leveloggers (L) measure the total pressure acting on a transducer at their zero point/sensor. The total pressure is caused by the column of water lying above the Levelogger pressure sensor and the barometric (atmospheric) pressure acting on the water surface. To compensate for barometric pressure fluctuations and get true height of water column measurements (H), a Barologger (B) is required

$$H = L - B$$ Equation 26

With L=levelogger Reading; B=Barologger Reading and Height of H =Water Column

Levelogger is rated for a specific submergence depth. The choice of model largely depends on the accuracy of the water level required and the submergence depth. The selection is based on the maximum anticipated water level fluctuation."

Verifying Readings

The best recommendation is to compare barometrically compensated Levelogger data **(**H**)** with a measured depth to water level value **(**d**)** (using a water level meter). The deployment depth of the Levelogger **(**D**)**, minus the manual depth to water measurement **(**d**)**, should equal the compensated Levelogger reading.

$$H = D - d$$ Equation 27

With Deployment depth =D; Depth to water =d and Height of water column=H

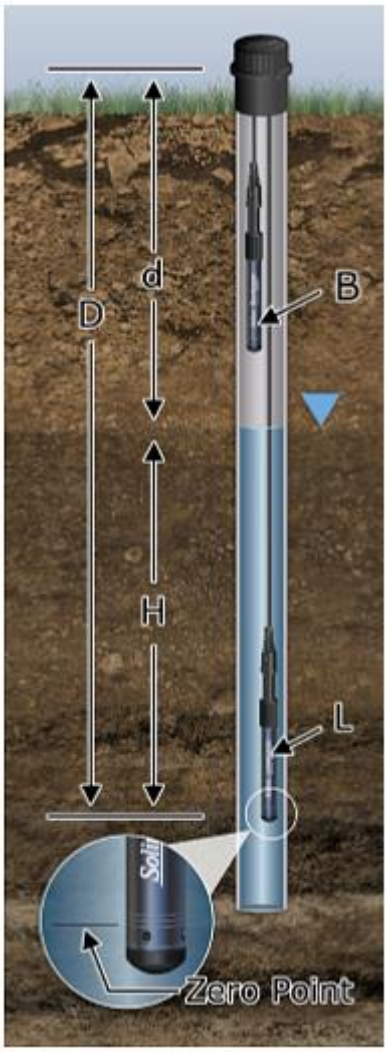

Figure 38: Principle of water level measurement with level loggers and baro loggers

3.5.3 Piezometric curves's map realization

Water levels measured in piezometer should be used to construct a water table map using the data from the other existing piezometers in the neighbourhood. Before constructing the potentiometric map fresh water level measurements should be taken from the all the piezometers and observation wells in the neighbourhood that will be used in the construction of the potentiometric map. The potentiometric surface should be in consistent with the neighbouring observation wells.

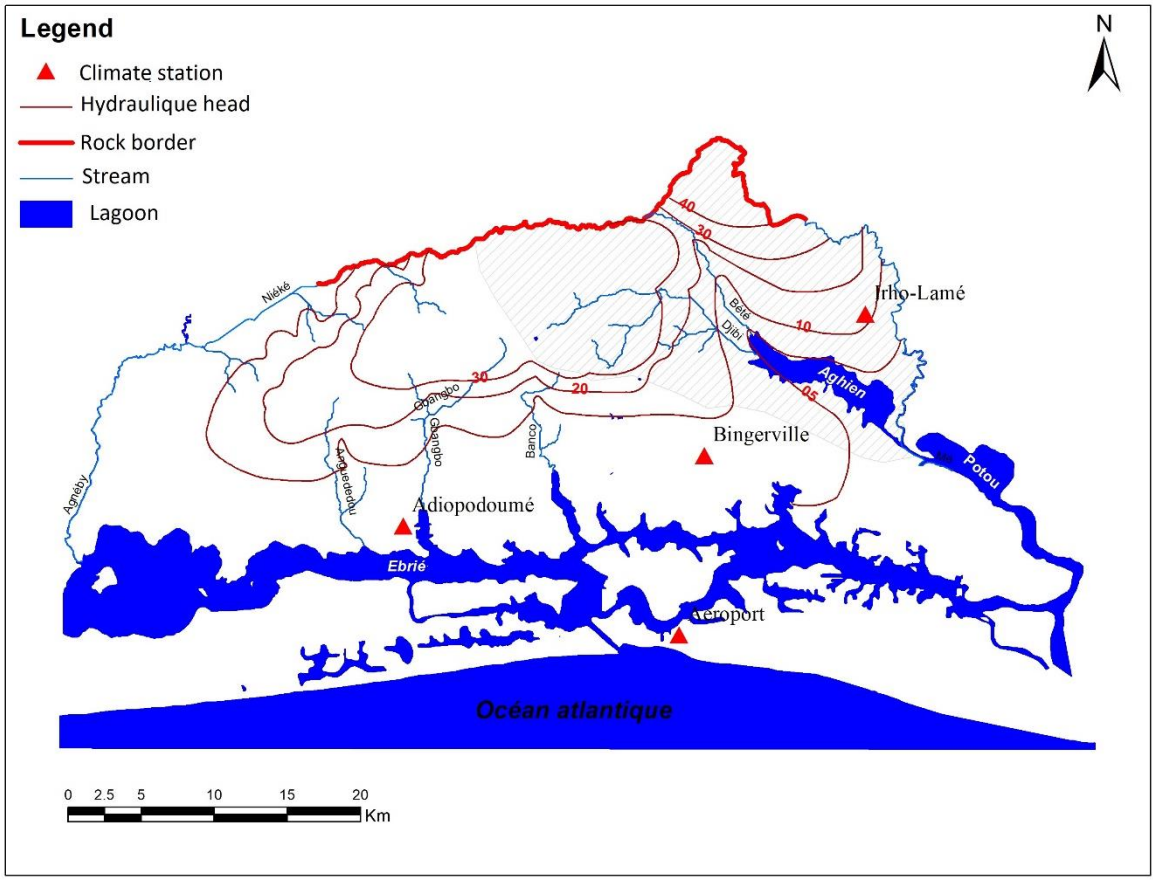

Figure 39: Initial hydraulic heads around Aghien lagoon

Chapter 4: Influence of Land Use Land Cover (LULC) on groundwater recharge

This chapter give an overview of analysis of land use-land cover influence on groundwater recharge of the Continental Terminal. The results consist of: (a) change analysis of land use/land cover types of the area, (b) The weight curve number value and runoff estimated and (c) groundwater recharge estimation and analysis.

4.1 Land Use-Land Cover dynamic of the Abidjan

Five LULC classes were identified in this study:

- Urban are
- Shrubs
- Agriculture
- Forest
- Water

All the items are detail in Table VIII

Table VIII: land use/ land cover classification scheme

LULC categories	Description
Urban area or built-up	urbanized areas and roads as well as land covered by buildings and other man-made structures, residential areas, commercial services, industrial areas, mixed urban and built up lands;
Shrubs	some woody plants, smaller than a tree, usually having multiple permanent stems branching from or near, the ground or woody plants of relatively low height, having several stems arising from the base and lacking a single trunk;
Agriculture	the farmland areas or the lands covered with temporary crops followed by harvest period, crop fields and pastures;
Forest	growth of trees and other plants covering a large area
Water	the stream line, lagoon

4.1.1 Land use/ land cover classification between 1990, 2000 and 2016

Image analysis and classification, revael that the land use/ land cover map for the year 1990 was dominated by Forest area with 593.22 km², which represent 33.05%, followed by Shrubs

area (590.75 km², 32.91%) ; Urban area (337,74 km², 18.82%) ; Water (256.89 km², 14.3%) and Agricultural area (16.28km², 0.91%).

In 2002, the land use/ land cover map showed that LULC was dominated by urban area which increase from (337,74 km² , 18.82%) in 1990 to (681.94km², 38.02%) in 2000 followed by an decrease in shrubs area. from (590.75 km² , 32.91%) in 1990 to (418.89 km², 23.35%) in 2000 and forest area (397.74km², 22.18%) while Agricultural area (43.76 km², 2.44%) was increasing and Water (251.33km², 14.01%) did not change.

For the year 2016, the land use/ land cover map showed that LULC was still dominated by urban area followed by shrubs area and agriculture was increasing. However, forest area was sitill decreasing. Urban areas were about 604.26 km² (39.29%), shrubs area 474.92 km² (26.31%), agricultureal area 88.01 km² (4.98%), forest 379.69 km² (16.51%) and water 248.06 km² (12.91%)

Table IX: LULC Classification Statistics with area in km^2 (%) from 1990 to 2016

LULC Class	**1990**	**2000**	**2016**	**Area coverage (%)**		
				1990	**2000**	**2016**
1-Urban area	337.74	681.94	604.26	18.82	38.02	39.29
2-Shrubs	590.75	418.89	474.92	32.91	23.35	26.31
3-Agriculture	16.28	43.76	88.01	0.91	2.44	4.98
4-Forest	593.22	397.79	379.69	33.05	22.18	16.51
5-Water	256.89	251.33	248.06	14.31	14.01	12.91

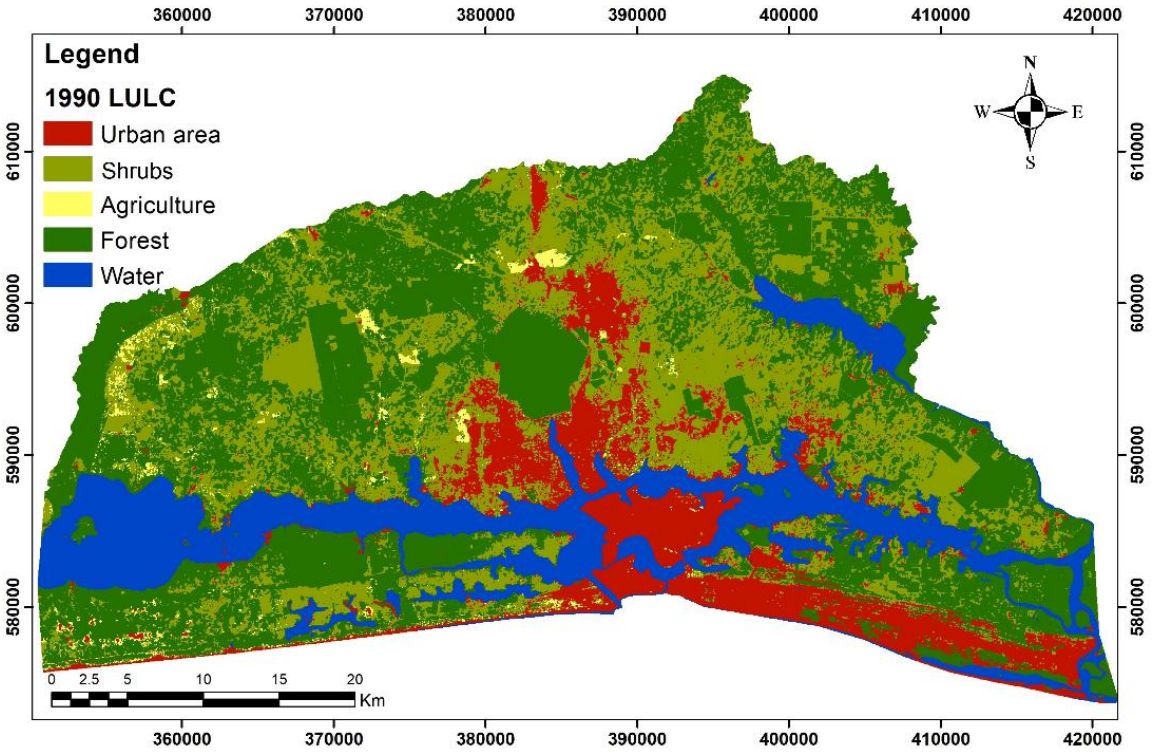

Figure 40: Spatial distribution of land use/cover maps of Abidjan in 1990

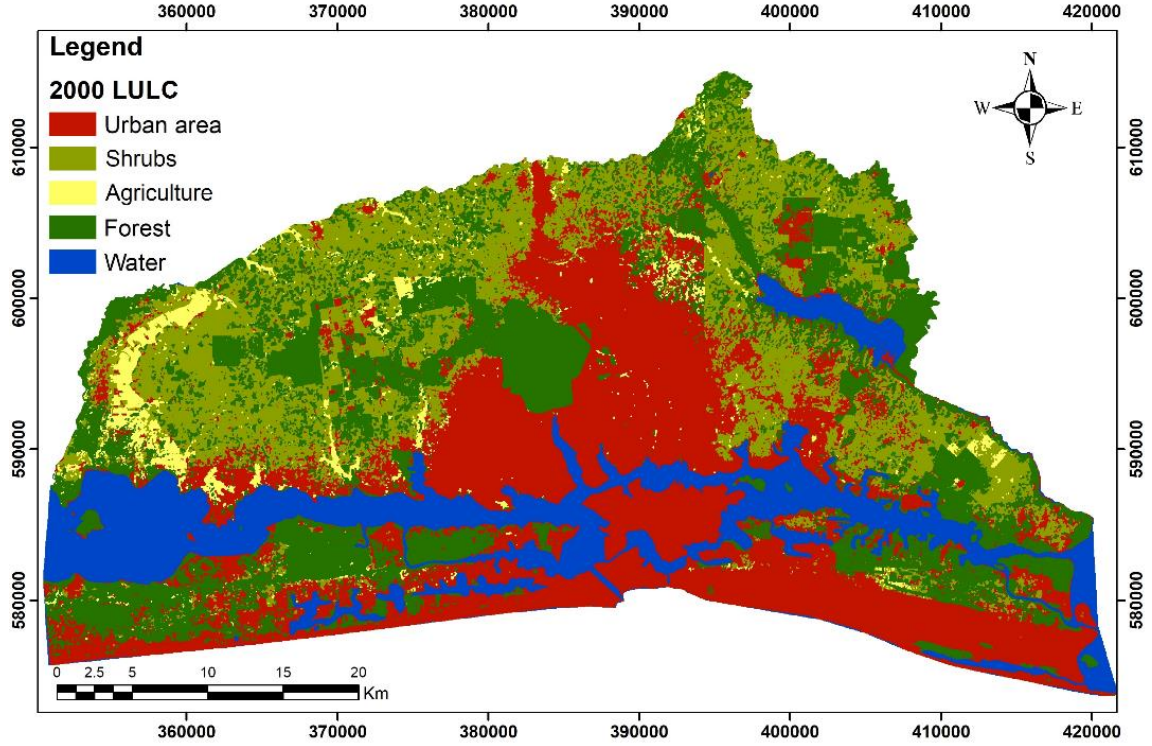

Figure 41: Spatial distribution of land use/cover maps of Abidjan in 2000

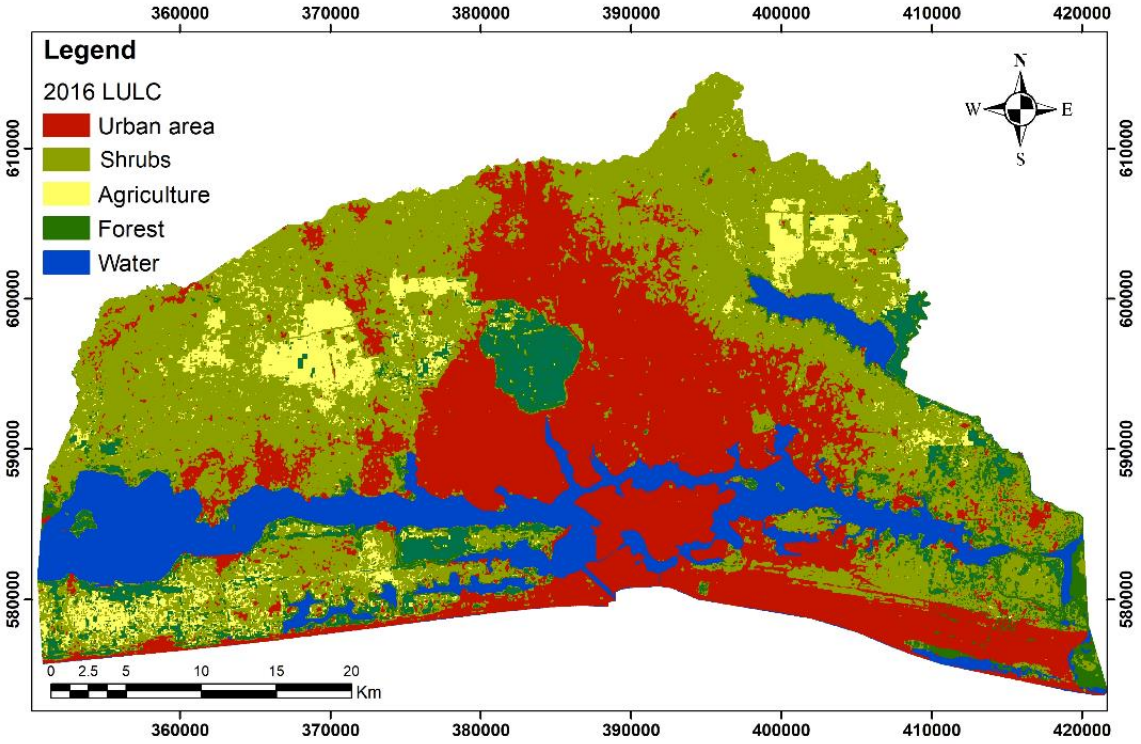

Figure 42: Spatial distribution of land use/cover maps of Abidjan in 2016

4.1.2 Validation of land use /land cover classification

4.1.2.1 Accuracy statistics and LULC change analysis

Table X: Accuracy statistics of the classified land use/land cover maps

(a) Year 1990, overall accuracy= 98.29%, Kppa=0.97

LULC	Reference image					Number of classified pixel	User accuracy (%)	Commission error (%)
	1	2	3	4	5			
1-Urban area	**100**	0.33	0.00	0.00	0.80	721	98.77	1.23
2-Shrubs	00.00	**96.08**	4.92	0.48	0.23	613	96.56	3.44
3-Agriculture	0.00	3.59	**94.10**	0.00	0.00	305	92.88	7.12
4-Forest	0.00	0.00	0.98	**99.52**	0.23	838	99.40	0.60
4-Water	0.00	0.00	0.00	00.00	**98.74**	872	100	00
Producer's accuracy (%)	100	96.08	94.10	99.52	98.74			
Omission error (%)	0.0	0.00	0.00	0.03	0.37			

(b) Year 2000, overall accuracy= 99.9%, Kppa=0.99

LULC	Reference image					Number of classified pixel	User accuracy (%)	Commission error (%)
	1	2	3	4	5			
1-Urban area	**100**	0.00	0.00	0.03	0.37	885	99.68	0.32
2-Shrubs	00.00	**100**	0.00	0.00	0.00	662	100	0.00
3-Agriculture	0.00	1.96	**100**	0.00	0.00	409	100	0.00
4-Forest	0.00	0.00	0.00	**99.97**	0.23	1059	100	0.00
4-Water	0.00	0.00	0.00	00.00	**99.63**	858	100	00
Producer's accuracy (%)	100	100	100	99.97	98.74			
Omission error (%)	0.0	3.92	5.90	0.48	1.26			

(c) Year 2016, overall accuracy= 93.80%, Kappa=0.92

LULC	Reference image					Number of classified pixel	User accuracy (%)	Commission error (%)
	1	2	3	4	5			
1-Urban area	**96.25**	0.00	0.00	0.78	1.47	1894	98.38	1.62
2-Shrubs	1.37	**78.01**	3.32	0.28	0.00	1064	95.62	4.38
3-Agriculture	0.00	18.61	**96.68**	1.35	0.00	241	51.78	48.22
4-Forest	2.38	3.38	0.00	**97.59**	0.23	1412	94.45	5.55
5-Water	0.00	0.00	0.00	00.00	**98.53**	1294	100	00
Producer's accuracy (%)	96.25	78.01	96.68	97.59	98.53			
Omission error (%)	3.74	21.99	3.32	2.41	1.47			

4.1.2.2. Land Use/ Land Cover dynamic

The overall accuracy of the post classification derived from the confusion matrix was estimated at 98.29 %, 99.90 % and 93.80 % for 1990, 2000 and 2016 LULC maps, respectively. The study area has known important land use/cover conversion from one type to another.

4.2 Curve Number change and impacts on runoff and recharge in the study area

Twelve curve numbers were derived from the three HSG and five LULC classes as shown in the Curve Number maps in Figure 43, Figure 44 and Figure 45and Table XI: Weighted curve number

of the group of soil and surface of land cover type. for the three LULC maps for the year 1990, 2000 and 2016. The curve number range from 30 to 100; the lower numbers indicate low runoff potential while the larger numbers indicates high runoff potential. The lower curve numbers the more permeable the soil. These maps reveal that in 1990, the study area was dominated by low weighted curve number which led to a low runoff and higher recharge, while 2000 is marked by an increase of weighted curve number zone which favor an increase in the runoff and the decline of recharge in the study area. However, recharge areas identifying areas with low runoff capacity, therefore having a low weighted curve number reappear in 2016.

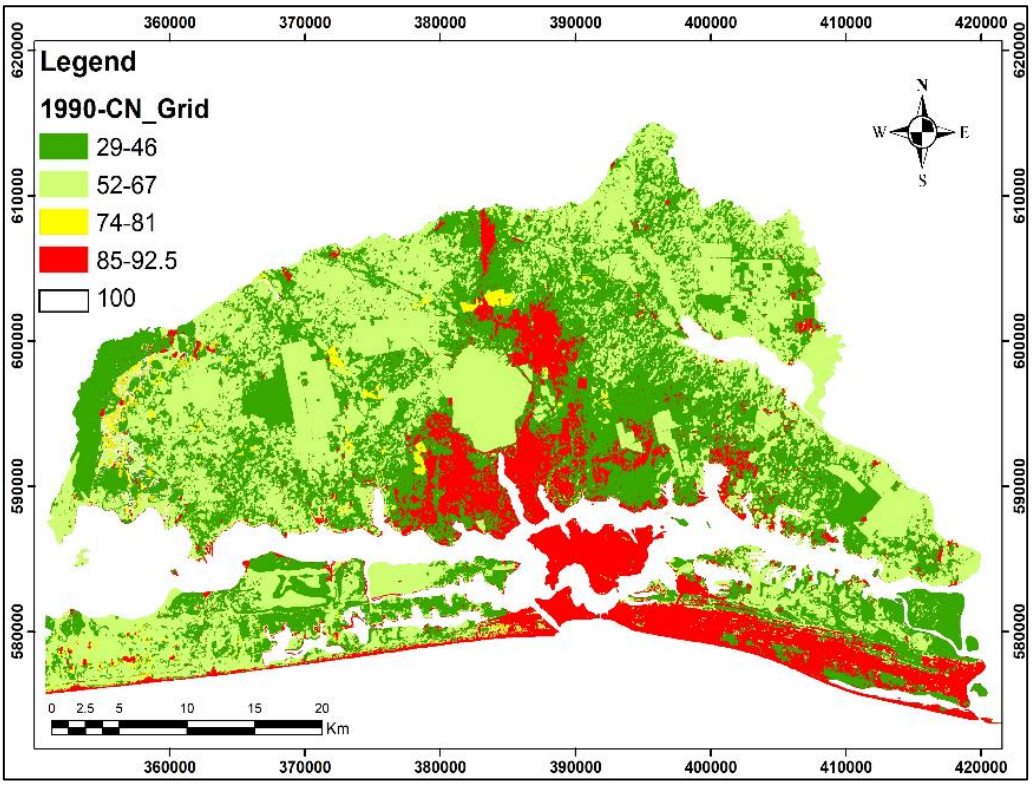

Figure 43: Weighted curve number map based on different soil groups and LULC types.in 1990

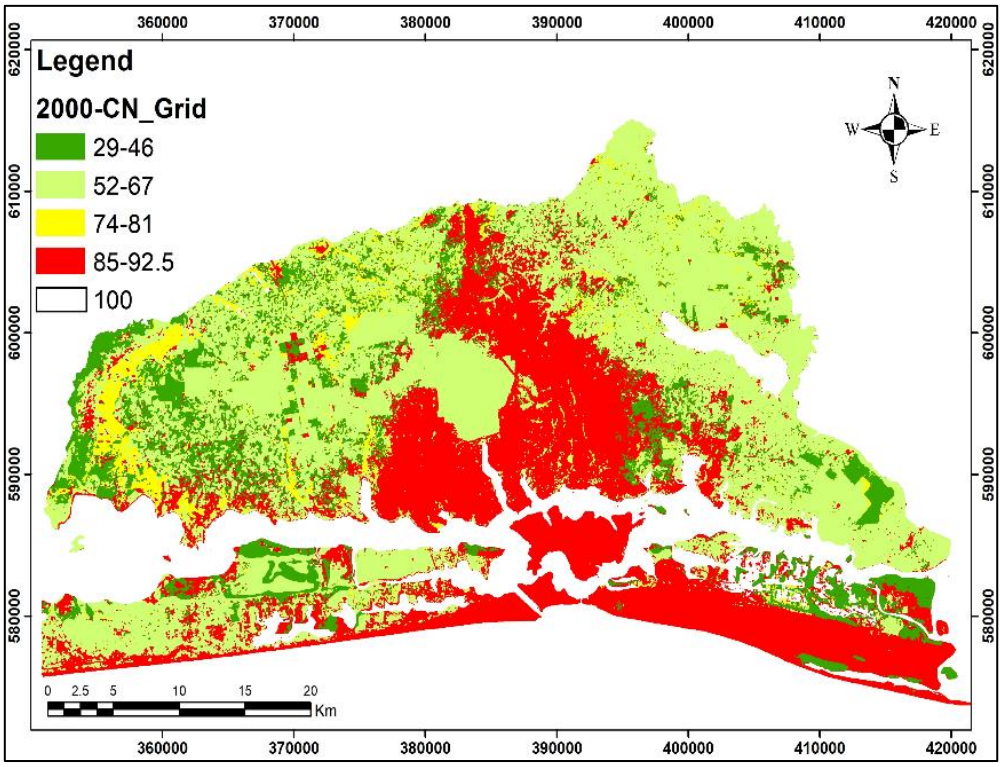

Figure 44: Weighted curve number map based on different soil groups and LULC types.in 2000

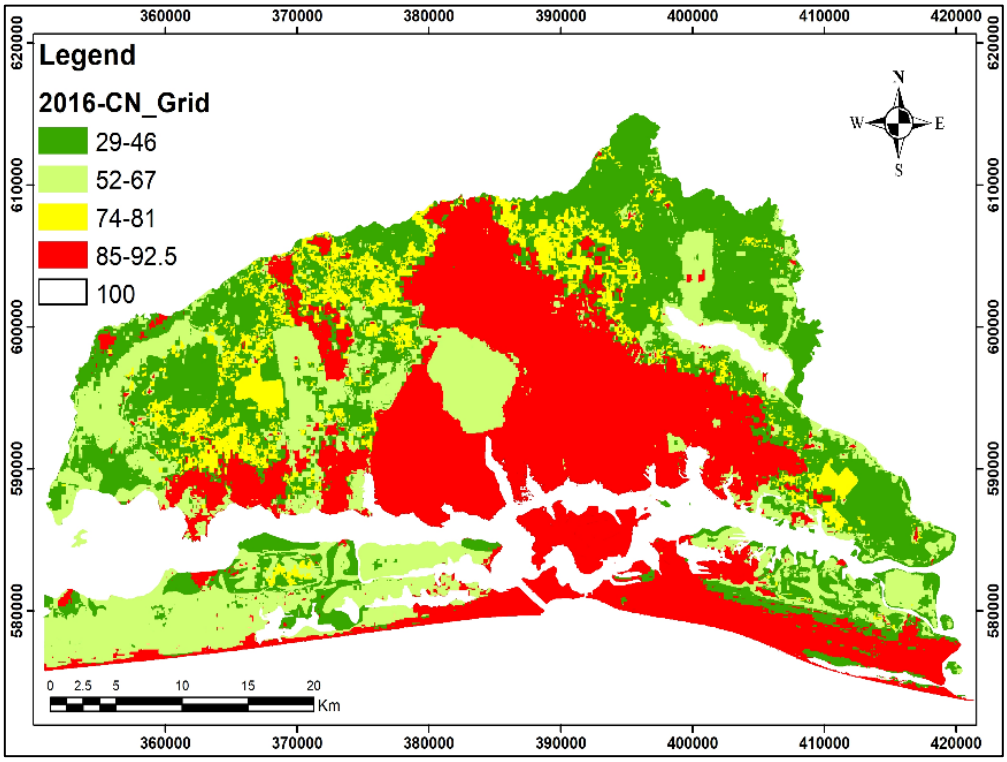

Figure 45: Weighted curve number map based on different soil groups and LULC types.in 2016

Table XI: Weighted curve number of the group of soil and surface of land cover type.

			1990			2000			2016		
Land cover	**Soil**	**CN**	**Surface (km^2)**	**Percent Area**	**CN*Percent Area**	**Surface (km^2)**	**Percent Area**	**CN*Percent Area**	**Surface (km^2)**	**Percent Area**	**CN*Percent Area**
Urban area	A	85	130.96	8.27	702.55	170.10	10.74	912.52	124.81	7.88	669.56
	B	90	29.10	1.84	53.26	29.60	1.87	54.18	74.54	4.70	136.43
	C	92.5	3.48	0.22	14.06	20.47	1.29	82.68	2.08	0.13	8.40
Shrubs	A	29	126.64	7.99	231.79	75.4	4.76	138.00	90.57	5.72	165.77
	B	46	16.82	1.06	106.16	11.44	0.72	72.20	15.01	0.95	94.73
	C	62	3.64	0.23	20.68	10.17	0.64	57.77	1.17	0.07	6.65
Agriculture area	A	64	8.65	0.55	25.11	5.08	0.32	14.75	11.95	0.75	34.69
	B	74	0.74	0.05	3.46	3.51	0.22	16.39	0.39	0.02	1.82
	C	81	29.27	1.85	96.06	24.32	1.53	79.82	29.34	1.85	96.29
Forest	A	29	2.14	0.14	13.51	1.36	0.09	8.58	1.55	0.10	9.78
	B	52	201.67	12.73	1177.35	445.06	28.09	2598.25	462.53	29.19	2700.24
	C	67	523.53	33.04	2048.59	170.95	10.79	668.93	396.26	25.01	1550.58
Water	A	100	12.50	0.79	63.90	60.57	3.82	309.64	85.81	5.42	438.68
	B	100	447.81	28.26	1893.61	518.45	32.72	2192.32	245.39	15.49	1037.66
	C	100	47.50	3.00	299.79	37.97	2.40	239.64	43.01	2.71	271.45
TOTAL			1584.45	100.00	6749.86	1584.45	100.00	7445.69	1584.41	100.00	7222.73

4.3 Groundwater recharge estimation using water balance method

This recharge (Table XII) was computed by monthly mean area precipitation (1983-2017) based on the Thornthwaite flowchart (Annex1). This method has been used by SOGREAH (1996) on the Abidjan aquifer.

4.4 Seasonal and Inter-annual variability of rainfall, recharge and runoff

The results reveal a decrease in rainfall over time while the recharge shows a decrease from the year 1990 to 2000 and an increase in the year 2016. However, runoff increased considerably from 1990 to 2000 and decreased in 2016 (Figure 46). Inter-annual variability shows that in 2000 when rainfall and recharge were decreasing, runoff was increasing. This period is marked by a strong increase in urbanization in the study area. Figure 47;Figure 48 , Figure 49 and Figure 49 show the inter-annual variability and seasonal trends of rainfall, runoff and recharge for the year 1990, 2000 and 2016. The seasonal recharge from April to July was high and the peak was observed in June (174 mm) during the year 1990.The recharge decreased in September, November and December. In 2000, the higher values of recharge were observed in May and June and get down in April, July and October. The peak was also in June with 139 mm. The year 2016 is characterized by a high value of recharge in May and June where the peak was observed in June (175 mm). The low value of recharge is observed in March, April and October. Runoff is proportional to recharge and presents lower values compared to recharge. Seasonal variability shows that the recharge is changing from one month to the next and that is due to rainfall variability.

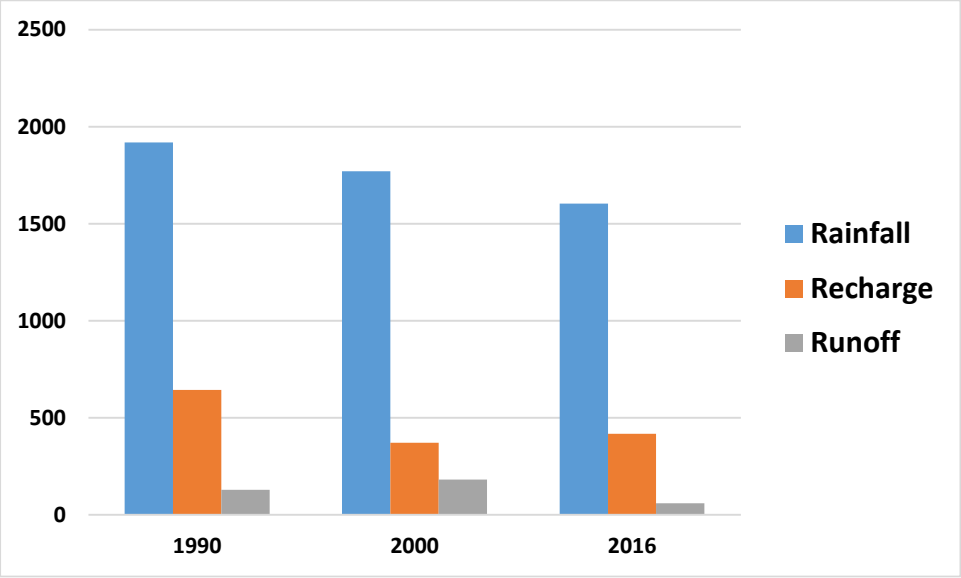

Figure 46: Interannual variability of rainfall, recharge and runoff

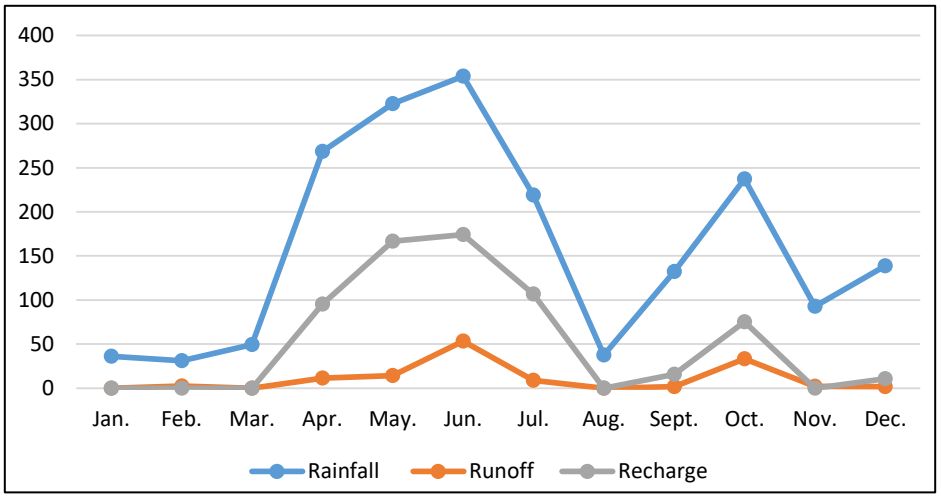

Figure 47: Seasonal variability of rainfall, recharge and runoff in 1990

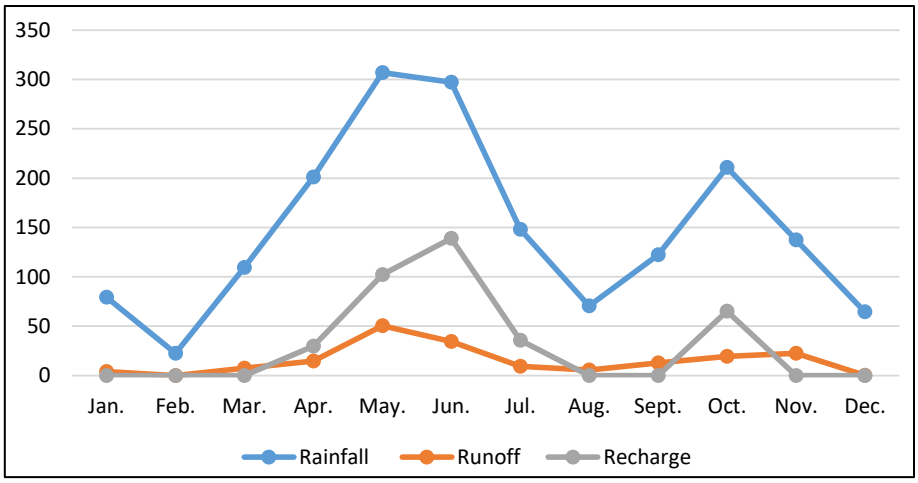

Figure 48: Seasonal variability of rainfall, recharge and runoff in 2000

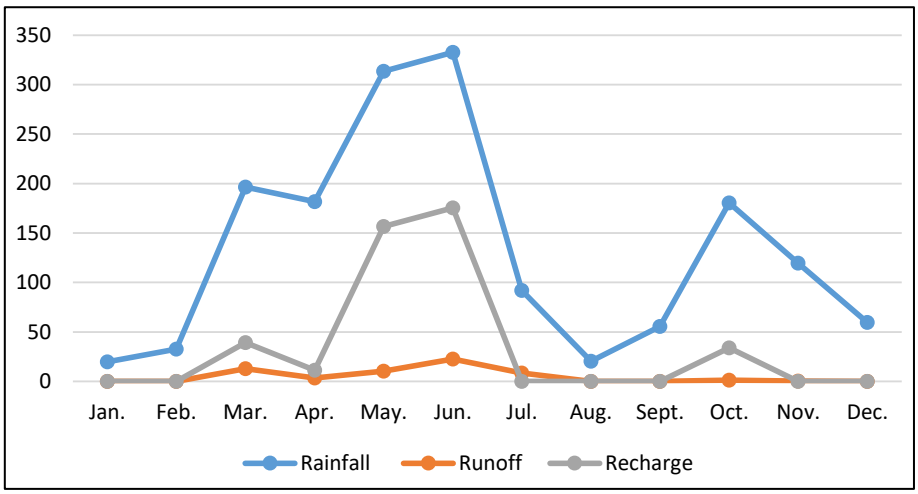

Figure 49: Seasonal variability of rainfall, recharge and runoff in 2016

Table XII: Monthly rainfall, runoff and recharge.

	1990			2000			2016		
Date	**Rainfall (mm)**	**Runoff (mm)**	**Recharge (mm)**	**Rainfall (mm)**	**Runoff (mm)**	**Recharge (mm)**	**Rainfall (mm)**	**Runoff (mm)**	**Recharge (mm)**
Jan	36	0	0	79	4	0	20	0	0
Fev	31	2	0	23	0	0	33	0	0
March	49	0	0	110	7	0	197	13	39
April	269	11	95	201	15	30	182	3	11
May	323	14	167	307	51	102	314	10	157
June	354	53	174	297	34	139	333	23	175
Juill	219	9	107	148	9	36	92	8	0
Augt	37	0	0	70	6	0	20	0	0
Sept	132	2	16	122	13	0	56	0	0
Oct	237	33	75	211	20	65	180	1	34
Nov	93	2	0	137	22	0	120	0	0
Dec	138	2	11	65	0	0	60	0	0
Total	1919	128	644	1771	181	372	1604	59	417

4.5 Discussion

In this study, a spatial-temporal dynamics of LULC was assessed based on image classification and change detection method. The study highlights that the built-up and agricultural lands have increased rapidly in the study area. Such an increase in built-up area and agricultural lands can be explained by the increase in urbanized and cultivated areas, respectively. In addition, the decline of forestland can be explained by the expansion of agricultural and urbanized areas. In fact, forest areas are being reduced to enlarge the land use areas or, forest areas are converted in agricultural and built up area. This increase in urbanization after 2000 could be explained by rural exodus of urban center population, as well as population growth, and is supported by (Berthe et al. 2015) who indicated that urban sprawl in Abidjan from 2002 to 2014 is mainly due to population growth during the crisis (2002-2011) and its demand for development. Indeed, due to the country's crisis which started in 2001, population migration significantly increased (rapid uncontrolled urbanization) from the north to the southern part of the country, mainly to Abidjan. The urbanization is linked to the economic progress. The same conclusion was made by (Danumah et al. 2017), who explained that the economic capital of Ivory Coast with developmental projects including construction of roads, houses and industries, as well as population growth are still increasing and therefore areas covered by vegetation are expected to be further transformed to urban areas

Furthermore, three hydrological soil groups namely A, B and C were found to dominate the watershed with hydrological soil group C having the high runoff potential. This is because the hydrological soil group C lies in the urban area; hence limiting infiltration and favoring runoff. The southeastern parts of the watershed were found to be dominated by hydrological soil group A, which has low runoff potential. This is mainly due to the presence of agricultural lands in this section. The crops require more water hence increasing the rate of infiltration which in turn leads to lower runoff potential, and hydrological soil group B characterize by moderate runoff. It is important to mention that hydrological soil group must be associated with LULC to know the infiltration capacity of the soil. For instance, the hydrological soil group A located at the southeastern part of the study area is converted into urban area which is therefore favorable to high runoff. The LULC changes have an important effect on the catchment runoff generation (Kalnay and Ming 2003).

In addition, comparing maps of curve number during the years 1990, 2000 and 2016, the amount of weighted curve number value estimated for the study area was increased because of the increase in the urban area, showing human interventions in the landscape during that period.

During the years 2000 to 2016, the level of forestland decreased by 4% and some part were converted in croplands. This made possible the increasing of recharge in this period. A similar conclusion was reported by (Scanlon et al. 2005), who found that dry agricultural land could increase groundwater recharge in the southwestern US.

The results show a temporal variability of the recharge on Abidjan aquifer. The methodology uses to find the recharge highlight runoff variability which brings out the impact of urbanization, shrubs area and agricultural land on groundwater recharge. Thus, the changes in recharge are due to rainfall variability and LULC change over time. Moreover, it is observed that the recharge decreases considerably, almost to a half from 1990 to 2000. This period is marked by a strong increase of urbanization in the study area which favors the increase of runoff from 128 to 181mm. However, the study reveals an increase in recharge in 2016 which is due to the increase of afforested area and agricultural land. In fact, it was observed that covered area favored high infiltration and represents a low weight of curve number which expresses low runoff. However, low infiltration occurs in urban areas where weighted curve number is high and expresses high runoff. The results are in accordance with the study of (N. Soro et al. 2006) and some previous studies in West Africa (Oluseyi et al. 2015) and (Obuobie 2008) provide a numbered reference for Baier et *al.*, who affirm that the rapid growth of urban area has two basic effects on groundwater resources such as effects on natural recharge of aquifers due to sealing of ground with concrete and pollution of groundwater due to leakage from drainage and industrial waste and effluents. Furthermore the annual recharge was estimated at 400 mm/year in 2016, this value represents about the double of the results of the study undertaken by (Yao et al. 2015) this could be explained by the difference in methods used but this result is close to the previous study of Kouakou (2013) who assess the recharge at 342 mm/year in 2006.

These findings are in line with the study made by Kouame et al.(2008) which indicated that the land use of the study area especially that of the well fields by constructions can make the ground impermeable. This situation in certain places can lead to a reduction in the net recharge of the aquifer.

Chapter 5: Impact of climate change on groundwater recharge

This chapter presents the outcomes from the analysis of climate change for the catchment. The results consist of: (a) validation of CHIRPS precipitation data for the study area and (b) projections of rainfall, temperature and recharge for the study area under RCP4.5 scenario.

5.1 Rainfall analysis for the Continental Terminal catchment

5.1.1 Station and gridded precipitation data comparison

In this study, due to the lack of many station in the area, it has been used CHIRPS precipitation data which is the Climate Hazards Infrared Precipitation with Stations archive (Funk et al. 2015). The CHIRPS database comprises a quasi-global (50°S50°N, 180°E-180° W), 0.05° resolution, and 1981 to nearpresent gridded precipitation time series.This dataset merges three types of information: global climatology, satellite estimates, and in situ observations (Bai et al. 2018), generating several precipitation products with time steps from 6-hourly to 3-monthly aggregates. This database was mainly used for the assessment of monthly, seasonal, and annual precipitation variability in several regions of the world.

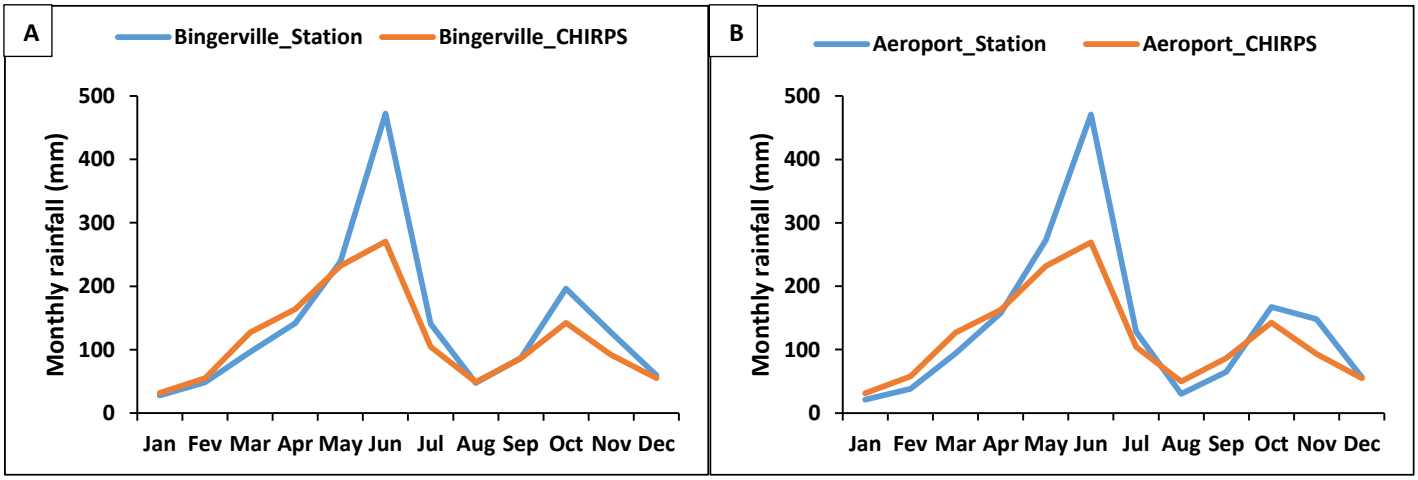

Figure 50: Performance evaluation of CHIRPS based on mean monthly distribution (A and B) of rainfall from 1982 to 2011 for the Bingerville and Aeroport station

However the CHIRPS gridded precipitation data and the rainfall station data at mean monthly scale in reproducing the current rainfall pattern of bingerville and Aeroport stations for the period 1982-2018 reveal that CHIRPS precipitation data for both stations showed a bimodal rainfall pattern with the peak of the raining season in june and october which is similar to the station data (Figure 50). The CHIRPS data simulated well the seasonal rainfall pattern with an overestimation at the peak month (June and October) of the raining season at both station bingerville and Aeroport. The CHIRPS precipitation data was able to reproduce the mean

monthly rainfall patterns for the two stations shown in Figure 50. The statistical analysis outcome at monthly scale showed in Table XIII reveal a good agreement with the station data which is comfirm by a correlation coefficient (r = 0.94), The percentage bias (PBIAS) indicated an overestimation for both station, Bingerville station (19.5%) and Aeroport station (17%). but in an acceptable range with PBIAS within ± 25 as indicated by Cohen et al. (2012). In general, the observed statistical results demonstrate that the CHRIPS precipitation data is able to reproduce the rainfall pattern of the catchment and therefore can be used for further analysis.

Table XIII: Mean monthly scale statistical analysis of rainfall for the station and CHIRPS data from 1982 to 2011 in the catchment

Monthly scale	**Bingerville**	**Aeroport**
Percentage bias (PBIAS)	19.50%	17%
Pearson correlation coefficient (r)	0.92	0.94
Root-mean-square error (RMSE) Nash-	63.11	63.98

5.2 Climate projections of the study area based on the ensemble mean

5.2.1 Rainfall Projections under climate change scenarios (RCP 4.5)

Changes in future rainfall (2020–2049) projected mean monthly and annual by different hydroclimate ensemble members under the RCP4.5 scenario with respect to the historical data (1982–2011) for the Continental Terminal were shown in Figure 51 with the statistics presented in Table XIV.The ensemble mean shows an increase of 37.32% in rainfall at a rate of 7.74 mm by year (Table XIV) between 2020 and 2049. At the monthly scale (Table XIV)
the ensemble mean projected an increase in mean monthly rainfall of 5.67% during the rainy season (MJJON) and a decrease of 60.05% during the dry season (DJFMASD),

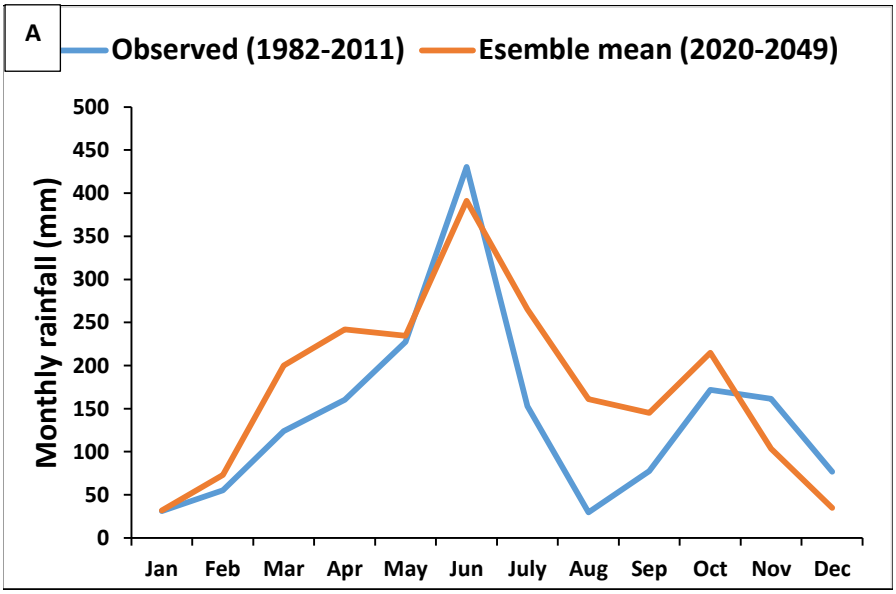

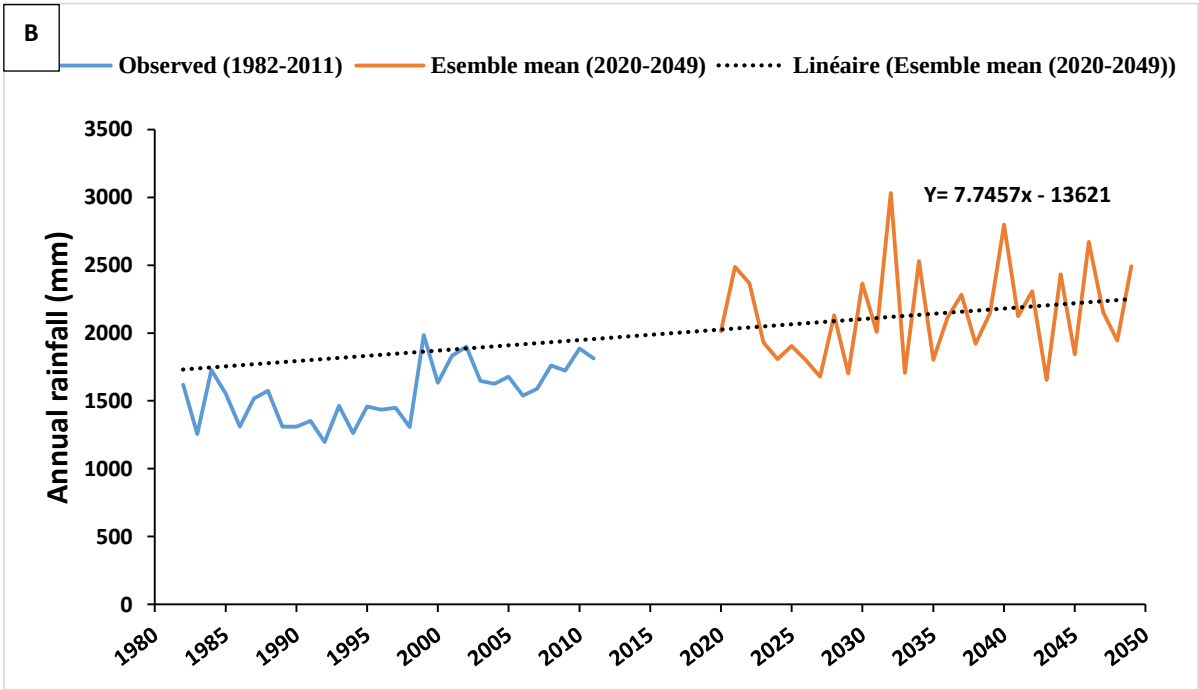

Figure 51: Rainfall projections of the study area under RCP4.5 scenario based the ensemble mean of the climate models for monthly scale (A) annual scale: (B)

Table XIV: Mean annual rainfall and temperature projections for the catchment

Variables	Baseline (1982-2011)	RCP4.5 (2020-2049)
		Ensemble mean
Tmax (ºC)	26.84	27.30 (0.46)
Tmin (ºC)	25.75	26.00 (0.25)
Tmean (ºC)	26.29	26.53 (0.25)
Rainfall (mm)	1556.99	2138.07 (37.32%)

NB: Projected changes in rainfall and temperature in the brackets

5.2.2 Temperature Projections under climate change scenarios (RCP 4.5)

Changes in future temperature (2020–2049) projected mean monthly and annual by different hydroclimate ensemble members under the RCP4.5 scenario with respect to the historical data (1982–2011) for the Continental Terminal were shown in Figure 52. The ensemble mean showed a warming trend of 0.03 ºC/ year with a projected increase in mean annual temperature of 1.73 ºC in the future 2020-2049. The annual maximum temperature is projected by the ensemble mean to increase by 1.73ºC while the minimum temperature increased by 1.34ºC (Table XVI). At the seasonal scale an increase in mean temperature (Tmean) of 1.25ºC in the raining season (MJJON) were projected by the ensemble mean. In the dry season (DJFMASD), a mean temperature change of 1.31 ºC is projected by the ensemble mean in the future 2020-2049. the models projected mean temperature change pattern in August indicating the lowest temperature months while April show highest temperature months (Figure 52).

Table XV: Mean monthly rainfall and temperature projections in the Continental Terminal for the raining season (MJJON)

Variables	Baseline (1982-2011)	RCP4.5 (2020-2049)
		Ensemble mean
Tmax (ºC)	24.2	25.9 (1.73)
Tmin (ºC)	25.3	26.7 (1.34)
Tmean (ºC)	24.8	26.1 (1.37)
rainfall (mm)	228.86	241.90 (5.67%)

NB: values in bracket indicate temperature change and percentage of rainfall in the future relative to the baseline period

Table XVI: Mean monthly rainfall and temperature projections in the Continental Terminal catchment for the dry season (DJFMASD)

Variables	Baseline (1982-2011)	RCP4.5 (2020-2049)
		Ensemble mean
Tmax (ºC)	24.3	25.6 (1.27)
Tmin (ºC)	26.0	27.6 (1.55)
Tmean (ºC)	25.2	26.5 (1.31)
rainfall (mm)	79.25	126.84 (60.05%)

NB: values in bracket indicate temperature change and percentage of rainfall in the future relative to the baseline period

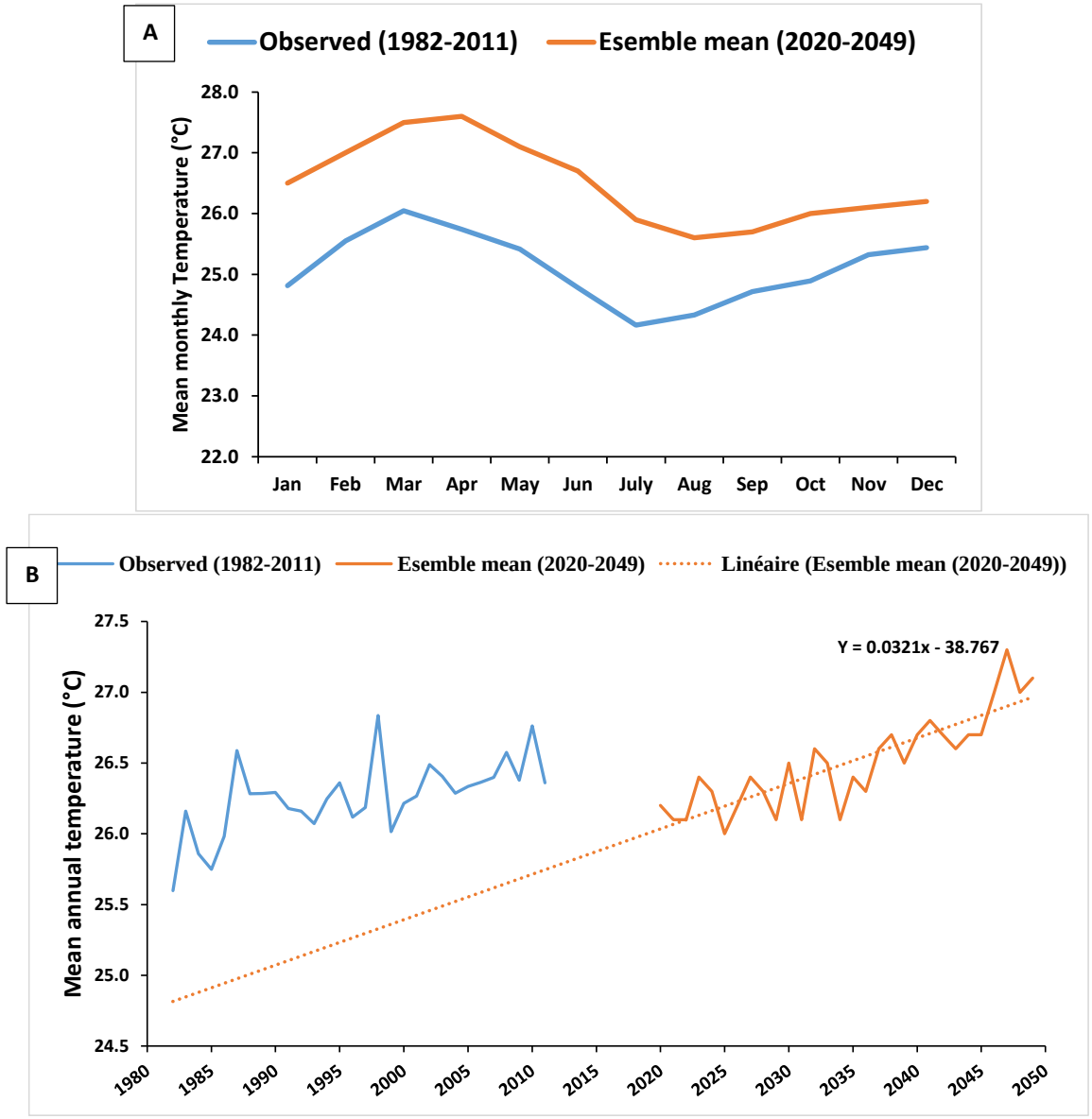

Figure 52: Temperature projections of the Continental Terminal for the ensemble mean in the future (2020-2049) under RCP 4.5 scenario relative to the baseline period for Mean monthly (A) and annual (B)

5.2.3 Recharge Projections under climate change scenarios (RCP 4.5)

Base on the projected mean annual temperature and rainfall found by the ensemble mean in the future (2020-2049), the projected mean annual recharge was computed and it is ranging from 1115.78 to 482.93 mm/year (Figure 53).

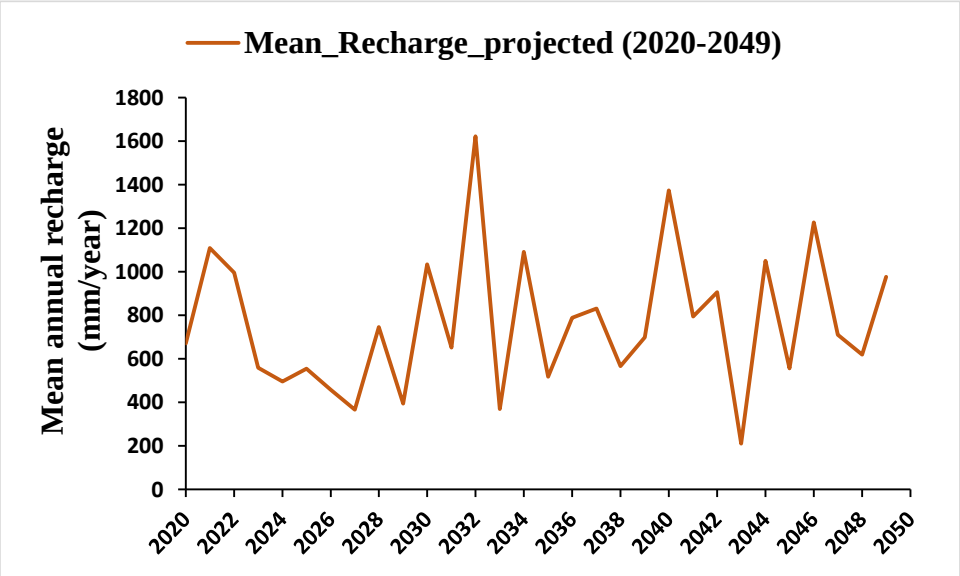

Figure 53: Recharge projections of the Continental Terminal base on rainfall and temperature the future (2020-2049) under RCP 4.5 scenario

5.2.4 Spatial distribution of rainfall and temperature projections

The spatial pattern of the projected changes in mean annual temperature and rainfall by the ensemble mean in the future (2020-2049) relative to the baseline (1982-2011) period are shown in Figure 54. The mean annual temperature is projected to increase from 26.5 to 25.1ºC (baseline) to 27.7 - 25.5ºC (future) with a change in temperature ranging from -0.30 to 1.40 ºC. The temperature change for the future 2020-2049 is higher in the center of the catchment compared to the east and the west part of the catchment. The annual rainfall ranges from 1827.17 to 1558.24mm as baseline (1982-2011) is also projeted to increase from 2169.32 to 1577.20 in the future (2020-2049), with the highest amount found in the southern and some part in the center of the catchment (Figure 54)

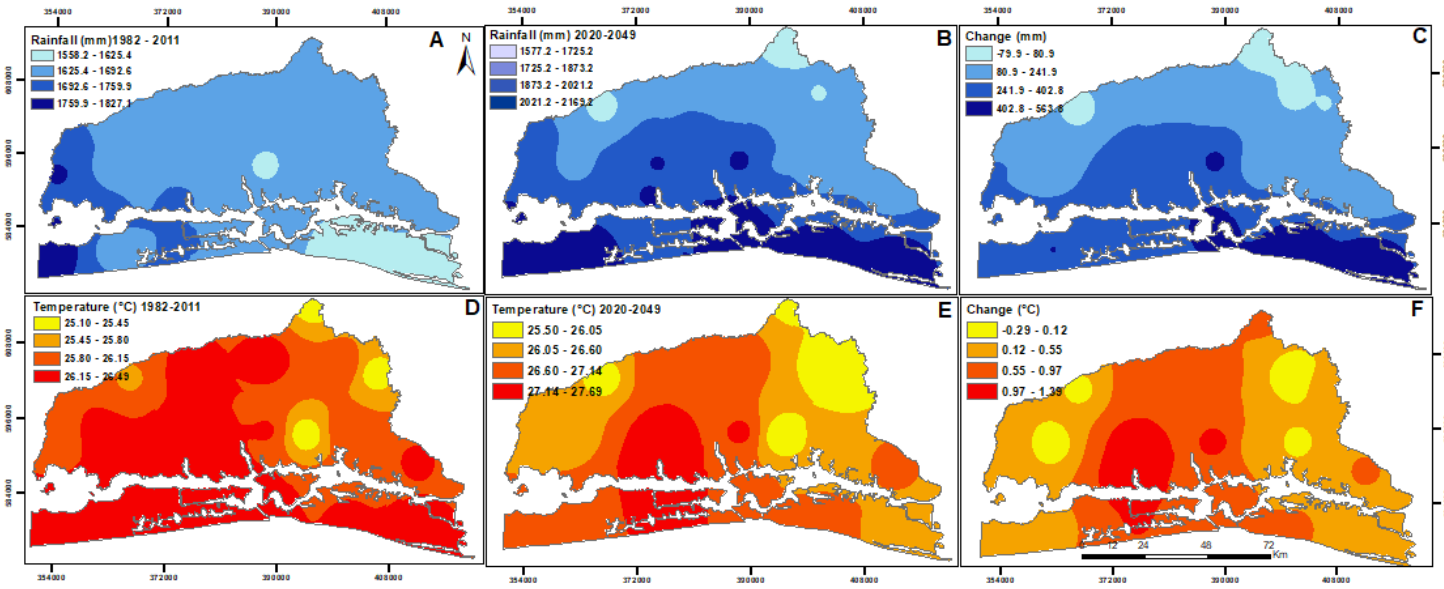

Figure 54: Spatial distribution of mean annual rainfall and temperature of the Continetal Terminal for the baseline (1982-2011), future (2020-2049) and projected changes.

5.2.5 Spatial distribution of recharge

The spatial pattern of the projected mean recharge by the ensemble mean in the future (2020-2049) base on the mean annual rainfall and temperature are shown in Figure 55. The recharge for the future 2020-2049 is higher in the south than the north part of the catchment

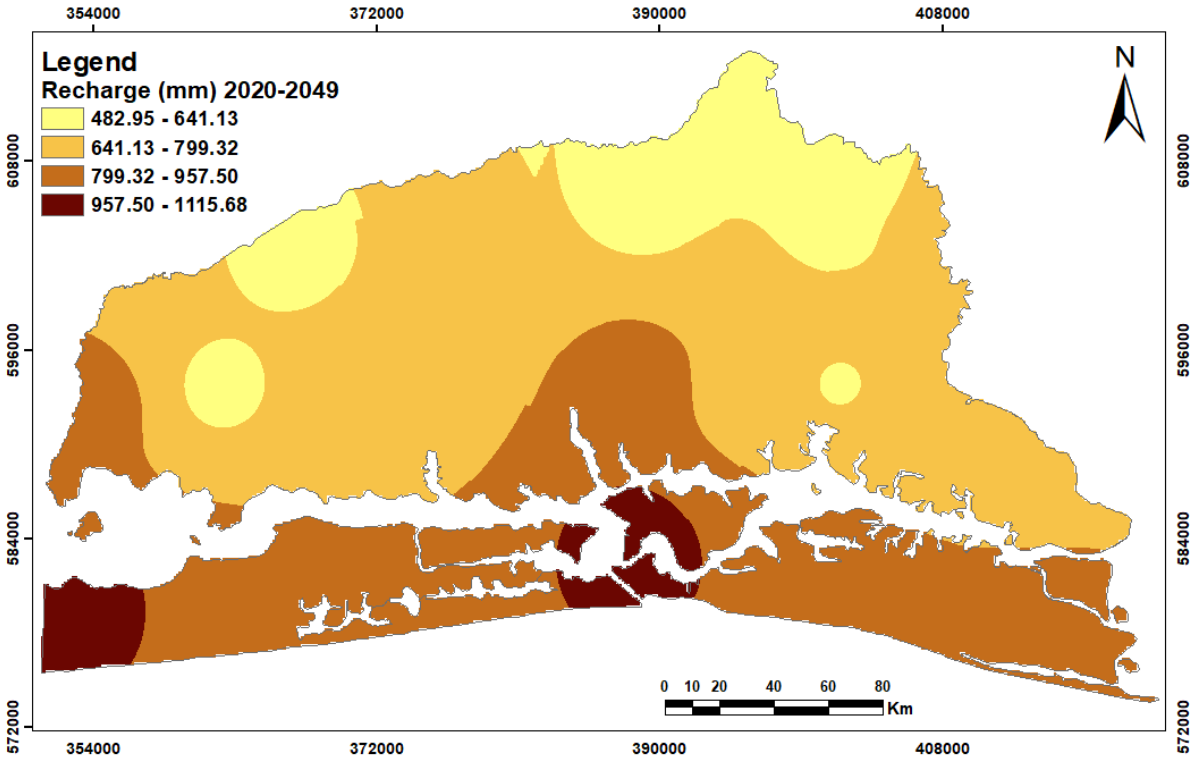

Figure 55: Spatial distribution of mean recharge of the Continental Terminal for future and projected changes

5.3 Discussion

This study show the capacity of CHIRPS precipitation data to reproduce the current climate of the Cotinental Terminal. In fact, due to the deficiency of long term and quality climate data on the study area, it has been compared CHIRPS precipitation data with station data over the period of 1982 to 2011 due to limited and gap free station data. Most of the time the CHIRPS data indicated good performance in term of PBAIS and correlation coefficient which may be related to the fact that CHIRPS data have smaller systematic errors (Wu et al. 2019) and the smaller grid size (5km) as it reduces the effect of pixel-to-point comparison (Cohen *et al.,* 2012).. The CHIRPS data also performed better in the warm seasons (dry season) than the cold seasons (reaning season), which might be related to its limited ability to detect drizzle or frozen precipitation during the latter period (Kidd et al. 2012), this explaned why CHIRPS data were underestimated during the reaning season in this study. This finding suggests the CHIRPS data could be used as an alternative precipitation source. The evaluation and comparison of satellite reveal the conjunction with precipitation data and showed that CHIPRS data perform well in the study area and therefore can be used for further studies.

The principle focus of climate change research with regard to groundwater has been on quantifying the likely direct impacts of changing precipitation and temperature patterns(Kumar 2012), then the study shows that the changes in future rainffall (2020–2049) using RCP 4.5 scenario indicate an increase in future rainffall. This is consistent with the studies undertook by Yapo et al.(2020), that projected an increase intensity of precipitation events under future climates, This considerably impacts changes in dry spell length. The high increase in the extreme precipitation intensity associated to an extension of dry spell length and expand of urbanisation increases the risk of the occurrence of natural disasters such are floods and droughts which therefore impact groundwater recharge. Moreover the study of Abdellatif et al. (2012) reveal that extreme rainfalls are projected to increase in frequency under the high emission scenario.

The study analyse future temperature base one hydroclimate ensemble members under the RCP4.5 scenario and consider historical data (1982–2011). The results showed an increase of future temperature in all season. These findings are in line with the study made by the International Center for Tropical Agriculture (CIAT); International Crops Research Institute for the Semi-Arid Tropics (ICRISAT); Food and Agriculture Organization of the United Nations (FAO; ICRISAT; CIAT. 2018). The study shows that climate change is already an undeniable reality for Cote d'Ivoire(YAO et al. 2013). It is indicated that insolation increased

in the Guinean forest zone of the south, but changed very little in the northern half of the country. Temperatures have risen by 1.6°C throughout the country in the period 1960-2010, and projections indicate that temperatures will continue to increase by as much as 1.8 °C and 2.1°C in 2050 and 2070 respectively, West Africa on average is projected to experience a 3 to 6 °C summer temperature increase between 1981–2000 and 2031–2050 (Diallo et al. 2012) under the A1B emission scenario (IPCC 2014).

Under RCP 4.5, the climate change is likely to affect groundwater due to changes in precipitation and temperature. However it is find that the projected recharge of this study compared to the past recharge find in the literature reveal that the projected recharge is increasing. This result conforms to the study of Soro et al. (2017) that observed an increase in groundwater recharge of the coming decades. The evidence from the analysis indicates that under RCP 4.5, mean monthly runoff and groundwater recharge may increase for all seasons. Changes of runoffs and groundwater recharge are mainly due to projected precipitation variability. In fact the increase of projected precipitation in the long-term wet season will make it very wetter, resulting in higher runoff and aquifer recharge in the area. This phenomenon is due to the higth interaction between groundwater and suface water in the cactment. Therefore the increase in groundwater levels would lead to an increase in the flow of watercourses supplied by the aquifers. According to Owuor et al. (2016) these two parameters were decreasing under other scenario These results highlight the large uncertainties associated with the impacts of climate change on water resources.

Chapter 6: Groundwater and suface water interaction modelling

The chapter 7 describes the results obtained from the conceptual model. This includes both the results obtained from the calibrated model and scenario generated.

The results consist of: (a) MODFLOW model calibration, simulation groundwater head to 2060 horizon under 3 main scenario and validation, (b) analysis of groundwater and surface water interaction.

6.1 Steady State simulations

The steady state fully calibrated model showing in Figure 57 present the general hydraulic head in the domain of the model as well as the groundwater flow patterns in the study area. The distribution of hydraulic heads in the basin was the observed water levels during the field work carried out in 2017, and they range from -1.71 m to 62.92 m. It is highest at the north part of the domain, more specifically at the highest elevated areas. However, the hydraulic heads are lowest in the topographic lows. This indicates that recharge areas are from the topographic highs to the topographic lows (Fetter, 2001). The groundwater contours portray the nature of the geology and indicates a flow of groundwater from the northwest part of the area to the Aghien and Potou lagoons. The lagoon system therefore receives groundwater flow (N. Soro 2004). The general piezometric trend after calibration is well reproduced by the model, which allow to obtain a good representation of the general flow directions of the aquifer presented in Figure 56 below.

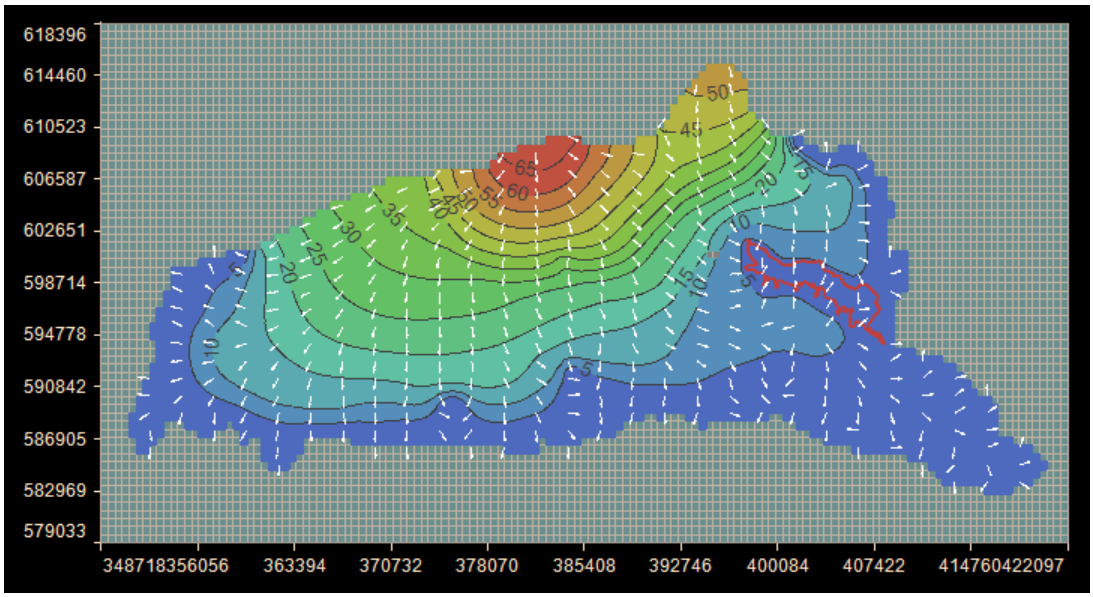

Figure 56: Flow direction simulated

The model was calibrated by matching the observed groundwater heads against predicted heads in fifty (55) wells within the model domain. The model was deemed calibrated when the

computed heads for all the wells were within 1.0 m of the observed heads. The results of the calibrated groundawater level versus the observed level have a mean error of -0.46 m, a mean absolute error of 2.69 m and a root mean square error of 0.98. These values indicate that; the model is well calibrated. The relationship between observed and model calculated hydraulic heads in the basin is presented in Figure 58. A good match between the computed and the observed hydraulic head suggest that the model is reasonably calibrated within the limits of the data used and is therefore representative of the hydrogeological conditions. Thus, the model realistically simulates the groundwater elevation and flow direction across the model domain

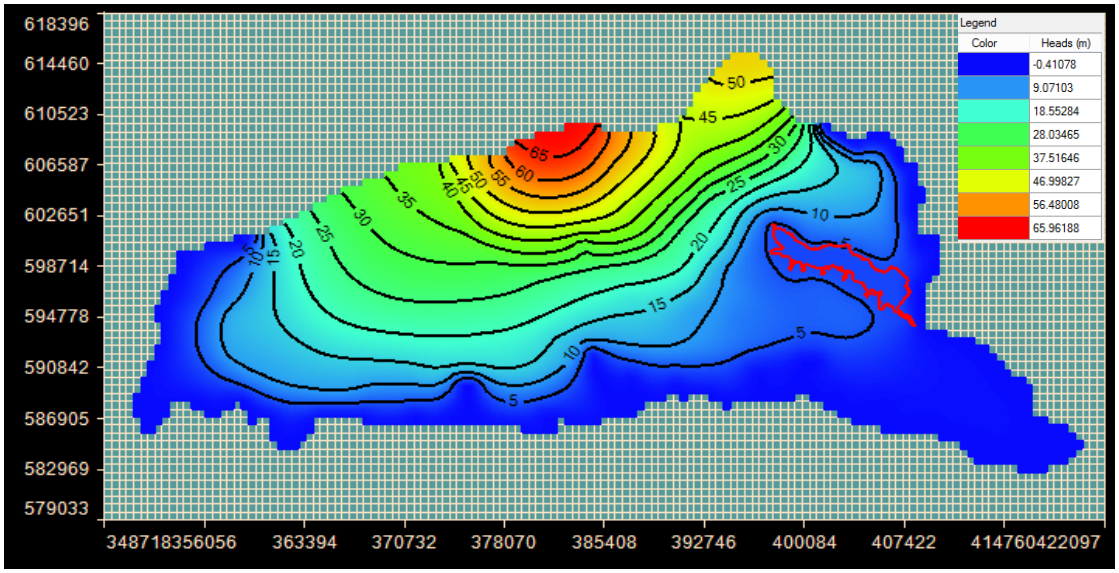

Figure 57: Hydraulic head Simulation

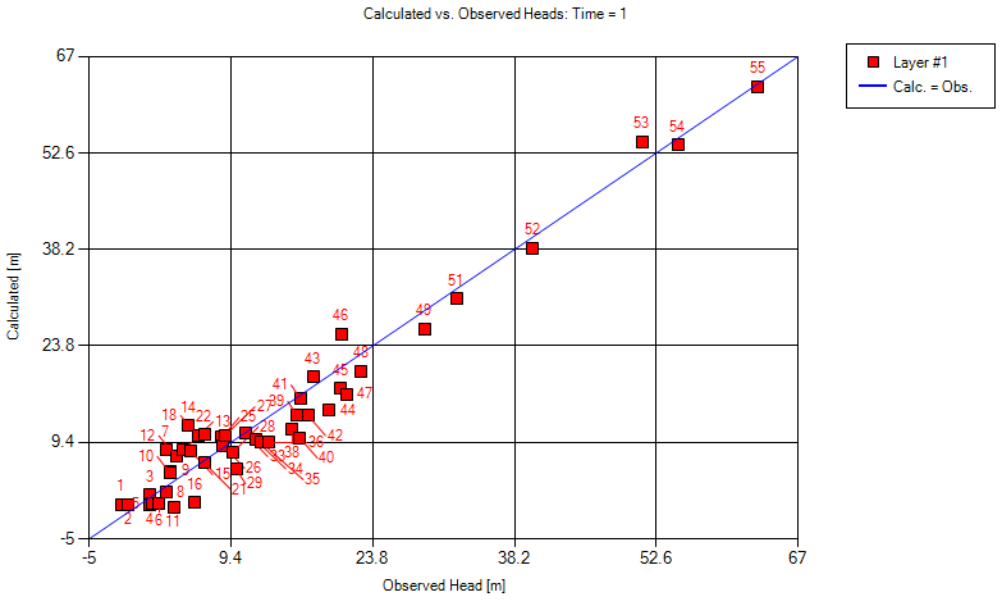

Figure 58: A comparison between observed and model computed hydraulic heads

6.1.1 Water budget

A water budget is a quantitative measurement of the balance between water inflow and outflow of a watershed during a specific period (Seneviratne 2007). One of the best ways to assess model simulation efficiency is by analyzing the water budget. A water budget provides an indication on acceptability on a numerical model solution. However, a good water balance cannot guarantee a good simulation, a bad water balance indicates problems in the model. In steady state simulation, the difference between total inflow and total outflow should be equal to zero, while it should be a total change in storage in a transient simulation. Although the water budget is used for calibration purpose, it also provides a measure of the relative importance of each component to the total budget (Konikow and Reilly 1998). The percentage discrepancy that quickly checks the water budget acceptability should be equal to zero in both cases. In this study, the percentage discrepancy of all the stress periods for the model is nearly zero. Thus, the model equations have been correctly solved (Chiang and Kinzelbach 1998). The average annual water budget is summarized in Figure 59 and indicates that Aghien lagoon drains the aquifer to 1.10^4 m^3 /day in certain areas where the aquifer is deeper, the lagoon supplies the groundwater by drainage up to 41.10^3 m^3 /day

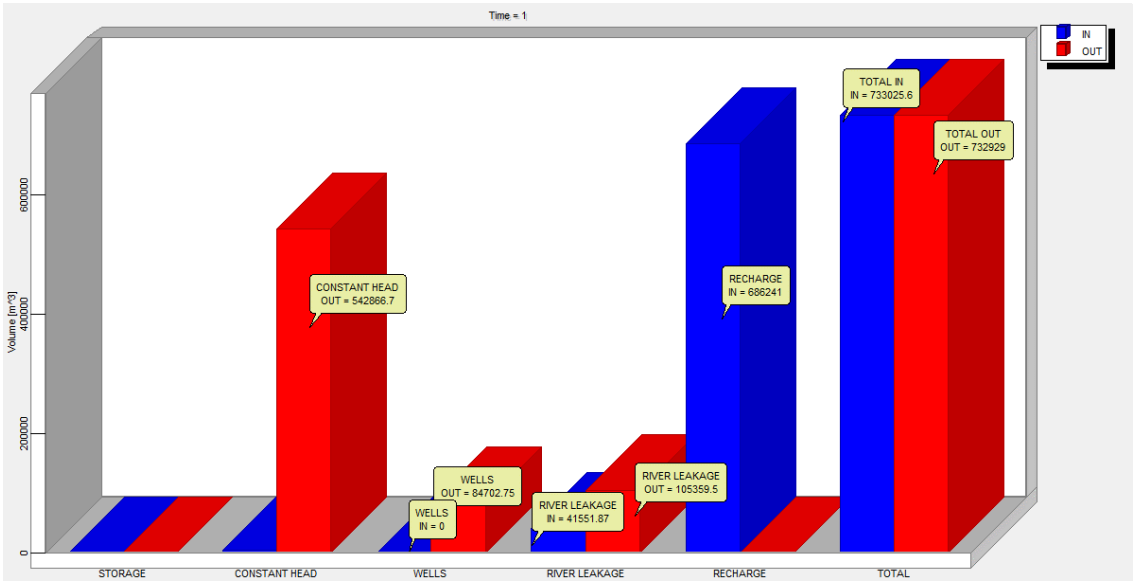

Figure 59: hydraulic balance after calibration

Table XVII: Mean annual water budget for groundwater in m^3/day in the Continental Teminal from 2010 to 2017

Flows	Water inflows (m^3/day)	Water ouflows (m^3/day)
Potential requires	0	54422866
Aghien lagoon	41551	105359
Recharge	686241	0
Total	733025	732929

To better understand the interaction between the groundwater and the lagoon, a focus on the immediate environment of the lagoon is carried out with the ZoneBudget2000 Package available with Modflow Flex to simulate the inflows and outflows. Thus, the lagoon is assigned Zone 2 (blue), Zone 1 for groundwater and the Constant head limits in Zone 3(Figure 60)

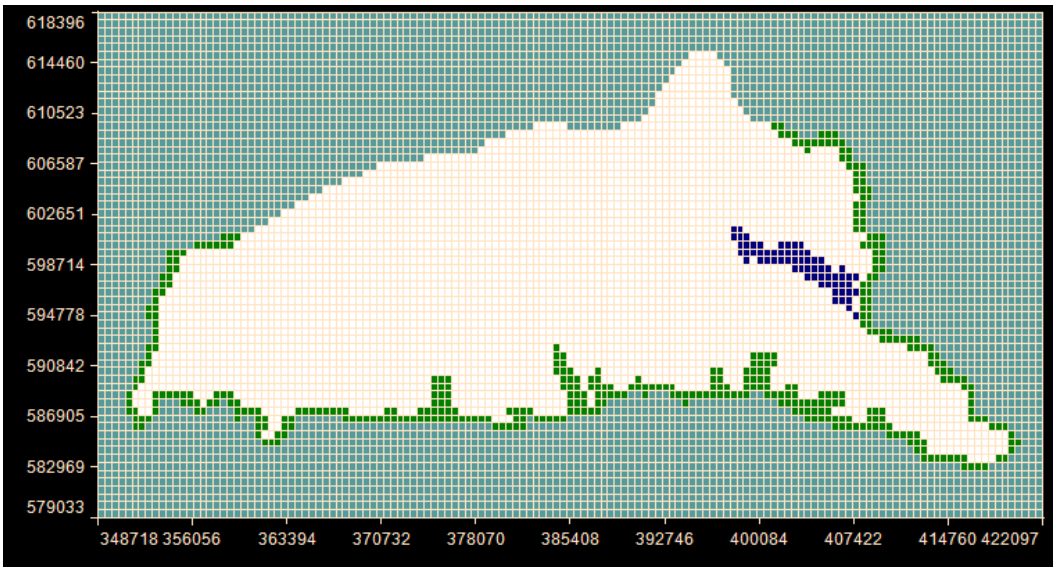

Figure 60: Budget zone

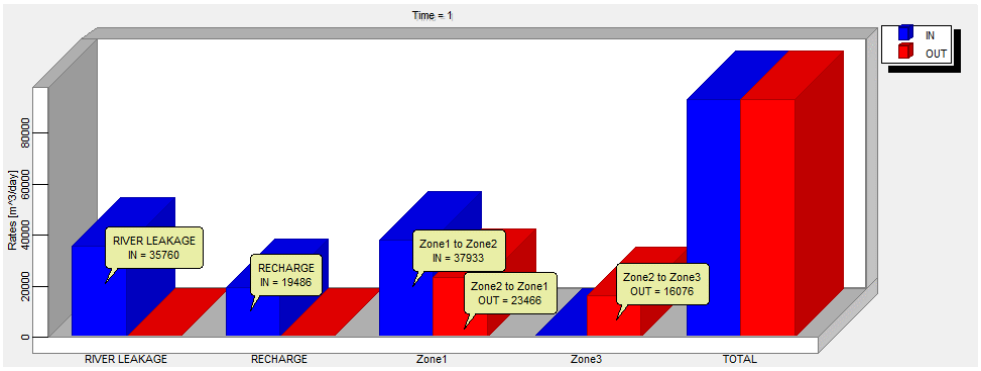

Figure 61: The inflows and outflows simulation

6.2 Modeling of future conditions

6.2.1 Scenarios analysis

After calibration, the models were used to simulate possible future scenarios of groundwater head and changes in recharge rates that might result from climate variability. A total of three scenarios were simulated for the period 2017 to 2060, the first scenarios (S1) assume the establishment of new boreholes (20) surrounding Aghien lagoon that assume no change in recharge (i.e., no impact of climate variability). The second one (S2) deal with groundwater behaviour under climate change. Assuming that most of CMIP5 projection revealed a decreasing recharge rate over time. A third scenario (S3), the most resource-intensive of the tree is the combination of the two, (S1) abstraction and (S2) climate change.

6.2.1.1 Initial condition without additional pumping

In the initial condition, groundwater flow is meanly directed toward Aghien lagoon (Figure 62). that confirm that the fact that Aghien lagoon drains the aquifer. Therefore it could be useful to satisfy water demand. However in context of water demand increasing due to the develepment of unbanisation and climate change impact on groundwater recharge, will this resource satify water demand by the year 2060?

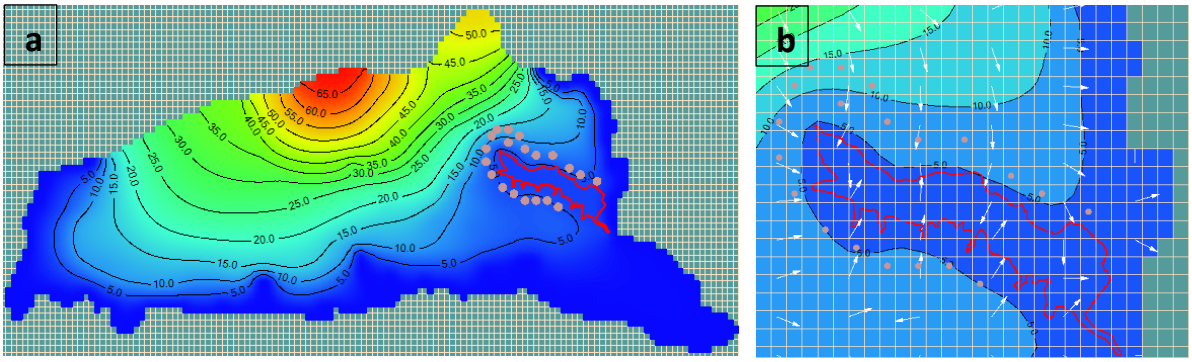

Figure 62: a) Initial Hydraulic head distribution b) Initial flow direction

6.2.1.2 First Scenario

In this scenario, the establishment of 20 boreholes surrounding Aghien logon were dicided. Different pumping rate are used to simulate the groundwater dynamic and the possibility to get 150Mm^3/day in order to satisfy water demand. Pumping rates estimated at steady state were using to increasing groundwater abstractions for all wells by Q_1= 2000m^3/day; Q_2= 3500m^3/day and Q_3=5000m^3/day. Pumping water in the wells show that water circulation is changing around the lagoon from the baseline 2017 to the projected year 2060 (Figure 64). When the rate of pumping is increasing from 2000 to 5000 m^3/day, the hydraulic head is drop from 0.1 to 2.8m.

The residuel map showed that a depression cone is created around the well (Figure 63) that will extend with time (transient state) and could reach new sources of water also hydraulic head is decreasing.Groudwater flow direction (Figure 65) around the lagoon reveal that the lagoon is not draining by the goundwater.

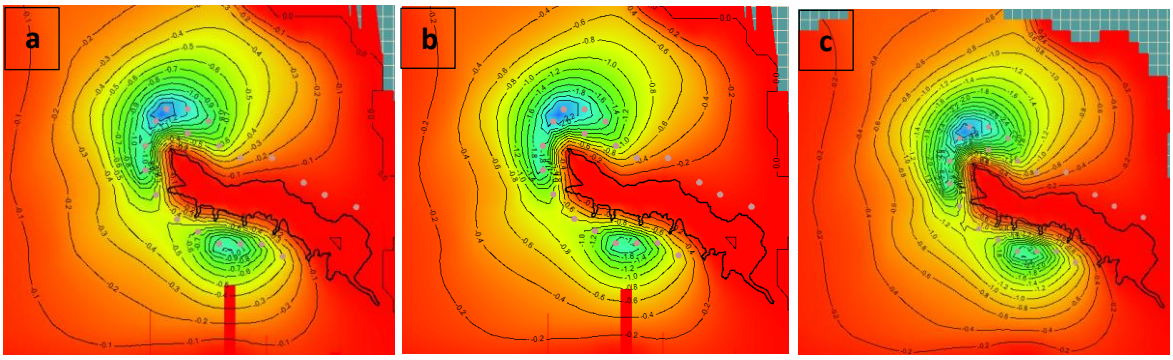

Figure 63: Residual map showing: a) pumping of Q1=2000m^3/day/well; b) pumping of Q2=3500m^3/day/well; c) after pumping of Q2=3500m^3/day/well

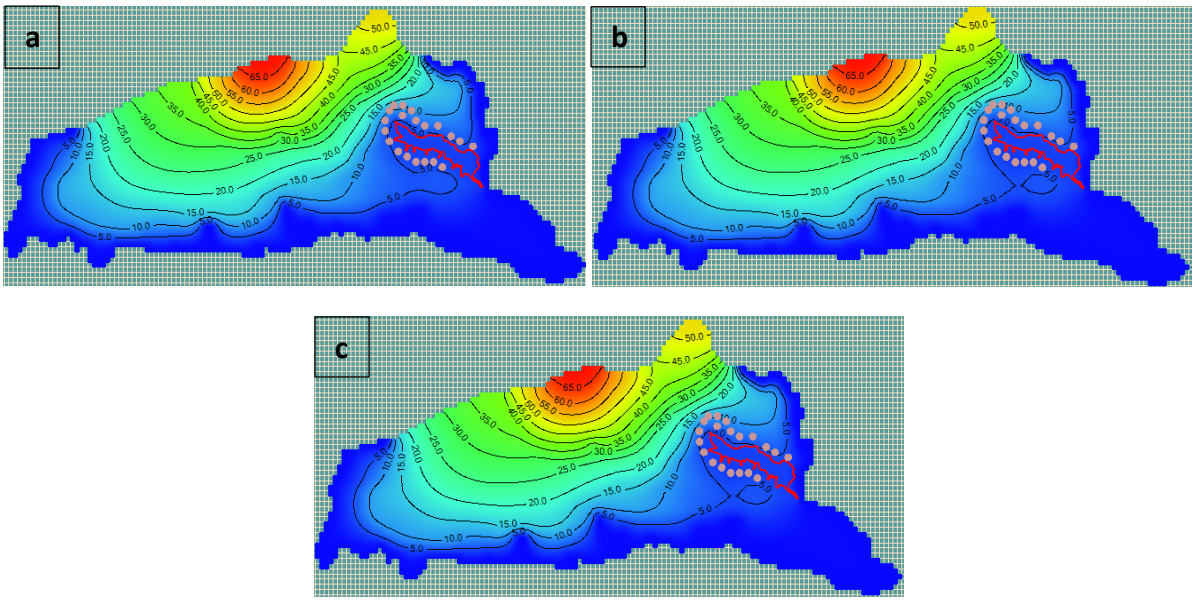

Figure 64: Hydraulic head distribution after pumping of a) Q1=2000m^3/day/well; b) Q2=3500m^3/day/well; c) Q2=3500m^3/day/well in 2060

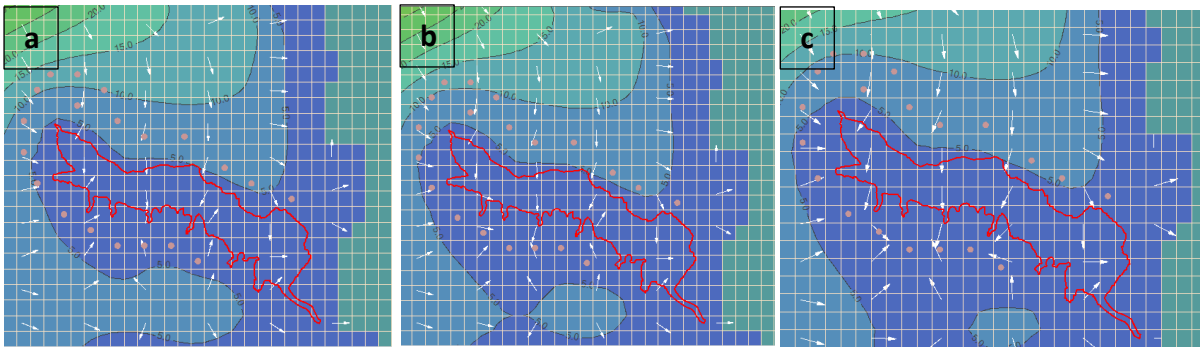

Figure 65: Groundwater flow direction after pumping of a) Q1=2000m^3/day/well; b) Q2=3500m^3/day/well; c) Q2=3500m^3/day/well in 2060

6.2.1.3 Sencod Scenario

This scenario considers the climate change with only recharge reduction at 15% and 30%. The residuel map showed that climate induced changes in water elevations are respectively on the order of 0.5 m and 0.2 m around the lagoon for 30% and 15% of recharge reduction (Figure 67) and the hydraulic head in 2060 is decreasing from 0.2 to 3 m (Figure 66)

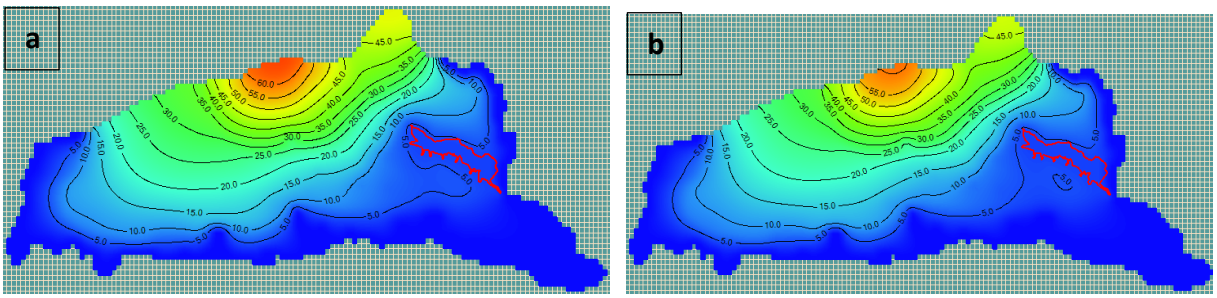

Figure 66: Hydraulic head distribution after recharge decrease at a) 15% and b) 30% up to 2060

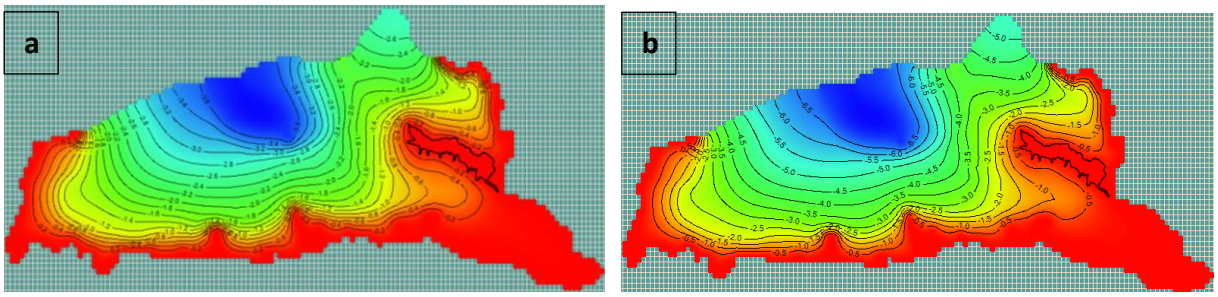

Figure 67: Residual map showing hydraulic head difference between initial condition after recharge decrease at a) 15% and b) 30%

6.2.1.4 Third Scenario

In the third case, worse case scenarios were analyzed. Firstly, 15% reduction in recharge rates and an increment in the abstraction rates up to Q=2000 m^3/day was performed and changes in the hydraulic heads were noted. Secondly, 15% reduction in recharge rates and an increment in the abstraction rates up to Q=5000 m^3/day reveal also the shifting in hydrlic head around the lagoon (Figure 68, Figure 69)

The residuel map showed that a depression cone is created around the well (Figure 68) and groundwater decreased around 4m

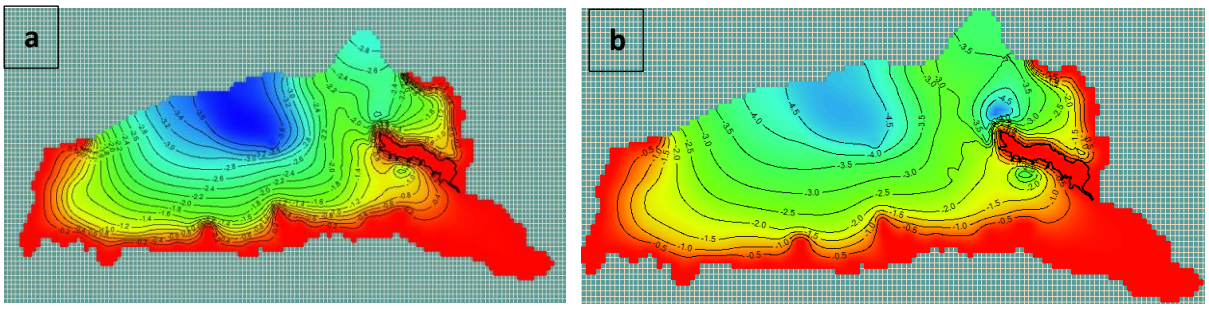

Figure 68:Residual map showing hydraulic head distribution after a) conbining recharge reduction at 15% +pumping rate Q= 2000 m^3/day and b) conbining recharge reduction at 15% +pumping rate Q= 5000 m^3/day

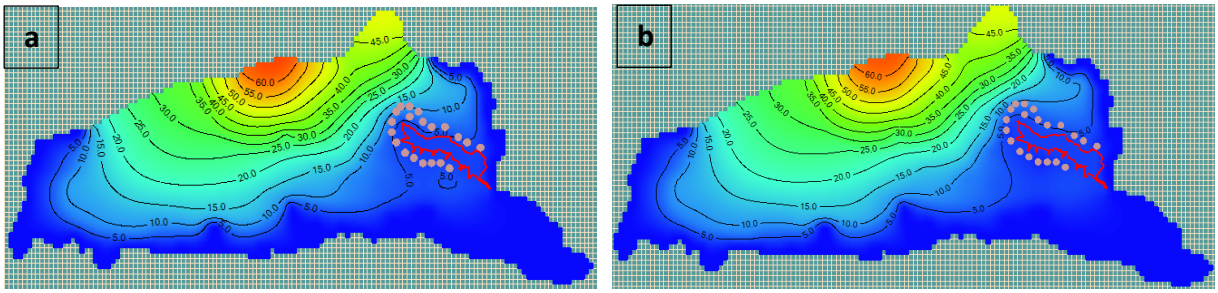

Figure 69: Hydraulic head distribution after a) combining recharge reduction at 15% +pumping rate Q= 2000 m^3/day b) 30% and b) combining recharge reduction at 15% +pumping rate Q= 5000 m^3/day

6.3 Discussion

The dynamics Continental Termional's groundwater has been modeled in order to estimate the future intaraction between the groundwater and surface water from 2017 to 2060.To estimate this interaction, three scenarios have been etablish. All the scenarios reveal that groundwater water level is decreasing and this could impact surface water reseve

In the first scenario base on the pumping rate it is found that more the pumping rate is increasing, the groundwater level is decreasing. Drawdowns occur when pumping continues. This result conforms to the study of Kouame et al.(2008) which reveal the drawdown caused by the additional withdrawal will vary between 1 and 16 m compared to initial head values. The highest drawdown cone was calculated at piezometers, Anonkoua kouté 2 with 15.71 m, Niangon 1 with 6.86 m and Adonkoua with 6.24 m. Western and south-eastern parts of the model are slightly influenced by this additional exploitation. In the same way Wada et al. (2012) affirm that in some semi-arid and arid regions with intensive irrigation, abstraction rates exceeding groundwater recharge have resulted in strong groundwater depletion. Furthermore the study of Inge et al. (2019) reveal that already, unsustainable groundwater pumping exceeds

recharge, leading to substantial drops in the levels of groundwater and losses of groundwater from its storage, especially in intensively activity regions When groundwater levels drop, discharges from groundwater to streams decline, reverse in direction or even stop completely, thereby decreasing streamflow, with potentially devastating effects on aquatic ecosystems .

Projected Climate change under CMIP5 scenario on groundwater highlights the fact the drawdowns is projected to be more intense in the future (2060). The shift in grandwater level will reach respectively 3.6 m and 4.5 m for 15% and 30% of recharge reduction. These findings are in line with Soro et al.(2017) study in the Bandaman aquifer (the lithology is characterized by the Birimian formations (volcanic, volcanogenic, and sedimentary formations)) which reveal that The groundwater recharge may decrease from 136.6 mm to 73.8 mm by 2025 and 2075, groundwater may decrease from 60.2% to 55.4% compared to the baseline period.

The climate change is likely to affect groundwater due to changes in precipitation and temperature. Pumping Groundwater withdrawal from a well causes lowering of heads in the area around the well. Both Associted could affect deeply groundwater level in the future (2060) and reach 4 m of deacreasing and this was also observe in the study of Kouame et al.(2008)in which he drawdown contour obtained in 2030 progresses towards the lagoons (Aghien, Ebrié, Lamé). This behaviour of the drawdown may result in salt-water intrusion. This salt-water intrusion will occur when the withdrawals projected by the SODECI reverse the groundwater flow direction from south towards north.

Chapter 7 - General conclusion and perspectives

7.1 Conclusions

Water availability used to supply Abidjan's city is indeed subject to more pressure such as: climate change and urbanization. However, to overcome this insufficiency, it is important to understand the process that links surface water and groundwater. Therefore modflow was used to set up the aquifer model in order to understand groundwater and surface water interaction. This study focused on Continetal Terminel aquifer and the results enhance knowledge about (i) assess groundwater recharge regarding the changing in climate and LULC of the Continental Terminal catchment using water balance method after determined the runoff based on the SCS curve number method, (ii) assess the impact of the Representative Concentration Pathways (RCP4.5) climate change scenario on rainfall, temperature, and groundwater recharge in the future 2020-2049, and (iii) model and analyze locally impact of climate and LULC change on groundwater balance using MODFLOW model to assess interaction between groundwater and surface water. LULC change's historical data analysis showed a development of urban area at the expense of forest area. Population growth increase built-up area, road construction, demands on resources etc. Besides, the study reveal that the gradual regression of groundwater recharge is benefit to runoff which is increasing. Therefore it is clear that urbanization has an effect on groundwater recharge.

The CHIRPS data was able to mimic the seasonal rainfall pattern of the study area reasonably well indicating its capability for further usage in other analysis at the study location. The impact of climate change based on the RCP 4.5 scenario on future recharge of the aquifer, for the period 2020-2049 based on an ensemble mean of two climate models (GFDL and HadGEM) were also studied. The analyses of the climate simulation under RCP4.5 scenario shows a warmer climate in the future 2020-2049. The study observed an increase in mean annual rainfall and temperature in the future 2020-2049. The projected recharge under RCP 4.5 scenario is increasing but this could change under RCP 8.5 scenario

MODFLOW was configured for the Continent Terminal Aquifer to study groundwater and surface water interaction by driving the model with piezometer head .Groundwater dynamic show that Aghien lagoon drains the aquifer to 1.10^4 m^3 /day in certain areas where the aquifer is deeper, the lagoon supplies the groundwater by drainage up to $41.10^3 m^3$/day. All the scenarios made to assess future groundwater water level (2060) such as pumping rate increasing, Climate change under CMIP5 scenario and both of them associated reveal a drop of hydraulic head and this could impact surface water reseve

7.2 Recommendations

Considering the various information gathered, it is recommended that, further efforts must be done in order to make the model better so as to simulate alternative scenarios of groundwater development in the Continental Terminal aquifer. Such simulations can provide planners and decision makers with guidance to minimize undesirable impacts from pumping and climate change

Furthermore, it is recommended that

i) Policy makers should strengthen urbanization legislation, land use planning and enforcement to regulate and control urbanization.

ii) The groundwater recharge zones of high hydraulic head identified in the catchment must be protected to safeguard the quality of groundwater in the area.

iii) Modelize future LULC unsing SWAT model in order to to well predict groundwater recharge on the study area

iv) Using new indicator for standardising groundwater level time series, the Standardised Piezometric Level Index (SPLI) to compare groundwater level time series and to characterize the severity of extreme events such as long dry period or groundwater overflows

7.3 Perspectives or Future works

Regarding actual situation of land use / land cover, urbanization rate and climate change in groundwater recharge, projections of rainfall and temperature for the study area under RCP4.5 scenario could under estimate the impact on the groundwater recharge. Therefore future study can look at to project rainfall and temperature and temperature under RCP8.5 scenario. Besides future works should focus on land use / land cover projection using SWAT model in order to amphasize future recharge value

.

References

Abdellatif, Mawada, William Atherton, Rafid Alkhaddar, and . 2012. “Climate Change Impacts on the Extreme Rainfall for Selected Sites in North Western England.” *Open Journal of Modern Hydrology* 02 (03): 49–58. https://doi.org/10.4236/ojmh.2012.23007.

Aghui, N., and J. Biemi. 1984. “Géologie et Hydrogéologie Des Nappes de La Région d’Abidjan et Risques de Contamination.” *Ann. l’Université Natl. Côte d’Ivoire* 20: 331–347.

Ahern, J.A. 2005. “Ground-Water Capture-Zone Delineation: Method Comparison in Synthetic Case Studies and a Field Example on Fort Wainwright, Alaska (M.Sc). University of Alaska Fairbanks, United States. Available at: Http://Issuu.Com/Universityofalaskafairbanks/Docs/Jahern.”

Ahmed, S., J. C. Marechal, E. Ledoux, and G. De Marsily. 2007. “Groundwater FLow Modelling in Hard-Rock Terrain in Semi-Arid Areas: Experience from India.” *Hydrological Modelling in Arid and Semi-Arid Areas*, 157.

Alemaw, B.F, and T.R. Chaoka. 2003. “A Continental Scale Water Balance Model: A GIS-Approach for Southern Africa.” *Physics and Chemistry of the Earth* 28: 957–966.

Alley, W. M., T. E. Reilly, and O. L. Franke. 1999. “Sustainability of Ground-Water Resources.” *US Department of the Interior, US Geological Survey*. 1186.

Anderson, M.P., and W.W. Woessner. 1992. “Applied Groundwater Modeling: Simulation of Flow and Advective Transport.” *Academic Press, San Diego*.

Asquith, W.H., and M.C. Roussel. 2007. “An Initial-Abstraction Constant-Loss Model for Unit Hydrograph Modeling for Applicable Watersheds in Texas: U.S Geological Survey Scientific Investigations Report 2007-5243.”

Atteia, O. 2011. “Modelisation Du Devenir Des Composé Organiques Dans Les Aquiferes: Logiciel Rflow 2D et Application.” *Lavoisier, France*.

Baalousha, H. 2007. “Application of Automatic Differentiation in Groundwater Sensitivity Analysis. In Oxley, L. and Kulasiri, D. (Eds) Modelling and Simulation Society of Australia and New Zealand, December 2007, ISBN : 978-0-9758400-4-7.” *MODSIM 2007 International Congress on Modelling and Simulation.*, 2728–33.

———. 2009. “Fundamentals of Groundwater Modelling, in: König, L.F., Weiss,J.L. (Eds.), New York.” *Groundwater: Modelling, Management and Contamination. Nova Science Publishers*, 149–166.

Baalousha, H, and J Köngeter. 2006. “Stochastic Modelling and Risk Analysis of Groundwater Pollution Using Form Coupled with Automatic Differentiation.” *Advances in Water*

Resources 29 (12): 1815–32.

Bai, L., C. Shi, L. Li, Y. Yang, and J. Wu. 2018. "Accuracy of CHIRPS Satellite-Rainfall Products over Mainland China." *Remote Sensing* 10 (3).

Banton, O., and L. M. Bangoy. 1997. "HYDROGEOLOGIE. Multiscience Environnementale Des Eaux Souterraines." *Presses de l'Université Du Quebec.,AUPELF-UREF,* 460.

Barlow, P.M., and A. Harbaugh. 2006. "USGS Directions in MODFLOW Development." *Ground Water 44* 6: 771–774.

Bear, J., and A. Verruijt. 1987. "Modeling Groundwater Flow and Pollution." *Springer*, 432.

Belay, E.A. 2009. "Growing Lake with Growing Problems: Integrated Hydrogeological Investigation on Lake Beseka, Ethiopia (PhD)." University of Bonn, Germany.

Berthe, Yao Affoué, Kouame Kouassi Innocent, Kouassi Kouamé Auguste, Koffi Kouadio, Bi Tié Albert Goula, and Issiaka Savane. 2015. "Estimation de La Recharge d ' Une Nappe Côtière En Zone Tropicale Humide : Cas de La Nappe Du Continental Terminal d ' Abidjan (Côte d ' Ivoire) [Assessment of Coastal Groundwater Recharge in a Humid Tropical Zone by the Method of Thiessen : Case of Th." *International Journal of Innovation and Applied Studies* 12 (4): 888–98.

Bigot, S., T. Brou, J. Oszwald, A. Diedhiou, and C. Houdenou. 2005. "Facteurs de La Variabilité Pluviométrique En Côte d'Ivoire et Relations Avec Certaines Modifications Environnementales." *Sécheresse* 16 (1): 14-21.

BNETD. 2008. "Impact Environnemental et Social de La Mise En Œuvre Des Périmètres de Protection Autour Des Points de Captage d'eau Souterraine Du District d'Abidjan." *Rapport Définitif Février 2008.*, 97.

Bonta, J. V., C. R. Amerman, T. J. Harlukowicz, and W. A. Dick. 2007. "Impact of Coal Surface Mining on Three Ohio Watersheds." *Surface-water Hydrology* 33 (4): 907–17.

Box, G., and N. Draper. 1987. "Empirical Model-Building and Response Surfaces," 669.

Bredehoeft, J.D., and L.F. Konikow. 2012. "Reflectionsonourmodelvalidationeditorial." *Groundwater* 50 (4): 495. https://doi.org/10.1111/j.1745-6584.2012.00951.x.

Bundschuh, J., and M.C.S. Arriaga. 2010. "Multiphysics Modeling. CRC/Balkema,Taylor & Francis Group."

Campbell, J. B., and R. H. Wynne. 2011. "Introduction to Remote Sensing. Fifth Edn. New York:" *Guilford Press*.

Castany, G. 1998. *Hydrogéologie : Principes et Méthodes. 2e Cycle, DUNOD, Paris*.

Chenini, I., and A. Ben Mammou. 2011. "Groundwater Recharge Study in Arid Region: An Approach Using GIS Techniques and Numerical Modeling." *Comput. Geosci. UK* 36:

801–817.

Chiang, W.H., and W. Kinzelbach. 1998. “Processing Modflow A Simulation System for Modeling Groundwater Flow and Pollution.”

Cohen, L.T., J. Matos, J.L. Boillat, and A. Schleiss. 2012. “Comparison and Evaluation of Satellite Derived Precipitation Products for Hydrological Modeling of the Zambezi River Basin.” *Hydrol. Earth Syst. Sci.* 16: 489–500. https://doi.org/10.5194/hess-16-489-2012.

Collins, M.A., and L.W. Gelhar. 1971. “Seawater Intrusion in Layered Aquifers.” *Water Resources Research* 7 (4): 971–79. https://doi.org/10.1029/WR007i004p00971.

Council, G.W. 1999. “A Lake Package for MODFLOW (LAK2).”

Crosbie, R.S., P. Binning, J.D. Kalma, and .. 2005. “A Time Series Approach to Inferring Groundwater Recharge Using the Water Table Fluctuation Method.” *Water Resour Res* 41. https://doi.org/10.1029/2004WR003077.

Dakoure, D. 2003. “Etude Hydrogeologique et Geochimique de La Bordue Sud-Est Du Bassin Sadimentaire de Taoudeni (Burkina Faso- Mali) Essai de Modelisation Université Pierre et Marie Curie-Paris VI.”

Danumah, J.H., M.B. Saley, S.N. Odai, M. Thiel, and L.Y. Akpa. 2017. “Remote Sensing Based Analysis of the Latest Development and Structure of Abidjan District, Cote d’Ivoire.” *Geoinfor Geostat: An Overview* 5 (1).

Danumah, Jean Homian. 2016. “Assessing Urban Flood Risks under Changing Climate and Land Use in Abidjan District , South Cote d ’ Ivoire.” KWAME NKRUMAH UNIVERSITY OF SCIENCE AND TECHNOLOGY KUMASI GHANA.

Darcy, H.P.G. 1856. “Determination of the Laws of Water Flow through Sand, the Public Fountains of the City of Dijon, Appendix De Filtration ,Section2 of Appendix Don Natural Filtration. Translated from the French by Patricia Bobeck. Kendall/Hunt Publishing Company, Iowa,” 455–59.

Delin, G.N., R.W. Healy, D.L. Lorenz, and J.R. Nimmo. 2007. “Comparison of Local- to Regional-Scale Estimates of Ground-Water Recharge in Minnesota,.” *USA. J. Hydrol.* 334: 231–249. https://doi.org/10.1016/j.jhydrol.2006.10.010.

Delor, C., I. Diady, Y. Simeon, B. Yao, J. P. Tastet, M. Vidal, and A. CHiron, J. P. Dommanget. 1992. “Notice Explicative de La Carte Géologique de La Côte d’Ivoire à 1/200000, Feuille Grand-Bassam, Mémoire de La Direction de La Géologie de Côte d’Ivoire, N°4, Abidjan, Côte d’Ivoire,.”

Diallo, I, M B Sylla, F Giorgi, A T Gaye, and M Camara. 2012. “Multimodel GCM-RCM Ensemble-Based Projections of Temperature and Precipitation over West Africa for the

Early 21st Century." *International Journal of Geophysics*, 19. https://doi.org/10.1155/2012/972896.

Dingman, S. L. 2008. "Physical Hydrology. 2 Ed. Long Grove, Illinois." *Waveland Press, Inc.*

Doherty, J., L. Brebber, P. Whyte, and . 1994. "PEST - Model-Independent Parameter Estimation. ." *User's Manual,Watermark Computing. Australia*.

Drouin-Brisebois, I.A. 2002. "Predicting Local and Regional Effects of Urbanisation on the Subsurface Water Balance of North Pickering Agricultural Lands: Unpublished M.S. Thesis, Univ. Toronto, Toronto, Ontario, Canada."

Ellis, E., and R. Pontius. 2007. "Land-Use and Land-Cover Change [Online]." *Available from <http://Www.Eoearth.Org/Article/Land-Use_and_land-Cover_change>*.

Essink, G.H.P.O. 2001. "Density Dependent Groundwater Flow Salt Water Intrusion and Heat Transport."

Essink, G.H.P.O. 2000. "Groundwater Modelling. University of Utrecht."

FAO; ICRISAT; CIAT. 2018. "Climate-Smart Agriculture in Côte d'Ivoire. CSA Country Profiles for Africa Series. International Center for Tropical Agriculture (CIAT); International Crops Research Institute for the Semi-Arid Tropics (ICRISAT); Food and Agriculture Organization of The." Rome, Italy.

FAO. 2011. "The State of the World's Land and Water Resources for Food and Agriculture (SOLAW) – Managing Systems at Risk. Food and Agriculture Organization of the United Nations, Rome and Earthscan, London."

Foster, S.S.D., A.R. Lawrence, and B.M. Morris. 1998. "Groundwater in Urban Development." *World Bank Technical Paper No 390, Washington DC.*

Foster, S.S.D, B.L. Morris, P.J. Chilton, and ... 1999. "Groundwater in Urban Development- a Review in the Linkages and Concerns. In: Ellis, J.B. (Ed) Impacts of Urban Growth on Surface Water and Groundwater Quality." *IAHS* 259: 3–12.

Franke, O.L., T.E. Reilly, G.D. Bennett, and . 1987. "Definition of Boundary and Initial Conditions in the Analysis of Saturated Ground-Water Flow Systems – An Introduction: Techniques of Water-Resources Investigations of the United States Geological Survey." In *Book 3, Chapter B5*, 15.

Freeze, R.A., and J.A. Cherry. 1979. *Groundwater. Englewood Cliffs, NJ: Prentice-Hall*.

Freeze, R.A, and J.A. Cherry. 1999. *Groundwater: Englewood Cliffs, NJ, Prentice-Hall*.

Fujinawa, K., T. Iba, Y. Fujihara, and T. Watanabe. 2009. "Modeling Interaction of FLuid and Salt in an Aquifer/ Lagoon System." *Groundwater* 47 (1): 35–48. https://doi.org//10.1111/j.1745-6584.2008.00482.x.

Funk, C, P Peterson, M Landsfeld, D Pedreros, and J Verdin. 2015. “The Climate Hazards Infrared Precipitation with Stations-a New Environmental Record for Monitoring Extremes.” *Scientific Data* 2 (150066).

Furman, A. 2008. “Modeling Coupled Surface-Subsurface FLow Processes: A Review.” *Vadose Zone Journal 7* 2: 741–756.

Geomines. 1982. “L’inventaire Hydrogéologique Effectué à Partir de Tous Les Ouvrages d’hydraulique Villageoise Existant En Côte d’Ivoire.”

Gerhart, J.M. 1986. “Groundwater Recharge and Its Effect on Nitrate Concentrations beneath a Manured Field Site in Pennsylvania.” *Groundwater* 24: 483–489.

Ghodoosipour, B. 2013. “Three Dimensional Groundwater Modeling in Laxemar-Simepevarp Guaternary Deposits.” *TRITA LWR Degree Project* 13 (36): 41.

Goula, A., I. Savané, K. Brou, F. Vamoryba, and B. Gnamien. 2006. “Impact de La Variabilité Climatique Sur Les Ressources Hydriques Des Bassins de N’ZO et N’ZI En Cote d’ivoire (Afrique Tropicale Humide).” *Vertigo* 7 (1): 12.

Hall, D.W., and D.W. Risser. 1993. “Effects of Agricultural Nutrient Management on Nitrogen Fate and Transport in Lancaster County, Pennsylvania.” *Water Resour Bull* 29: 55–76.

Harbaugh, A.W. 2005. “MODFLOW-2005, The U.S. Geological Survey Modular Ground-Water Model—the Ground-Water Flow Process. U.S. Geological Survey Techniques and Methods 6-A16, Variously Paginated.”

Hawkins, A.J.S., P.N. Salkeld, B.L. Bayne, E. Gnalger, and D.M. Lowe. 1985. “Feeding and Resource Allocation in the Mussel Mytilus Eduli: Evidence for Time-Averaged Optimization.” *Mar Ecol Prog Ser* 20: 273–87.

Hawkins, R. H. 1993. “Asymptotic Determination of Runoff Curve Numbers from Data.” *J. Irrig. Drain. Eng.* 119: 334–45. https://doi.org/10.1061/(ASCE)0733-9437(1993)119:2(334).

Hawkins, R. H., T. J. Ward, D. E. Woodward, and J. A. Van Mullem. 2009. “Curve Number Hydrology: State of the Practice.” *American Society of Civil Engineers, Reston,VA.*

Healy, R.W., and P.G. Cook. 2002. “Using Groundwater Levels to Estimate Recharge.” *Hydrogeol J.* 10 (91): 109.

Healy, R.W., and B.R. Scanlon. 2010. “Estimating Groundwater Recharge.” *Cambridge University Press, New York.*

Heinzeller, D., D. Dieng, G. Smiatek, C. Olusegun, C. Klein, I. Hamann, S. Salack, and H. Kunstmann. 2017. “The WASCAL High-Resolution Regional Climate Simulation Ensemble for West Africa: Concept, Dissemination, Assessment. Data Discuss.,

Https://Doi.Org/10.5194/Essd-2017-93." *Earth Syst. Sci.*

Heinzeller, D., C. Olusegun, H. Kunstmann, and . 2016. "Projected Future (2070-2099): High Resolution (12km) WRF-MPI Daily Near-Surface Relative Humidity over West Africa, (WASCAL Project).Https://Wascal-Dataportal.Org/Geonetwork/?Uuid=0cafe3f0-Adf5-43d7-9483-6fbd2b05d86d."

Heliotis, D.F., and C.B. DeWitt. 1987. "RAPID WATER TABLE RESPONSES TO RAINFALL IN A NORTHERN PEATLAND ECOSYSTEM1." *WATER RESOURCES BULLETIN. AMERICAN WATER RESOURCES ASSOCIATION* 23 (6): 6.

Hill, Mary. 2006. "The Practical Use of Simplicity in Developing Groundwater Models." *Ground Water Journal* 44 (6): 775–81.

Hjelmfelt, A. T. Jr., D. A. Woodward, G. Conaway, A. Plummer, Q. D. Quan, J. Van Mullen, R. H. Hawkins, and D. Rietz. 2001. "Curve Numbers, Recent Developments, in: Proc. of the 29th Congress of the Int. As. for Hydraul. Res., Beijing, China (CD ROM), 17–21 September, 2001."

Hjelmfelt, A.T. 1991. "Investigation of the Curve Number Procedure." *Journal of Hydraulic Engineering, ASCE* 117 (6): 725–37.

Huang, Mingbin, Jacques Gallichand, Zhanli Wang, and Monique Goulet. 2006. "A Modification to the Soil Conservation Service Curve Number Method for Steep Slopes in the Loess Plateau of China." *Hydrological Processes,* 20 (3): 579–89.

Igboekwe, M. U., and N. J. Achi. 2011. "Finite Difference Method of Modelling Groundwater Flow, Umudike, Nigeria." *Journal of Water Resource and Protection* 3. https://doi.org/10.4236/jwarp.2011.33025.

Illman, W.A., S.J. Berg, and T.-C.J Yeh. 2012. "Comparison of Approaches for Predicting Solute Transport: Sandbox Experiments." *Groundwater* 50 (3): 421–31. https://doi.org/17456584.2011.00859.

Inge, G., G. Tom, L. P. H. Van Beek, H. S Edwin, and F. P. Marc Bierkens. 2019. "Environmental Flow Limits to Global Groundwater Pumping." *Nature* 574 (7776): 90–94. https://doi.org/10.1038/s41586-019-1594-4.

INS. 2014. "Recensement Général de La Population et de l'habitat (RGPH),Données Socio-Démographiques et Économique de Localités, Résultats Définitif Par District, Région, Département et Sous-Préfecture, Secrétariat Technique Permanent Du Comité Technique Du RGPH », 2."

IPCC. 2007. "'Climate Change 2007: The Physical Science Basis.' Contribution of Working Group I to the Fourth Assessment Rep. of the Intergovernmental Panel on Climate Change,

S. Solomon, D. Qin, M. Manning, Z. Chen, M. Marquis, K. B. Averyt, M. Tignor, and H. L. Mill." In . Cambridge University Press, Cambridge, U.K., 996.

———. 2014. "Summary for Policymakers. In Climate Change 2013 – The Physical Science Basis: Working Group I Contribution to the Fifth Assessment Report of the Intergovernmental Panel on Climate Change." Cambridge: Cambridge University Press. https://doi.org/10.1017/CBO9.

Jansen, L. J., and A. Di Gregorio. 2002. "Parametric Land Cover and Land-Use Classifications as Tools for Environmental Change Detection." *Agriculture, Ecosystems & Environment.* 91 (1): 89-100.

Jha, M.K., A Chowdhury, S Chowdary, and V.M. Peiffer. 2007. "Groundwater Management and Development by Integrated Remote Sensing and Geographic Information Systems: Prospects and Constraints." *Water Resour Manag* 21 (427): 67.

Jourda, J. R. P. 1987. "Contribution à l'étude Géologique et Hydrogéologique de La Région Du Grand Abidjan,." Thèse de Troisième Cycle, Université de Grenoble.

Kalnay, E., and C. Ming. 2003. "Impact of Urbanization and Land-Use Change on Climate." *Nature* 423: 528–31.

Kanohin, F., P. Jourda, B. Saley, and I. Savané. 2009. "Impacts de La Variabilité Climatique Sur Les Ressources En Eau et Les Activités Humaines En Zone Tropicale Humide: Cas de La Région de Daoukro En Côte d'Ivoire." *European Journal of Scientific Research* 26 (2): 209–22.

Kidd, C, P Bauer, J Turk, G Huffman, R Joyce, K Hsu, and D. Braithwaite. 2012. "Intercomparison of High-Resolution Precipitation Products over Northwest Europe." *J Hydrometeorol.* 13 (1): 67–83.

Kim, J., D. E. Waliser, C. A. Mattmann, C. E. Goodale, A. F. Hart, P. A. Zimdars, J. Daniel, . Crichton, ..., and A. Favre. 2013. "Evaluation of the CORDEX-Africa Multi-RCM Hindcast: Systematic Model Errors." *Climate Dynamics* 42 (5–6): 1189–1202. https://doi.org/10.1007/s00382-013-1751-7.

Kinzelbach, W. 1986. "Groundwater Modelling: An Introduction with Sample Programs in BASIC." *Developments in Water Science. Elsevier ; Distributors for the United States and Canada, Elsevier Science Pub, New York.*

Kollet, Stefan J, and Reed M Maxwell. 2008. "Capturing the Influence of Groundwater Dynamics on Land Surface Processes Using an Integrated , Distributed Watershed Model." *Water Resour. Res* 44 (February 2007): 1–18. https://doi.org/10.1029/2007WR006004.

Konikow, L.F., and T. Reilly. 1998. “Groundwater Modeling.” *Delleur JW(Ed) the Handbook of Groundwater Engineering. CRC Press, Boca Raton*.

Kouadio, B. H. 1997. “Quelques Aspects de La Schématisation Hydrogéologique : Cas de La Nappe d’Abidjan. DEA, Université de Cocody.”

Kouakou, Deh Serge. 2013. “Contributions de l’évaluation de La Vulnérabilité Spécifique Aux Nitrates et d’un Modèle de Transport Des Organochlorés a La Protection Des Eaux Souterraines Du District d’abidjan (Sud de La Côte d’ivoire).” Thèse de l’université félix houphouët-boigny , hydrogéologie.

Kouakou, E. 2011. “Impacts de La Variabilité Climatique et Du Changement Climatique Sur Les Ressources En Eau En Afrique de l’Ouest : Cas Du Bassin Versant de La Comoé.” Thèse Unique de Doctorat, Université d’Abobo Adjamé.

Kouakou, E., S. Bachir, A. Goula, and I. Savane. 2007. “Impacts de La Variabilité Climatique Sur Les Ressources En Eau de Surface En Zone Tropicale Humide: Cas Du Bassin Versant Transfrontalier de La Comoé (Côte d’Ivoire – Burkina Faso).” *European Journal of Scientific Research* 16 (1): 31–43.

Kouame, K. I. 2007. “Pollution Physico -Chimique Des Eaux Dans La Zone de La Décharge d’Akouédo et Analyse Du Risque de Contamination de La Nappe d’Abidjan Par Un Modèle de Imulation Des Écoulements et Du Transport Des Polluants.” Thèse unique, université d’abobo-adjamé.

Kouame, K. J., J. P. Jourda, J. Biemi, and Y. Leblanc. 2008. “Groundwater Modelling and Implication for Groundwater Protection: Case Study of the Abidjan Aquifer, Côte d’ivoire.” *Applied Groundwater Studies in Africa*, 457–72.

Kouassi, K. A. 2013. “Modélisation Hydrodynamique En Milieu Poreux Saturé Par Approche Inverse via Une Paramétrisation Multi-Échelle : Cas de l’aquifère Du Continental Terminal d’Abidjan (Côte d’Ivoire).” Thèse université nangui abrogoua.

Kouassi, M., Kouame F., B. Saley, and K. Yao. 2007. “Identification de Tendances Dans La Relation Pluie-Débit et Recharge Des Aquifères Dans Un Contexte de Variabilité Hydroclimatique: Cas Du Bassin Versant Du N’zi (Bandama) En Côte d’Ivoire.” *EuropeanJournal of Scientific Research* 12 (3): 412–27.

Kouli, M., N. Lydakis-Simantiris, P. Soupios, and . 2009. “GIS-Based Aquifer Modeling And Planning Using Integrated Geoenvironmental And Chemical Approaches, in: König, L.F., Weiss, J.L. (Eds.), , New York.” *Groundwater: Modelling, Management and Contamination. Nova Science Publishers*.

Kowalik, T., and A. Wałęga. 2015. “Estimation of CN Parameter for Small Agricultural

Watersheds Using Asymptotic Functions." *Water* 7 (3): 939–955.

Kresic, N., and A. Mikszewski. 2013. "Hydrogeological Conceptual Site Models : Data Analysis and Visualization." *CRC Press, Boca Raton*, 584.

Kumar, C P. 2012. "Climate Change and Its Impact on Groundwater Resources." *International Journal of Engineering and Science* 1 (5): 43–60. www.researchinventy.com%0AClimate.

Kunstmanna, H., and M. Kastensb. 2006. "Direct Propagation of Probability Density Functions in Hydrological Equations." *Journal of Hydrology* 325 (1–4): 82–95.

Lambin, E. F., H. J. Geist, and E. Lepers. 2003. "Dynamics of Land-Use and Land-Cover Change in Tropical Regions'." *Annual Review of Environmental Resources* 28 (205): 41.

Lambin, E. F., B. L. Turner, H. J. Geist, S. B. Agbola, A. Angelsen, J. W. Bruce, and J. Xu. 2001. "The Causes of Land-Use and Land-Cover Change: Moving beyond the Myths." *Global Environmental Change,* 11 (4): 261-269.

Langevin, C. D., and W. Guo. 2006. "MODFLOW/MT3DMS–Based Simulat Ion of Variable-Density Ground Water Flow and Transport." *Groundwater* 44 (3): 339–51.

Lerner, D.N. 2002. "Identifying and Quantifying Urban Recharge: A Review." *Hydrogeology Journal* 10: 143–52.

Liou, T., and H. Der Yeh. 1997. "Conditional Expectation for Evaluation of Risk Groundwater Flow and Solute Transport: One-Dimensional Analysis." *Journal of Hydrology* 199 (3–4): 378–402.

Loroux, B.F.E. 1978. "Contribution à L'étude Hydrogéologique Du Bassin Sédimentaire de Côte d'Ivoire." *Ph.D. Thesis, Université de Bordeaux I, Bordeaux, France.*, 93.

Mahé, G., Y. L'Hôte, J. C. Olivry, and G. Wotling. 2001. "Trends and Discontinuities in Regional Rainfall of West and Central Africa (1951-1989)." *Hydrological Sciences Journal* 46 (2): 211-226.

Mamer, E.A., and C.S. Lowry. 2013. "Locating and Quantifying Spatially Distributed Groundwater/Surface Water Interactions Using Temperature Signals with Paired FIber-Optic Cables." *Water Resources Research* 1 (11): 49. https://doi.org/10.1002/2013WR014235.

Mandle, R.J. 2002. "Groundwater Modeling Guidance (Groundwater Modeling Program). Michigan Department of Environmental Quality."

McCabe, G.J., and S.L. Markstrom. 2007. "A Monthly Water-Balance Model Driven by a Graphical User Interface." *U.S. Geological Survey, Open-File Report*.

McDonald, M.G., and A.W. Harbaugh. 1988. "A Modular Three-Dimensional Finite-Difference Groundwater Flow Model. U.S. Geological Survey Techniques of Water-

Resources Investigations, Book 6, Chp A1," 586.

Meinzer, O.E. 1923. "The Occurrence of Ground Water in the United States: With a Discussion of Principles. University of Chicago," 1923.

Meinzer, O.E., and N.D. Stearns. 1929. "A Study of Groundwater in the Pomperaug Basin, Conn. with Special Reference to Intake and Discharge." *US Geol Surv Water-Supply Pap* 597B: 73–146.

Meyer, S.C. 2005. "Analysis of Base Flow Trends in Urban Streams, Northeastern Illinois,USA." *Hydrogeology Journal* 13: 871–85.

Middlemis, H. 2001. "Groundwater Flow Modeling Guideline (No. 125)." *Aquaterra Consulting Pty Ltd, Australia.*

Mishra, S.K., and V.P. Singh. 2003. "Soil Conservation Service Curve Number (SCS-CN) Methodology." *Kluwer Academic Publishers, Dordrecht.* https://doi.org/10.1007/978-94-017-0147-1.

Moore, J.E. 2002. "Field Hydrogeology: A Guide for Site Investigations and Report Preparation." *Lewis Publishers, Boca Raton.*

Morris, B.L., A.R. Lawrence, P.J. Chilton, B. Adams, R. Calow, and B.A. Klinck. 2003. "Groundwater and Its Susceptibility to Degradation: A Global Assessment of the Problems and Options for Management." *Early Warning and Assessment Report Series,RS, 03-3. UNEP, Nairobi,Kenya.*

Mukherjee, S. 1996. "Targeting Saline Aquifer by Remote Sensing and Geophysical Methods in a Part of Hamirpur-Kanpur, India." *Hydrogeol J* 19 (53): 64.

Niswonger, R.G., and D.E. Prudic. 2006. *Documentation of the Streamflow-Routing (SFR2) Package to Include Unsaturated FLow beneath Streams—A Modification to SFR1. U.S. Geological Survey Techniques and Methods, Book 6, Chap. A13. Carson City, Nevada: USGS.*

Obuobie, E. 2008. "Estimation of Groundwater Recharge in the Context of Future Climate Change in the White Volta River Basin, West Africa, Dissertation." Rheinische Friedrich-Wilhelms- Bonn University.

Olsthoorn, T. 1985. "The Power of the Electronic Worksheet- Modelling without Special Programs." *Ground Water Journal* 23: 381–90.

Oluseyi, O. A., M. Victor, O. E. Ayobami, F. D. Oluwaseun, O. O. Akintayo, and J. A. Taiwo. 2015. "Estimation of Groundwater Recharges Using Empirical Formulae in Odeda Local Government Area, Ogun State, Nigeria." *Challenges*, no. 6: 271–81. https://doi.org/10.3390/challe6020271.

Oreskes, N., K. Shrader-Frechette, K. Belitz, and . 1994. “Verification, Validation, and Confirmation of Numerical Models in the Earth Sciences.” *Science* 263 (5147): 641–46.

Owuor, S O, A C Guzha, M C Rufino, D E Pelster, and L Breuer. 2016. “Groundwater Recharge Rates and Surface Runoff Response to Land Use and Land Cover Changes in Semi-Arid Environments.” *Ecological Processes* 5 (16): 21. https://doi.org/10.1186/s13717-016-0060-6.

Papon, A., and R. Lemarchand. 1973. “Géologie et Minéralisation Du Sud- Ouest de La Cote d’Ivoire : Synthèse Des Travaux de l’opération SASCA, SODEMI-Abidjan.,” 285.

Pidwirny, M. 2006. “Actual and Potential Evapotranspiration, Fundamentals of Physical Geography.” 2nd Edition . date viewed.http// www.physicalgeography.net/fundamentals/8j.html.

Poeter, E.P., and M.C. Hill. 1998. “Documentation of UCODE, a Computer Code for Universal Inverse Modeling.” *U.S. Geological Survey, Water-Resources Investigations* 98 (4080).

Prudic, D.E. 1989. “Documentation of a Computer Program to Simulate Stream-Aquifer Relations Using a Modular, FInitedifference, Ground-Water FLow Model. U.S. Geological Survey Open-File Report . Carson City. Nevada: USGS.”

Prudic, D.E., L.F. Konikow, E.R . Banta, and . 2004. “A New Stream FLow Routing (SFR1) Package to Simulate Stream-Aquifer Interaction with MODFLOW-2000. U.S.” *Geological Survey Open- Carson City, Nevada: USGS.*

Rasmussen, W.C, and G.E. Andreasen. 1959. “Hydrologic Budget of the Beaverdam Creek Basin, Maryland.” *US Geol Surv Water- Supply Pap* 1472: 106.

Reilly, T., and A. Harbaugh. 2004. “Guidelines for Evaluating Ground-Water Flow.” *Scientific Investigations Report . U.S. Department of Interior,. U.S. Geological Survey.* Vol. 2004–5038.

REMP, (Rufiji Enironment Management Project). 2003. “Development of a Computerized Flood Warning Model and Study of Hydrological Characteristics of the Lower Rufiji Floodplain and Delta, u.o.: U.N.”

Roose, E., and M. Cheroux. 1966. “Les Sols Du Bassin Sédimentaire de Côte d’Ivoire. O.R.S.T.O.M. Adiopodoumé, Multig.”

Ruelland, D., A. Dezetter, C. Puech, and S. (2008) Ardoin - Bardin. 2008. “Long - Term Monitoring of Land Cover Changes Based on Landsat Imagery to Improve Hydrological Modelling in West Africa.” *Int. J. Remote Sens.* 29: 3533–3551.

Sawyer, A.H., M.B. Cardenas, and J. Buttles. 2012. “Hyporheic Temperature Dynamics and Heat Exchange near Channel-Spanning Logs.” *Water Resources Research* 48.

https://doi.org/10.1029/ 2011WR011200.

Scanlon, B. R., R. C. Reedy, D. A. Stonestrom, and ..... 2005. “Impact of Land Use and Land Cover Change on Groundwater Recharge and Quality in the Southwestern US.” *Global Change Biology* 11 (10): 1577–1593. https://doi.org/10.1111/j.1365-2486.2005.01026.x.

Schelesinger, W.H. 1991. *Biogeochemistry–An Analysis of Global Change: Academic Press, San Diego, California*.

Schneider, Lauren E., and Richard H. McCuen. 2005. “Statistical Guidelines for Curve Number Generation.” *Journal of Irrigation and Drainage Engineering* 131 (3). https://doi.org/10.1061/(ASCE)0733-9437(2005)131:3(282).

Schueler, T.J. 1994. “Importance of Imperviousness.” *Watershed Protection Techniques* 1: 100-111.

Seneviratne, A.A.A.K.K. 2007. “Development of Steady State Groundwater Flow Model in Lower Walawa Basin-Sri Lanka (Integrating GIS, Remote Sensing and Numerical Groundwater Modelling) (M.Sc). International Institute for Geoinformation.” *Science and Earth Observation EnschedeX, The Netherlands.*

Sharp, J.M., Jr., L.E. Llado, and T.J. Budge. 2009. “Urbanization-Induced Trends in Spring Discharge from a Karstic Aquifer – Barton Springs, Austin, Texas, USA: In Proceedings,.” In *15th International Congress of Speleology (White, W.B., Ed.), Kerrville, TX,* 2:1211-1216.

Sharpley, A.N., and J.R. Williams. 1990. “EPIC-Erosion/Productivity Impact Calculator: 1. Model Determination. USDepartment of Agriculture.” *Tech. Bull* 1768.

Shelton, C.W. 2011. “An Analytical and Numerical Investigation of Stream/Aquifer Interaction Methodologies (M.Sc).” *University of Washington State, Washington.*

Simmons, C.T., P. Bauer-Gottwein, T. Graf, W. Kinzelbach, H. Kooi, L. Li, V. Post, et al. 2010. “Variable Density Groundwater Flow: From Modelling to Applications, in: Wheater, H.S., Mathias, S.A., Li, X. (Eds.), Groundwater Modelling in Arid and Semi-Arid Areas.” *Cambridge University Press,, New York*, 87–117.

Singhal, B.B.S., and R.P. Gupta. 2010. “Applied Hydrogeology of Fractured Rocks.” *Springer Science+Business Media Dordrecht ; New York.* 2nd ed.

Skibitzke, H.E. 1961. “Electronic Computers as an Aid to the Analysis of Hydrologic Problems. Comm. Subterranean Waters, Gentbrugge, Belgium.” *International Association of Scientific Hydrology* 52: 347–58.

Skole, D. L. 1994. “Data on Global Land-Cover Change: Acquisition, Assessment and Analysis.” *In Changes in Land Use and Land Cover: A Global Perspective. Ed. by Meyer,*

W. B. and Turner II, B. L. Cambridge: Cambridge University Press, 437–71.

Sogreah. 1996. "Etude de La Gestion et de La Protection de La Nappe Assurant La Production En Eau Potable d'Abidjan. Etude Sur Modèle Mathématique. Rapport Final ; Synthèse Des Résultats, Volume 2, République de Côte d'Ivoire, Ministère Des Infrastructure."

Soro, Gneneyougo Emile, Affoué Berthe Yao, Yao Morton Kouame, and Tié Albert Goula Bi. 2017. "Climate Change and Its Impacts on Water Resources in the Bandama Basin, Côte D'ivoire." *Hydrology* 4 (1): 13. https://doi.org/10.3390/hydrology4010018.

Soro, N. 2004. "Variabilité Du Régime Pluviométrique Du Sud de La Côte d'Ivoire et Son Impact Sur L'alimentation de La Nappe d'Abidjan." *Sud Sciences & Technologies*.

Soro, N., T. Lasm, B. H. Kouadio, G. Soro, and K. E. Ahoussi. 2006. "Variabilité Du Régime Pluviométrique Du Sud de La Côte d'Ivoire et Son Impact Sur l'alimentation de La Nappe d'Abidjan." *Sud Sciences et Technologies* 14: 30–40.

Soulis, K. X., and J. D. Valiantzas. 2012. "SCS-CN Parameter Determination Using Rainfall-Runoff Data in Heterogeneous Watersheds-the Two-CN System Approach." *Hydrology and Earth System Sciences* 16 (3): 1001–15. https://doi.org/10.5194/hess-16-1001-2012.

Spudis, PD. 2005. "The Geology of Multi-Ring Impact Basins: The Moon and Other Planets." *1st Pbk. Ed. Cambridge University Press, Cambridge [England] ; New York, NY*.

Tanina, S., S. Nagnin, S. Yéi, L. Théophile, S. Gbombélé, A. Kouassi, and J. Biémi. 2011. "La Variabilité Climatique et Son Impact Sur Les Ressources En Eau Dans Le Degré Carré de Grand-Lahou (Sud-Ouest de La Côte d'Ivoire)." *Physio-Géo* 5: 55–73.

Tapsoba, S. A. 1995. "Contribution à l'étude Géologique et Hydrogéologique de La Région de Dabou (Sud de La Côte d'Ivoire): Hydrochimie, Isotopie et Indice Cationique de Vieillissement Des Eaux Souterraines." Thèse de doctorat de l'Université Nationale de Côte d'Ivoire.

Tastet, J.P. 1979. "Environnements Sédimentaires et Structuraux Quaternaires Du Littoral Du Golfe de Guinée (Côte d'ivoire, Togo, Bénin)." Thèse de Doctorat d'Etat ès sciences, Université de Bordeaux.

Thornthwaite, C. W. 1948. "An Approach toward a Rational Classification of Climate." *Geographical Review* 38 (1): 55-94.

Thorntwaite, C.W., and J.R. Mather. 1955. "The Water Balance." *Publ. Climatol* 8 (1): 14.

Thorntwaite, C.W., and J.R Mather. 1957. "Instructions and Tables for Computing Potential Evapotranspiration and the Water Balance." *Publ. Climatol.* 10 (3).

Todini, E. 2007. "Hydrological Catchment Modelling: Past, Present and Future." *Hydrology & Earth System Sciences* 11: 468–82.

Txomin, H. L., A. Ruiz, L. José, Gil-Yepes, A. R. Jorge, and E.P-P. Josep. 2013. "Multi-Level Object-Based Urban Mapping from Remote Sensing and GIS Data." *GIS Ostrava 2013 - Geoinformatics for City Transformation*, 10.

UNDESA. 2018. "The United Nation Department of Economies and Social Affairs, the 2018 Revision of the World Urbanization Prospects." *Http/Www.Un.Org/Development/Desa/Plublications/2018 Revision of the World Urbanization Prospects.Html Update: 16/05/2018*. http/www.un.org/development/desa/plublications/2018 revision of the world urbanization prospects.html update: 16/05/2018.

UNEP. 2003. "United Nations Environment Programme, GEO-Global Environmental Outlook. UNEP Website: Http://Www.Unep.Org/Geo/Geo3/English/Index.Htm."

USGS. 2017. "(United States Geological Survey) (2017). Earth Resources Observation and Science Center (EROS), USGS, Sioux Falls, SD, USA. Available Online: Http://Earthexplorer.Usgs.Gov/."

Wada, Y, L P H van Beek, F C Sperna Weiland, B F Chao, Y H Wu, and M F Bierkens. 2012. "Past and Future Contribution Ofglobal Groundwater Depletion to Sea-Level Rise." *Geophys. Res.Lett.* 39.

Wang, H.F., and M. P. Anderson. 1982. "Introduction to Groundwater Modeling: Finite Difference and Finite Element Methods." *W.H Freeman and Co. New York.*

Wheater, H.S. 2010. "Hydrological Processes, Groundwater Recharge and Surface Water/Groundwater Interactions in Arid and Semi-Arid Areas, in: Wheater, H.S., Mathias, S.A., Li, X. (Eds.), Groundwater Modelling in Arid and Semi-Arid Areas." *International Hydrology Series. Cambridge University Press, New York*, 5–20.

Wilby, R. L., C. W. Dawson, E. M. Barrow, and .. 2002. "SDSM - a Decision Support Tool for the Assessment of Regional Climate Change Impacts." *Environ. Modell. Software* 17 (2): 147–59.

Williams, W. D. 1999. "Salinisation: A Major Threat to Water Resources in the Arid and Semi-Arid Regions of the World." *Lakes and Reservoirs: Research and Management* 4 (3–4): 85–91.

Wilson, Alicia M. 2005. "Fresh and Saline Groundwater Discharge to the Ocean : A Regional Perspective." *Water Resour. Res.* 41: 1–11. https://doi.org/10.1029/2004WR003399.

WPP. 2017. "Le Département Des Affaires Économiques et Sociales Des Nations Unies, Https://Population.Un.Org/Wpp/."

WRI, UNEP, UNDP and WB. 1998. *World Resources 1998-99: A Guide to the Global*

Environment (and the World Resources Database Diskette). Oxford University Press, New York, United States, and Oxford, United Kingdom .

Wu, Wenqi, Yungang Li, Xian Luo, Yueyuan Zhang, Xuan Ji, and Xue Li. 2019. "Performance Evaluation of the CHIRPS Precipitation Dataset and Its Utility in Drought Monitoring over Yunnan Province, China." *Geomatics, Natural Hazards and Risk* 10 (1): 2145–62. https://doi.org/10.1080/19475705.2019.1683082.

Xu, C. Y., and V. P. Singh. 2001. "Evaluation and Generalization of Temperature-Based Methods for Calculating Evaporation." *Hydrological Processes* 15: 305–19.

Yao, Affoué Berthe, Kouassi Innocent Kouame, Kouamé Auguste Kouassi, Kouadio Koffi, and Issiaka Goula, Bi Tié Albert SAVANE. 2015. "Estimation de La Recharge d'une Nappe Côtière En Zone Tropicale Humide: Cas de La Nappe Du Continental Terminal d'Abidjan (Côte d'Ivoire)." *International Journal of Innovation and Applied Studies* 12 (4): 888–98. https://doi.org/ISSN 2028-9324.

YAO, N. R., A. F. Oule, N.B. Kouadio, and . 2013. "Etude de La Vulnérabilité Du Secteur Agricole Face Aux Changements Climatiques En Côte d'Ivoire.," 105.

Yao, Y.Y., C.M. Zheng, J. Liu, G.L. Cao, H.L. Xiao, H.T. Li, and W.P. Li. 2015. "Conceptual and Numerical Models for Groundwater FLow in an Arid Inland River Basin." *Hydrol. Process.* 29 (1480–1492).

Yapo, Assi Louis Martial, Adama Diawara, Benjamin K. Kouassi, Fidèle Yoroba, Mouhamadou Bamba Sylla, Kouakou Kouadio, Dro T. Tiémoko, Dianikoura Ibrahim Koné, Elisée Y. Akobé, and Kouassi P.A.T. Yao. 2020. "Projected Changes in Extreme Precipitation Intensity and Dry Spell Length in Côte d'Ivoire under Future Climates." *Theoretical and Applied Climatology* 140 (3–4): 871–89. https://doi.org/10.1007/s00704-020-03124-4.

Yin, L., G. Hu, J. Huang, D. Wen, J. Dong, X. Wang, and H. Li. 2011. "Groundwater-Recharge Estimation in the Ordos Plateau, China: Comparison of Methods." *Hydrogeol. J.* 19 (8): 1563– 1575.

Zhang, L., N. Potter, K. Hickel, Y. Zhang, and Q. Shao. 2008. "Water Balance Modeling over Variable Time Scales Based on the Budyko Framework – Model Development and Testing." *Journal of Hydrology* 360: 117–34.

Zhang, Y., and G. Pinder. 2003. "Latin Hypercube Lattice Sampling Selection Strategy for Correlated Random Hydraulic Conductivity Fields." *Water Resources Research* 39 (8). https://doi.org/111/11-3.

Zheng, C., and G. Bennett. 2002. "Applied Contaminant Transport Modeling." *Wiley*

InterScience: New York, NY. 2nd Ed.

Zhou, Y., and W. Li. 2011. "A Review of Regional Groundwater Flow Modelling." *Geoscience Frontiers* 2 (2): 205–14.

Zoungrana, B.J.B., C. Conrad, L.K. Amekudzi, M. Thiel, and E.D. Da. 2015. "Land Use/Cover Response to Rainfall Variability: A Comparing Analysis between NDVI and EVI in the Southwest of Burkina Faso." *Climate* 3: 63–77.

Annex

Annex 1: Thornthwaite flowchart

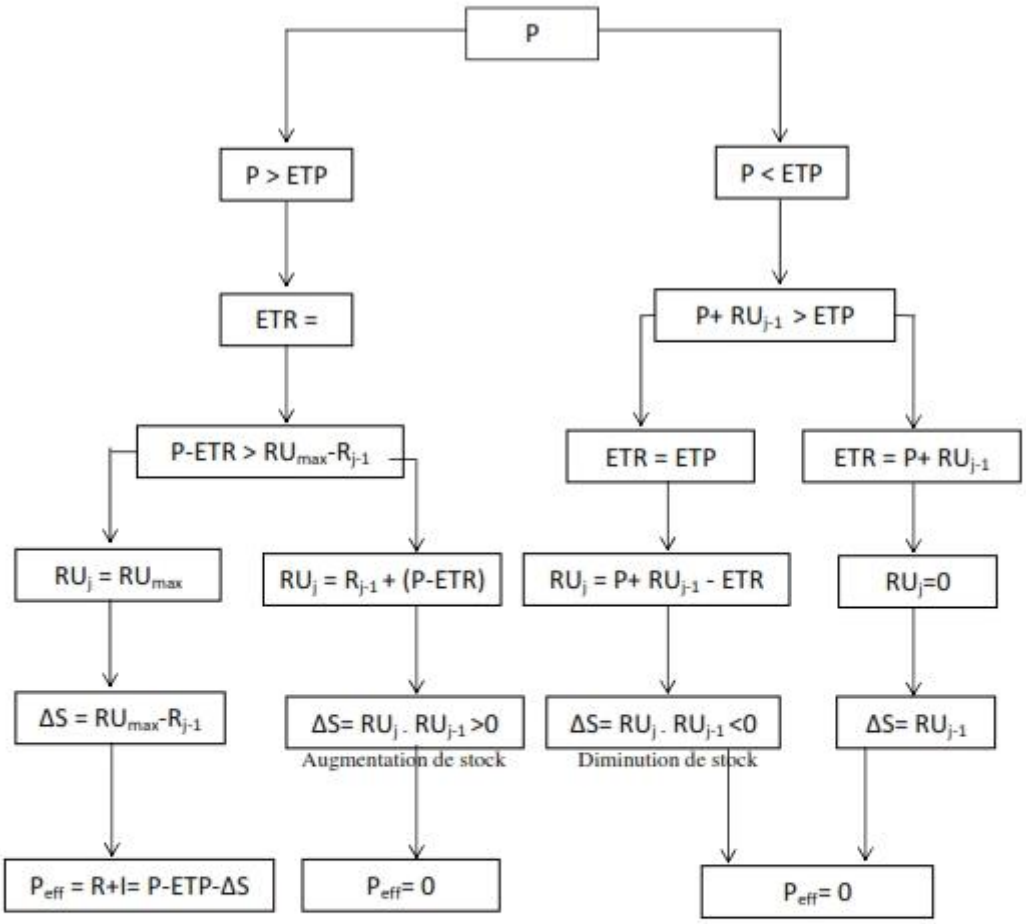

P : précipitation

ETP : évapotranspiration potentielle

ETR : évapotranspiration réelle

RUmax : réserve utile maximale

RU_j et RU_{j-1} : réserve utile du mois j et réserve utile du mois du mois j-1

ΔS : variation du stock d'eau dans le sol

P_{eff} : pluie efficace

R : écoulement rapide

I : infiltration profonde

Annex 2: Characteristics of the piezometers used

WELL_NAME	X	Y	Z	BOTTON	OBSERVE_TIME	WATER DEPH	WATER HEAD
PZ4-92	367143	601090	63.85	0.83	01/02/2018	43.62	21.06
PZ5-92	360667	591534	31.93	0.935	01/02/2018	21.4	11.465
PZ6	360805	588045	11.16	0.95	29/09/2017	10.08	2.03
PT01	362927	588312	21.97	0.67	01/02/2018	17.05	-4.94
PT02	368471	586761	7.8	0.3	27/09/2007	2.35	5.75
PZ7	381017	592740	86.17	0.8	27/03/2012	65.36	21.61
PZ8	381617	592816	85	0.94	25/09/2015	68.71	17.23
PZ1-92	407686	591111	68.97	1.01	31/01/2018	67.98	2
PZ2-92	401136	595676	89.78	1.01	31/01/2018	85.54	5.25
PZ9	391880	595437	93.38	0.9	27/01/2018	87.03	7.25
PZ10	390933	594597	59.39	0.98	02/02/2018	52.8	7.57
PZ11	391209	594468	50.477	0.53	02/02/2018	43.15	7.857
PZ12	391214	594465	50.33	0.3	02/02/2018	42.69	7.94
F6	382149	592583		0.94	22/08/2006	58.21	-57.27
PZ13	401589	605782	93.73	0.4	30/01/2018	72.29	21.84
PZ14	400031	604870	101.92	0.39	30/01/2018	81.48	20.83
PZ03	401531	603088	98.73	0.95	30/01/2018	83.47	16.21
PZ15	385690	606903	89.11	0.43	31/01/2018	36.7	52.84
PZ16	383488	600206	116.61	0.86	31/01/2018	47.08	70.39
PZ17	386054	594054	72.47	0.7	31/01/2018	67.3	5.87
PZ18	386849	596529	104.38	0.87	31/01/2018	88.85	16.4
PZ19	385593	592071	42.71	0.25	31/01/2018	38.42	4.54
PZ20	386442	589515	34.426	0.29	02/02/2018	32.59	2.126
PZ21	386497	589515	32.55	0.37	02/02/2018	31.56	1.36
PZ22	386530	588970	25.58	0.3	02/02/2018	27.64	-1.76
PZ23	395555	595231	44.604	0.5	29/01/2018	29.61	15.494
PZ24	395128	594757	48.81	1	29/01/2017	39.23	10.58
PZ1-2010	359233	598123	6.84	0.2	01/02/2018	3.47	3.57
PZ2-2010	379234	607334	82.04	0.2	31/01/2018	19.91	62.33
PZ3-2010	383813	600083	114	0.2	31/01/2018	82.68	31.52
PZ4-2010	391104	605756	103.65	0.2	31/01/2018	60.95	42.9
PZ5-2010	405758	602977	25.23	0.2	30/01/2018	13.36	12.07
PZ6-2010	397921	600679	7.83	0.2	30/01/2018	2.62	5.41
PZ7-2010	411233	587587	48.03	0.2	31/01/2018	46.7	1.53
PZ8-2010	417108	585881	40.77	0.2	31/01/2018	41.47	-0.5
F5	391968	595321		0.24	27/12/2005	73.35	-73.11
PZ-C2D-01	398102.86	598321.97	91	0.89	04/12/2017	81.03	10.86
PZ-C2D-02	398575.09	598808.93	86	0.91	04/12/2017	76	10.91
PZ-C2D-03	400739.07	598029.98	90	0.72	04/11/207	83.56	7.16

PZ-C2D-04	396939.93	602211.89	13.34	0.75	29/11/2017	5.33	8.76
PZ-C2D-05	395200.99	600157.04	84	1	04/12/2017	70.79	14.21
PZ-C2D-06	400486.85	600624.06	60	0.75	29/11/2017	47.39	13.36
PZ-C2D-07	403136.85	600571.97	15	0.8	29/11/2017	3.64	12.16
PZ-C2D-08	405521.1	599544.11	73	0.69	29/11/2017	63.37	10.32
PZ-C2D-09	403218	590519	45.22	0	04/12/2017	39.15	6.07
PZ-C2D-10	402652.14	595894.13	97	0.68	04/11/2017	90.75	6.93
PZ-C2D-11	395480	593521	56.57	0	04/12/2017	47.13	9.44
PZ-C2D-14	384133	592554	6	0.5	27/09/2017	2	4.5
PZ-C2D-15	383368	595296	25	0.5	31/07/2017	1.62	23.88
PZ-C2D-16	380286	598158	105	0.5	09/08/2017	64.63	40.87
PZ-C2D-17	381386	599911	101	0.5	11/08/2017	55.67	45.83
PZ-C2D-18	366050	598875	61	0.5	02/08/2017	34.27	27.23
PZ-C2D-19	364154	596911	59	0.5	30/11/2017	34.17	25.33
PZ-C2D-21	373013	593260	94	0.5	23/09/2017	77.39	17.11
PZ-C2D-22	374727	589585	29	0.5	23/09/2017	3.57	25.93
PZ-C2D-23	381073	594709	110	0.5		87.27	23.23
PZ-C2D-24	363970	596956	50	0.5		66.29	-15.79
PZ-C2D-25	367184	594219	90	0.5		58.01	32.49
DJIBI PUITS	391640	603220	36.00		10/10/1977	28.44	7.56
CAFE CI ANC	394.160	599.100	24.96	0.00	11/12/1978	16.62	8.34
PLANTATION SAPA	382.440	602.230	122.46	0.00	07/10/1977	48.83	73.63
SONGON MBRA CAR	359.800	588.450	15.33	0.35	29/10/1992	3.53	12.15
SONGON AGBAN VIL	360.600	587.750	11.16	0.75	29/10/1992	1.69	10.22
SONGON AGBAN PUITS	362.100	588.450	9.05	0.39	29/10/1992	6.38	3.06
SONGON TE ECOLE	362.600	587.925	21.97	0.67	29/10/1992	4.56	18.08
SONGON DAGBE VIL	363.250	587.225	12.08	0.74	29/10/1992	8.07	4.75
SONGON KASS VIL	365.200	587.225	3.16	0.57	29/10/1992	1.41	2.32
ADIAPO TE	369.680	586.440	1.52	0.48	29/10/1992	-0.35	2.35
ADIAPO MORO	368.880	589.695	36.57	0.05	29/10/1992	8.27	28.35
ANGUEDEDOU	369.800	590.025	29.54	0.38	04/11/1992	8.58	21.34
BIMBRESSO CAR	372.400	590.220	43.55	0.26	30/10/1992	6.43	37.38
ABADJIN KOUTE VIL	372.300	588.640	26.81	0.13	30/10/1992	2.42	24.52
ABADJIN KOUTE EC	371.650	588.275	12.23	0.20	30/10/1992	1.25	11.18
BIMBRESSO VIL	372.030	587.020	2.83	0.22	30/10/1992	0.32	2.73
ABADJIN DOUME	372.600	586.350	2.55	0.32	29/10/1992	0.41	2.46

INSTITUT PASTANC	374.300	587.420	17.72	0.00	30/10/1992	-6.42	24.14
ADIAPO DOUME MAR	374.400	589.500	26.19	0.40	30/10/1992	2.05	24.54
IRSDA	374.420	589.000	45.00	0.36	10/12/1992	12.02	33.34
NIANGON LOKOUA	377.200	586.350	3.50	0.03	31/10/1992	0.78	2.75
AZITO	380.200	585.825	3.00	0.20	31/10/1992	0.38	2.82
YOP PZ A8	380.980	589.440	35.64	0.14	25/02/1992	4.29	31.49
YOP PZ A8	380.980	589.440	35.64		16/05/1979	4.99	30.65
BIMBRESSO PUITS	371.600	586.825	5.37	0.64	30/10/1992	0.44	5.57
DCH6 YOP MACA	379.300	595.700	97.28	0.49	26/10/1992	18.25	79.52
GARDER FOREST 2	380.100	596.500	95.38	0.93	26/10/1992	18.51	77.8
GARDER FOREST 3	382.175	599.300	110.05	0.26	26/10/1992	32.29	78.02
GARDER FOREST 4	383.400	598.600	114.12	0.24	26/10/1992	28.06	86.3
YAPI 1 SAPA 2	378.700	601.575	68.91	0.40	26/10/1992	60.28	9.03
YAPI 2 ACHOKOI	377.600	601.750	52.39	0.85	26/10/1992	40.04	13.2
YAPI 3 AGBASSI	375.700	602.625	39.66	0.76	26/10/1992	35.68	4.74
AKOUPE	372.450	605.790	51.76	0.24	26/10/1992	14.05	37.95
ATTINGUIE PIEZO	368.300	603.270	64.04	0.25	28/10/1992	39.90	24.39
SAPH V2 NORD	369.720	596.920	61.19	0.22	26/10/1992	24.35	37.06
SODEFOR HORTIVEX	375.650	595.720	21.73		10/10/1977	17.94	3.79
SODEFOR IVOIR	374.900	595.450	25.00	0.50	26/10/1992	17.76	7.74
ATINGUIE FORAGE	368.250	602.270	22.40	0.47	24/05/1986	6.93	15.94
ADJAME F9	386.100	592.125	42.71	0.00	07/07/1995	1.57	41.14
ZONE NORD F4	386.375	602.230	72.47	0.25	07/07/1995	3.99	68.73
FILTISAC	386.425	595.450	104.38	0.82	07/07/1995	14.93	90.27
SAPH V2 NORD	369.720	596.920	61.19		20/12/1977	28.74	32.45
VP SODEPALM	374.550	598.440	44.65	0.01	26/10/1992	36.80	7.86
ALOKOUA	372.800	595.975	91.93	0.77	26/10/1992	21.94	70.76
SODEFOR HORTIVEX	375.650	595.720	21.73	0.44	26/10/1992	17.80	4.37
ZONE OUEST P9	377.700	590.725	86.17	0.80	06/07/1995	22.28	64.69
ANONKOUA KOUTE	383.500	600.175	116.61	0.61	06/07/1995	30.25	86.97
PLATEAU CHAT D'EAU	386.300	589.150	32.55	0.31	10/07/1995	1.36	31.5
ZONE EST P2	391.300	593.175	59.39	0.98	07/07/1995	1.85	58.52

NIANGON 1	376.300	593.875	19.79	0.58	30/03/1995	8.24	12.13
BANCO 2	383.600	590.900	14.33		24/10/1979	0.58	13.75
ZOO 1 SUD	388.220	594.225	32.24	0.66	27/10/1994	7.40	25.5
ADONKOI NOUV	365.840	598.040	67.04	0.45	27/10/1992	19.14	48.35
ATINGUIE PZ4 92	366.600	599.300	63.85	0.84	27/09/1993	17.37	47.32
ADONKOI PUITS	366.200	598.425	29.90	0.25	28/10/1992	19.39	10.76
ADONKOI 2	364.1	596.5	22.91	0.85	28/10/1992	13.43	10.33
SONGON AGBAN BA	363.900	595.625	51.24	0.70	28/10/1992	17.30	34.64
SONGON AGBAN AT	363.900	594.400	66.66	0.70	28/10/1992	16.97	50.39
NIEKY VILLAGE	360.200	598.250	11.39	0.88	27/10/1992	3.15	9.12
NIEKY ECOLE	359.100	597.550	9.81	0.37	27/10/1992	2.78	7.4
NIEKY EGLISE	357.000	596.150	12.58	0.90	27/10/1992	3.02	10.46
SONDJABONOU	356.200	594.575	43.26	0.45	27/10/1992	5.13	38.58
BETEKRO PUITS	357.000	593.350	18.81	0.82	27/10/1992	7.49	12.14
SONGON MBRA PZ5	358.250	591.250	31.93	0.96	29/09/1993	8.67	24.22
BETEKRO VILLAGE	357.800	593.000	32.52	0.70	28/10/1992	8.34	24.88
SONGON MB ATIE	359.200	593.350	52.28	0.48	28/10/1992	9.39	43.37
SONGON A ATIE 2	362.080	591.480	38.81	0.39	28/10/1992	5.62	33.58
AYOU WAHI	368.200	592.300	51.52	0.48	29/09/1992	15.94	36.06
NIANGONATIE	375.500	591.250	10.21	0.22	29/09/1992	5.04	5.39
ADONKOI ANC	365.250	598.200	67.39	0.00	07/11/1977	23.47	43.92
M'POUTO EGLISE	394.076	588.080	3.45	0.43	11/12/1978	1.42	2.46
M'BADON P47	396.25	588.95	11.22	0.12	07/11/1977	7.97	3.37
AKOUEDO	395.650	591.190	52.41	0.60	10/07/1995	3.96	49.05
ABATA	398.400	588.275	3.30	0.33	21/10/1992	-0.04	3.67
CARRIERE ECOLE	398.200	592.475	35.13	0.53	21/10/1992	3.43	32.23
DAHLIA FLEUR	398.690	590.880	21.96	0.38	20/10/1992	1.85	20.49
ANNA	402.600	588.450	3.13	0.76	21/10/1992	-0.78	4.67
CPT DABA	406.200	589.675	45.52	0.62	10/03/1992	1.96	44.18
AKOUE AGBAN	405.100	586.525	7.28	0.29	21/10/1992	1.03	6.54
BRAGBO	408.800	585.825	4.98	0.17	21/10/1992	1.13	4.02
KOFFIKRO ATTIE	408.700	586.525	16.79	0.56	21/10/1992	0.76	16.59
ELOKA USINE	411.180	587.060	47.98	0.25	04/02/1992	1.28	46.95
ELOKA TE	417.100	585.125	45.00	0.00	11/11/1982	4.26	40.74

EBRA	418.200	582.850	4.33	0.34	21/10/1992	0.10	4.57
MBATO BOUAKE	412.200	591.070	76.46	0.00	06/01/1982		76.46
AKAKRO PZ1 92	407.500	590.725	68.97	1.07	23/02/1993	-8.28	78.32
AKAKRO	408.730	592.280	4.43	0.27	21/10/1992	0.13	4.57
ACHOKOI	407.200	593.875	2.53	0.48	21/10/1992	0.44	2.57
AKOYATE	406.175	594.925	2.59	0.23	21/10/1992	-0.49	3.31
ADJIN HV	405.300	595.975	19.74	0.20	21/10/1992	-1.27	21.21
AKANDJE PZ2 92	401.050	595.275	89.78	1.10	23/09/1993	3.02	87.86
AKANDJE	400.600	597.550	4.66	0.42	20/10/1992	0.29	4.79
KOFFIKRO ATTIE PIEZO	408.100	586.200	4.31	0.00	14/05/1982	1.75	2.56
ELOKA TO	416.200	586.125	36.00	0.00	11/11/1982	2.37	33.63
ADJIN TUBE PVC	405.100	595.825	10.70	0.00	11/11/1982	-0.44	11.14
ABOBO CIMETIERE	391.100	601.400	111.28	0,45	23/03/1992	28.95	83.73
DJIBI FORAGE	391.800	603.500	75.34	0.63	24/03/1992	26.87	49.1
DJOROGOBITE 2	394.200	597.725	94.93	0.72	24/03/1992	12.87	82.78
CAFE CI NOUV	394.280	599.940	16.87	0.56	24/03/1992	12.16	5.27
CPT KOUAKOU	395.760	601.620	10.80	0.46	24/03/1992	5.54	5.72
ANYAMA DEBAR	397.700	600.350	3.99	0.26	23/10/1992	0.88	3.37
BROFODOUME DISP	397.300	608.875	72.00	0.07	23/10/1992	40.68	31.39
AKEKOI	402.300	607.225	51.79	0.70	23/03/1982	21.34	31.15
PLANTATION CP	399.800	604.725	101.92	0.39	19/03/1992	18.27	84.04
BABEKOI ECOLE	397.800	603.500	49.62	0.22	24/03/1992	7.94	41.9
LAME PZ3 92	401.600	602.450	98.73	0.88	15/10/1993		99.61
KONGOFON	404.800	606.125	22.03	0.30	23/10/1992	12.78	9.55
KONGOFON ECOLE	403.400	606.300	70.49	0.22	23/03/1992	19.46	51.25
CPT DOGBO	401.200	606.125	93.73	0.38	03/11/1992	19.40	74.71
PLANTATION SABO	384.460	602.054	114.46	0.65	12/12/1978	48.15	66.96
ANYAMA ADJAME	385.710	606.360	89.11	0.55	07/02/1992	48.89	40.77
YAPOKOI	383.600	609.200	55.84	0.30	26/03/1992	46.41	9.73
EBIMPE COLLEGE	379.240	606.900	68.65	0.30	07/02/1977	49.28	19.67
DJIBI PUITS	391.640	603.220	36.00	0.00	07/11/1977	28.14	7.86
ZOO 1 SUD	388.220	594.225	32.24	0.66	10/10/1979	11.25	21.65
ZOO 2 NORD	388.420	595.100	57.51	0.78	07/07/1995	14.64	43.65
NORD RIVIERA 1	394.000	593.175	48.22	0.91	18/08/1992	8.52	40.61

ANYAMA F1	383.300	607.525	91.61	0.34	28/03/1995	55.42	36.53
M'POUTO SODECI	394.076	588.080	3.45	0.00	23/09/1993	0.79	2.66
INSTITUT PAST SOD	374.650	587.400	19.70	0.00	27/09/1993	0.53	19.17
BIMBRESSO IRFA	373.625	592.825	91.27	0.27	19/02/1993	13.01	78.53
ZONE OUEST P7	381.480	592.740	85.00	0.91	06/07/1995	19.22	66.69
ZONE OUEST ANC	381.540	593.090	85.98	0.73	10/10/1977	10.71	76
ANOKOUA KOUTE ANC	384.220	600.330	115.32	0.37	10/10/1979	41.92	73.77
NIANGON PIEZO	376.470	593.390	65.76	0.58	24/10/1979	12.07	54.27
NIANGON F ANC	377.160	593.240	26.67		22/09/1982	13.78	12.89
BANCO PIEZO	385.850	588.990	4.30		24/10/1977	-0.30	4.6
PLATEAU RAN	386.480	588.500	25.58	0.30	10/07/1995	-2.22	28.1
NORD RIVIERA SR4	394.270	593.290	48.24		24/10/1979	6.70	41.54
NORD RIVIERA SR1	395.700	595.000	34.90		24/10/1979	10.17	24.73
ANYAMA CHÂTEAU	383.500	605.370	95.10		06/07/1995	51.07	44.03
ANYAMA SUD F2	383.66	607.3	86.54	0.43	06/07/1995	56.97	30
PZ 77 61 RTE BINGER	393.210	592.310	20.10		12/10/1981	8.02	12.08
MAISON ET JARDIN	400.080	592.050	11.95		04/11/1980	5.77	6.18
EECI ECOLE	399.960	591.500	11.10		10/10/1977	6.73	4.37
YAPI PUITS TRAD	377.960	602.340	59.22		12/10/1981	44.88	14.34
GD SEMINAIRE	382.030	607.100	85.55		07/11/1977	53.80	31.75
ADIAPO DOUME MISS	373.800	589.510	47.63		07/11/1977	5.28	42.35
YOP SANTE PUITS	384.560	589.020	8.07		10/10/1977	-0.08	8.15
PZ 77 A 1	384.620	593.960	20.92		07/11/1977	8.35	12.57
PZ 77 A2	384.45	595.82	38.02		16/05/1979	20.08	17.94
DCH3	388.850	599.800	78.86		02/07/1979	34.06	44.8
DCH2	392.480	597.150	77.12		04/11/1980	18.33	58.79
DCH1	379.520	598.150	49.40		18/05/1982	30.93	18.47
HOTEL RETRAITE ANY	383.82	604.12	103.96	0.39	12/12/1978	52.73	51.62
IRCA	372.802	587.340	5.37	0,69	10/10/1978	0.24	5.82

Annex 3: Lithological sections and technical data sheets of some boreholes used for the conceptual model setting up

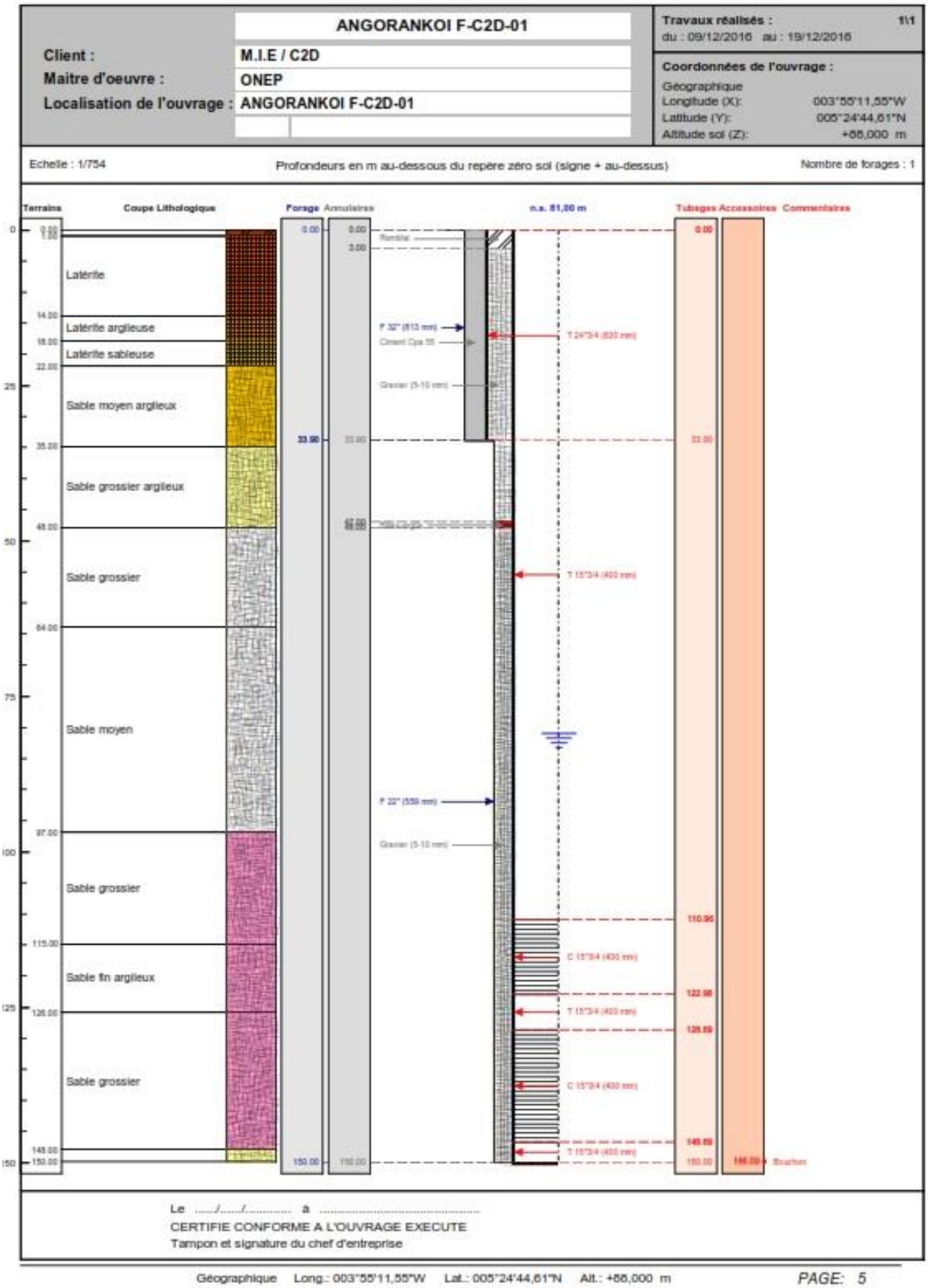

	ADJAME BINGERVILLE (PZ-C2D-09)	**Travaux réalisés :** du : 27/02/2017 au : 06/03/2017	1\2
Client :	**M.I.E / C2D**		
Maitre d'oeuvre :	**ONEP - ARTELIA (ASSISTANT TECHNIQUE)**	**Coordonnées de l'ouvrage :**	
Localisation de l'ouvrage :	**ADJAME BINGERVILLE (PZ-C2D-09)**	Géographique	
		Longitude (X):	003°52'24,57"W
		Latitude (Y):	005°20'30,64"N
		Altitude sol (Z):	+45,220 m

Echelle : 1/965 — Profondeurs en m au-dessous du repère zéro sol (signe + au-dessus) — Nombre de forages : 1

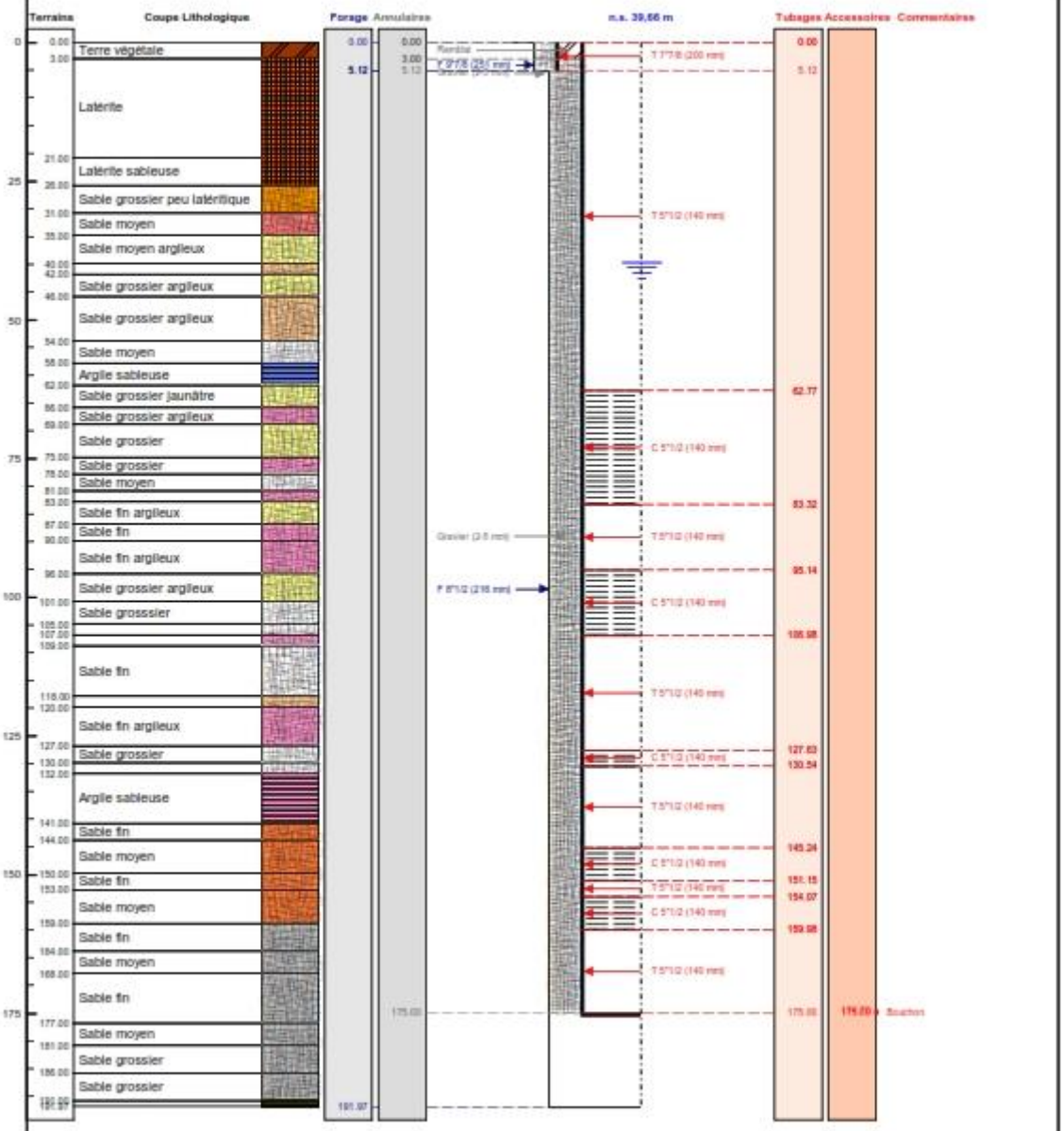

Le ...../...../..... à .....
CERTIFIE CONFORME A L'OUVRAGE EXECUTE
Tampon et signature du chef d'entreprise

Géographique Long.: 003°52'24,57"W Lat.: 005°20'30,64"N Alt.: +45,220 m

PAGE: 5

ADJAME BINGERVILLE (PZ-C2D-09)	**Travaux réalisés :** 1\2 du : 27/02/2017 au : 06/03/2017
Client : M.I.E / C2D	**Coordonnées de l'ouvrage :**
Maitre d'oeuvre : ONEP - ARTELIA (ASSISTANT TECHNIQUE)	Géographique Longitude (X): 003°52'24,57"W Latitude (Y): 005°20'30,64"N Altitude sol (Z): +45,220 m
Localisation de l'ouvrage : ADJAME BINGERVILLE (PZ-C2D-09)	

Echelle : 1/965 — Profondeurs en m au-dessous du repère zéro sol (signe + au-dessus) — Nombre de forages : 1

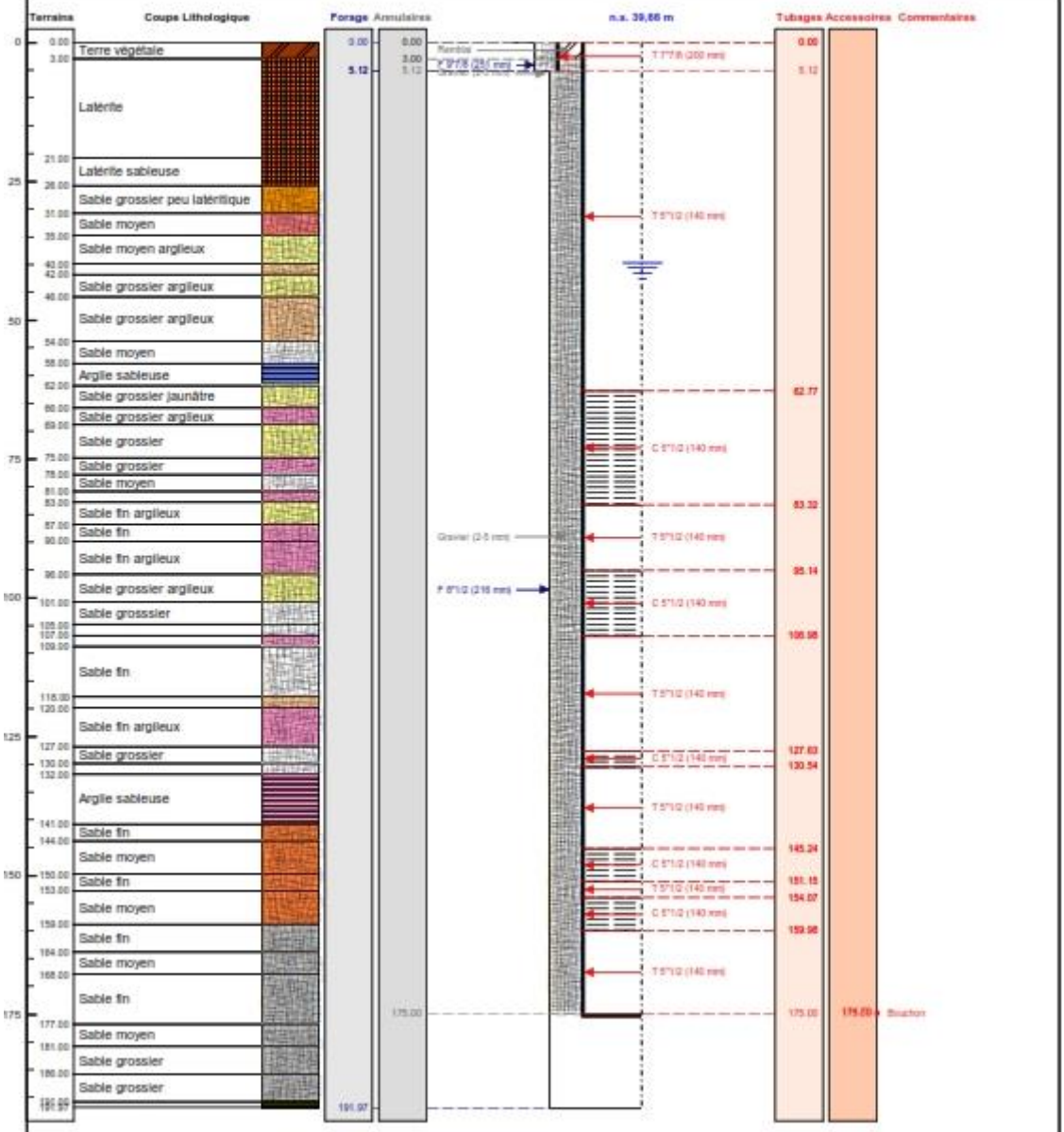

Le ...../...../..... à .....

CERTIFIE CONFORME A L'OUVRAGE EXECUTE

Tampon et signature du chef d'entreprise

Géographique Long.: 003°52'24,57"W Lat.: 005°20'30,64"N Alt.: +45,220 m

PAGE: 5

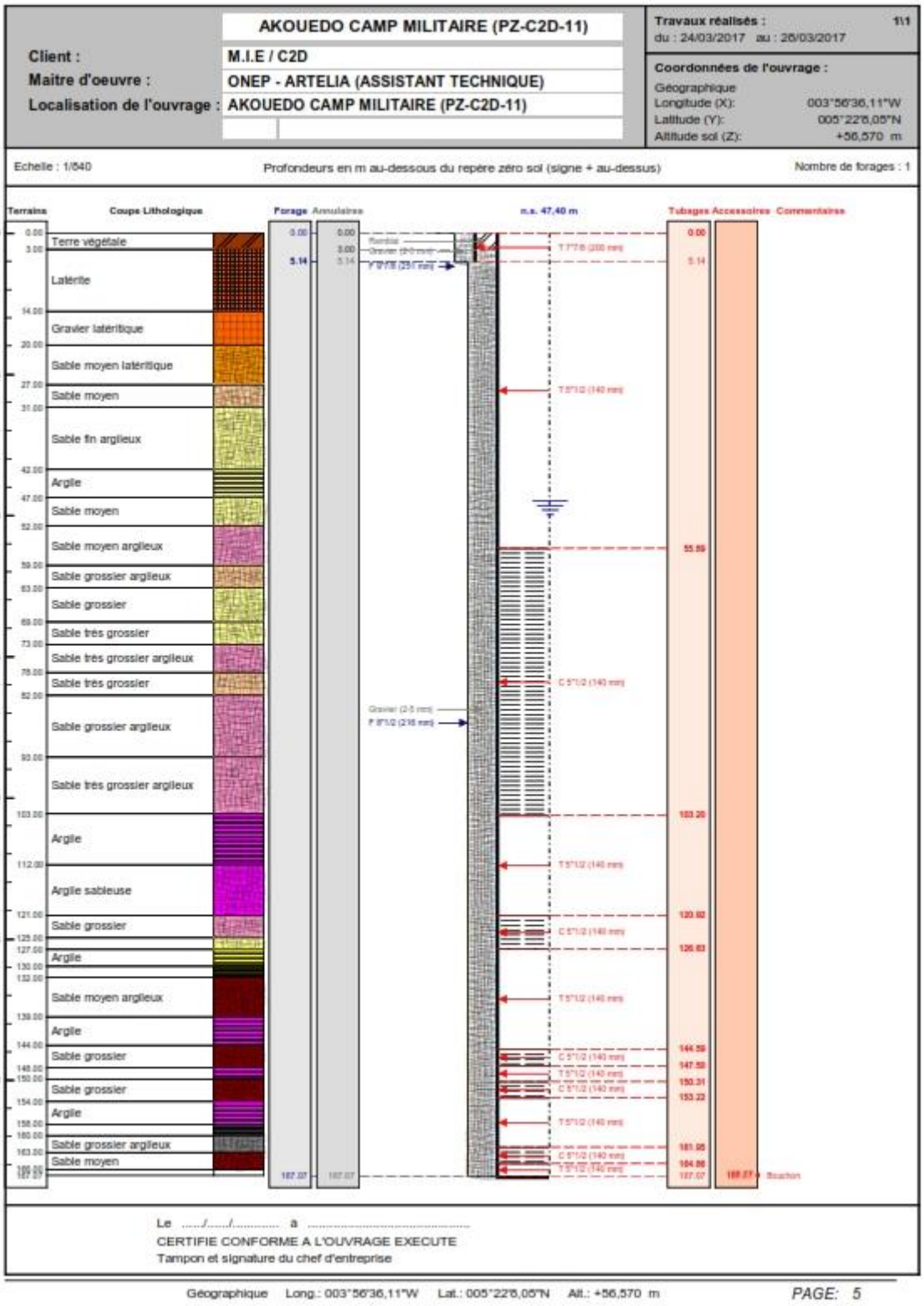
AKOUEDO CAMP MILITAIRE (PZ-C2D-11)
Client : M.I.E / C2D
Maitre d'oeuvre : ONEP - ARTELIA (ASSISTANT TECHNIQUE)
Localisation de l'ouvrage : AKOUEDO CAMP MILITAIRE (PZ-C2D-11)
Travaux réalisés : 1\1
du : 24/03/2017 au : 26/03/2017
Coordonnées de l'ouvrage :
Géographique
Longitude (X): 003°56'36,11"W
Latitude (Y): 005°22'6,05"N
Altitude sol (Z): +56,570 m
Echelle : 1/640
Profondeurs en m au-dessous du repère zéro sol (signe + au-dessus)
Nombre de forages : 1
Terrains
Coupe Lithologique
Forage Annulaires
n.s. 47,40 m
Tubages Accessoires Commentaires
Terre végétale
Latérite
Gravier latéritique
Sable moyen latéritique
Sable moyen
Sable fin argileux
Argile
Sable moyen
Sable moyen argileux
Sable grossier argileux
Sable grossier
Sable très grossier
Sable très grossier argileux
Sable très grossier
Sable grossier argileux
Sable très grossier argileux
Argile
Argile sableuse
Sable grossier
Argile
Sable moyen argileux
Argile
Sable grossier
Sable grossier
Argile
Sable grossier argileux
Sable moyen
Bouchon
Le ...../...../..... à .....
CERTIFIE CONFORME A L'OUVRAGE EXECUTE
Tampon et signature du chef d'entreprise
Géographique Long.: 003°56'36,11"W Lat.: 005°22'6,05"N Alt.: +56,570 m
PAGE: 5

	AKOUEDO CAMP MILITAIRE (PZ-C2D-11)
Client :	**M.I.E / C2D**
Maitre d'oeuvre :	**ONEP - ARTELIA (ASSISTANT TECHNIQUE)**
Localisation de l'ouvrage :	**AKOUEDO CAMP MILITAIRE (PZ-C2D-11)**

Travaux réalisés : 1\1
du : 24/03/2017 au : 26/03/2017

Coordonnées de l'ouvrage :

Géographique	
Longitude (X):	003°56'36,11"W
Latitude (Y):	005°22'6,05"N
Altitude sol (Z):	+56,570 m

Echelle : 1/640 — Profondeurs en m au-dessous du repère zéro sol (signe + au-dessus) — Nombre de forages : 1

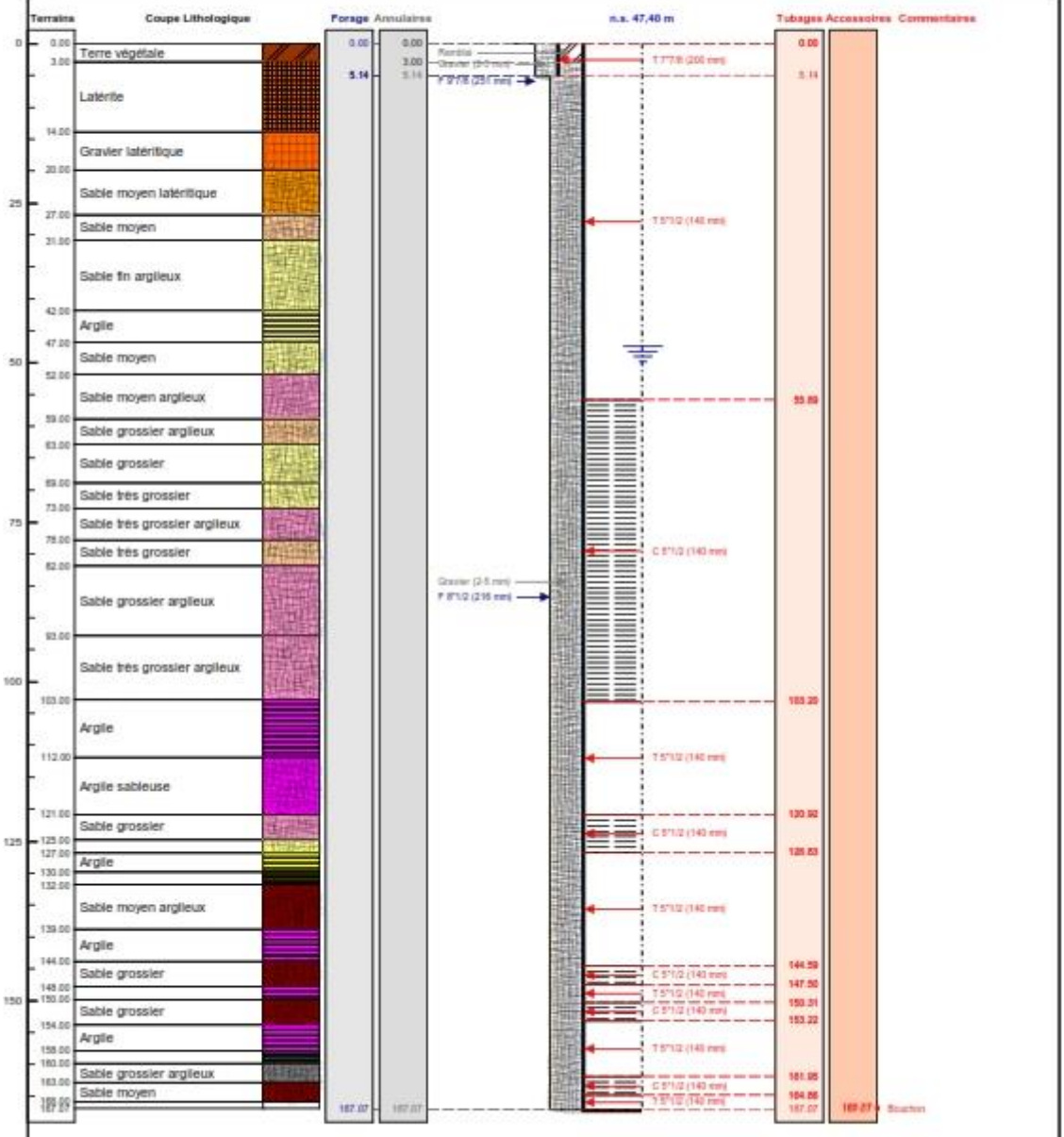

Le ...../...../..... à .....

CERTIFIE CONFORME A L'OUVRAGE EXECUTE

Tampon et signature du chef d'entreprise

Annex 4: Field pictures

Annex 5: List of Publications

Abdelaziz, K.K., Nicaise, Y., Séguis, L., Ouattara, I., Moussa, O., Auguste, K.K., Kamagaté, B. and Diakaria, K. (2020) Influence of Land Use Land Cover Change on Groundwater Recharge in the Continental Terminal Area of Abidjan, Ivory Coast. *Journal of Water Resource and Protection*, 12, 431-453. https://doi.org/10.4236/jwarp.2020.125026

Candidate biography

Mr. KOUAKOU Koffi Abdelaziz is PhD candidate in the GRP/ Climate Change and Water Resources Program at University of Abomey-Calavi, Benin in the framework of the WASCAL project. He holds a Master in Geosciences and Environment at Universty of Nangui Abrogoua. He is also author of an article on ". Journal of Water Resource and Protection" and worked as junior consultant for some projects in Côte d'Ivoire.

Abstract: This study focuses on the influence of climate and land use/land cover (LULC) change on groundwater recharge over the Continental Terminal catchment (Abidjan aquifer) in the context of urbanization and population growth. The specific objectives of the study were to, (i) assess groundwater recharge regarding the changing in climate and LULC of the Continental Terminal catchment using water balance method, (ii) assess the impact of the Representative Concentration Pathways (RCP4.5) climate change scenario on rainfall, temperature, and groundwater recharge in the future 2020-2049, and (iii) model and analyze locally impact of climate and LULC change on groundwater balance using MODFLOW model to assess interaction between groundwater and surface water. Many data have been used for the study such as, piezometric level data, observations (stations and CHIRPS) climate data, Landsat images (1990, 2000 and 2016) for LULC mapping, Regional Climate Models (RCMs) under RCP4.5 scenario for historical (1982-2011) and future (2020-2049) period for climate change impact assessment. The results show an increased in built-up and agricultural land, while the forest and shrub areas declined, with water body remaining unchanged over the period 1990-2016. The decline in forest could be imputed to the demographic and socio-economic growth as expressed by the expansion in agriculture and urbanization. Groundwater recharge represents 34%, 21% and 26% of rainfall respectively in 1990, 2000, and 2016. While the runoff during these same years is respectively 20%, 46% and 14% of rainfall total. The ensemble mean projected a warmer climate in the future (2020-2049) with a 1.73^{o}C increase in mean annual temperature and a 37.32% increase in mean annual rainfall relative to the baseline (1982-2011) period. Groundwater recharge projected was found more depending to climate change parameter especially changing in rainfall an temperature. Groundwater and lagoon Aghien intaraction show that Aghien lagoon drains the aquifer to 1.10^{4} m^{3} /day in certain areas where the aquifer is deeper, the lagoon supplies the groundwater by drainage up to $41.10^{3}m^{3}$/day and all the scenarios made to assess future groundwater water level (2060) reveal a drop of hydraulic head and this could impact surface water reseve

Key words: Land use and land cover change, climate change, MODFLOW, recharge, GW-SW interaction, Continental Terminal, Côte d'Ivoire

PhD

KOUAKOU Koffi Abdelaziz

IMPACT OF CLIMATE CHANGE AND URBANIZATION ON THE CONTINENTAL TERMINAL AQUIFER RECHARGE IN AGHIEN LAGOON AREA (ABIDJAN, CÔTE D'IVOIRE)

GRP/CCWR/INE/WASCAL – UAC Month, 2020